Universiteit
Leiden
The Netherlands

New developments in ablation of ventricular arrhythmias

Huls van Taxis, C.F.B. van

Citation
Huls van Taxis, C. F. B. van. (2019, February 14). *New developments in ablation of ventricular arrhythmias*. Retrieved from https://hdl.handle.net/1887/68644

Version:	Not Applicable (or Unknown)
License:	Licence agreement concerning inclusion of doctoral thesis in the Institutional Repository of the University of Leiden
Downloaded from:	https://hdl.handle.net/1887/68644

Note: To cite this publication please use the final published version (if applicable).

Cover Page

Universiteit Leiden

The handle http://hdl.handle.net/1887/68644 holds various files of this Leiden University dissertation.

Author: Huls van Taxis, C.F.B. van
Title: New developments in ablation of ventricular arrhythmias
Issue Date: 2019-02-14

New Developments in Ablation of Ventricular Arrhythmias

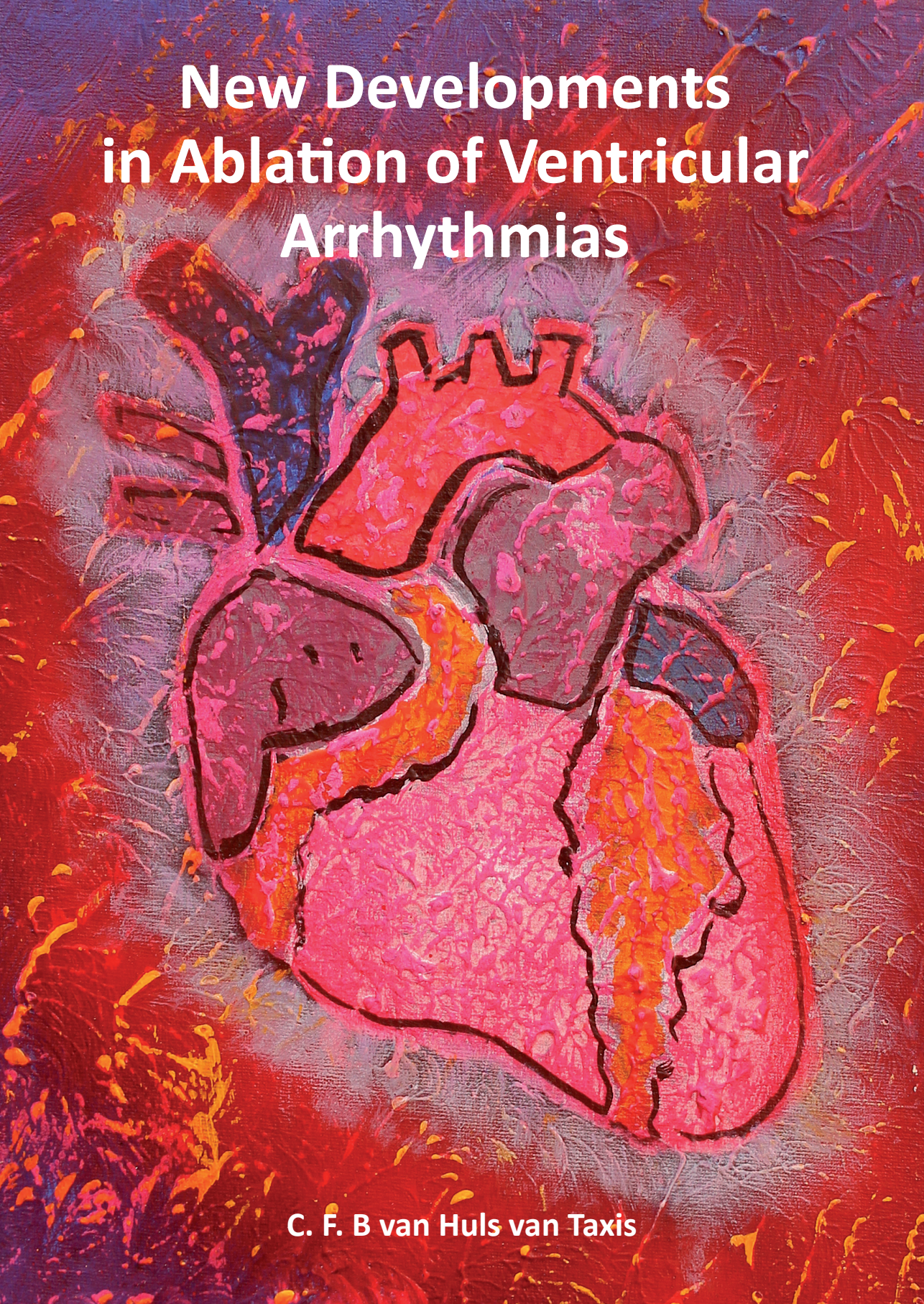

C. F. B van Huls van Taxis

New Developments in Ablation of Ventricular Arrhythmias

Carine Francine Belline van Huls van Taxis

The studies described in this thesis were performed at the Heart Lung Center of the Leiden University Medical Center, Leiden, The Netherlands.
Copyright © C.F.B. van Huls van Taxis 2019
All rights reserved. No part of this book may be reproduced, distributed or transmitted in any form or by any means without prior permission of the copyright owner.
Cover designed by: Philip de Bruijn
Layout and printed by: Optima Grafische Communicatie (www.ogc.nl)
ISBN: 978-94-6361-183-1
Financial support for the publication of this thesis by the following companies is gratefully acknowledged: Abbott Medical Nederland BV, Biotronik Nederland B.V., Boehringer Ingelheim B.V., Canon Medical Systems Nederland, ChipSoft B.V., Medis Medical Imaging Systems B.V. and Servier Nederland Farma B.V.

New Developments in Ablation of Ventricular Arrhythmias

Proefschrift

ter verkrijging van
de graad van Doctor aan de Universiteit Leiden,
op gezag van Rector Magnificus Prof. Mr. C.J.J.M. Stolker,
volgens besluit van het College van Promoties
te verdedigen op donderdag 14 februari 2019
klokke 13:45 uur

door

Carine Francine Belline van Huls van Taxis
geboren te Leiden in 1984

Promotoren:	Prof. Dr. K. Zeppenfeld
	Prof. Dr. M.J. Schalij
Co-promotor:	Dr. A.P. Wijnmaalen
Promotiecommissie:	Prof. Dr. R.J.M. Klautz
	Prof. Dr. H.J. Lamb
	Prof. Dr. J.L.R.M. Smeets (University of Maastricht)
	Dr. S. Kats (Maastricht Universitair Medisch Centrum)
	Dr. S.R.D. Piers

Financial support by the Dutch Heart Foundation for the publication of this thesis is gratefully acknowledged.
The research described in this thesis was supported by a grant of the Dutch Heart Foundation (2008B074).

TABLE OF CONTENTS

Chapter 1	General Introduction, Aim and Outline of the Thesis	7

Part I New Developments in Radiofrequency Catheter Ablation of Idiopathic Ventricular Arrhythmias

Chapter 2	The Neurohormonal, Structural and Functional Recovery Pattern after PVC Ablation is Independent of Structural Heart Disease Status in Patients with Depressed Left Ventricular Ejection Fraction; A Prospective Multicentre Study	25
Chapter 3	Fatigue as Presenting Symptom and a High Burden of Premature Ventricular Contractions are Independently Associated with Increased Ventricular Wall Stress in Patients with Normal Left Ventricular Function	41
Chapter 4	Reversed Polarity of Bipolar Electrograms to Predict a Successful Ablation Site in Focal Idiopathic Right Ventricular Outflow Tract Arrhythmias	59

Part II New Developments in Real-Time Image Integration During Radiofrequency Catheter Ablation

Chapter 5	Real-time integration of MDCT derived coronary anatomy and epicardial fat: Impact on epicardial electroanatomical mapping and ablation for ventricular arrhythmias	77
Chapter 6	Epicardial Substrate Mapping for Ventricular Tachycardia Ablation in Patients with Nonischemic Cardiomyopathy: A New Algorithm to Differentiate Between Scar and Viable Myocardium Developed by Simultaneous Integration of CT and Contrast-Enhanced MRI	97

Part III New Developments in Surgical Cryoablation of Ventricular Arrhythmias

Chapter 7	Programmed Electrical Stimulation Guided Encircling Cryoablation Concomitant to Surgical Ventricular Reconstruction for Primary Prevention of Ventricular Arrhythmias	119
Chapter 8	Endocardial/Epicardial- versus Endocardial Encircling Cryoablation for Ventricular Tachycardia; A Randomized Trial	135
Chapter 9	Summary, Conclusions and Future Perspectives	153
Chapter 10	Nederlandse Samenvatting	161
Appendix	List of Publications	171
	Dankwoord	177
	Curriculum Vitae	179

Chapter 1

General Introduction, Aim and Outline of the Thesis

BACKGROUND

The number of patients with structural heart disease is increasing due to advances in the treatment of acute and chronic coronary artery disease and heart failure.[1] As a consequence, the number of patients with ventricular arrhythmias (VA) has also increased, as many patients with structural heart disease are at risk for potentially life-threatening VA.[2] The mechanism for these VA is mostly reentry. The assumed substrate of reentrant tachycardias that occur in the chronic phase of myocardial infarction and other forms of structural heart disease is a circuitous 3-dimentional pathway formed by tracts of bundles of surviving myocytes that are located intramurally, subendocardially and epicardially within scarred myocardium.[3] Therapies targeting this substrate may prevent ventricular arrhythmia occurrence and recurrence.

Since the late 1950's several different treatment and preventative strategies for VA have been developed, some with better outcomes than others. However, despite great advances in knowledge and technology, VA cannot be fully prevented in patients with different substrates. In addition, invasive treatment remains associated with small but clinically significant risks. This illustrates the challenges and underlines the continuing need for improvement in this field.

In 1959 the first successful surgical ventriculoplasty for VA has been reported in a patient after remote myocardial infarction.[4] However, long-term results were disappointing and aneurysmectomy alone appeared not to be sufficient to control recurrent VA.[5] Since then surgical treatment for arrhythmias has evolved. From 1971 on coronary artery bypass grafting was utilized in attempts to treat recurrent VA in patients with ischemic heart disease.[6,7] Although results looked promising, even in addition to aneurysmectomy, uniform success was not achieved and significant morbidity and mortality was reported.[5,8,9] In 1980 Horowitz at al. described higher success rates with a new surgical technique; they performed endo- and epicardial mapping of the VA in patients with recurrent VA, followed by endocardial resection of the site of origin of the VA.[10] After 13.5±6 months follow-up none of the post-operative surviving patients experienced any VA.

Surgical cryoablation has increasingly been applied after its first description in 1977 when it was used to treat drug-refractory AV-node reentrant tachycardia.[11] The successful ablation procedure prompted the use of this technique to treat recurrent VA in a patient with sclerodemia.[12] Subsequently, it was further evolved into encircling cryoablation and has been applied in patients with refractory VA after myocardial infarction with promising results.[13,14]

Another major development in the treatment of VA was the introduction of implantable cardioverter defibrillators (ICD) in patients with ischemic heart disease and at high risk for sudden cardiac death.[2,15-18] ICD carriers had an improved long-term survival due to the termination of life-threatening arrhythmias compared to optimal medical therapy, only.[2,15-18] However, ICDs do not prevent VA recurrences. Of importance, ICD shocks have detrimental impact on the quality of life and have been associated with increased mortality.[19-21]Adequate additional therapies that prevent VA were therefore needed.

Even though surgical treatment of arrhythmias showed promising results in selected patients, the invasive character and possible complications led to the development of catheter based ablation strategies. In 1982 the first closed chest His-bundle ablation was performed using direct-current shocks up to 300 Joule from a standard cardioversion unit through an intracardiac catheter positioned at the His-bundle region.[22] Arguing that a high-energy discharge would also interrupt ventricular tachycardia reentry circuits, Hartzler used direct-current catheter ablation for VA with success.[23] This technique was however associated with a high rate of serious complications.[24] In 1987, Huang and co-workers were the first who performed closed chest catheter ablation of the atrioventricular junction with radiofrequency energy of up to 750kHz in 13 dogs.[25] Pathologic examination showed well delineated coagulation necrosis at the atrioventricular junction without surrounding hemorrhage or mural thrombus. It was concluded that radiofrequency catheter ablation (RFCA) of the AV junction was safe and had distinct advantages compared to direct current or laser energy catheter ablation. This technique was subsequently implemented for the treatment of scar-related recurrent VA.[26] The introduction of irrigated tip catheters in conjunction with electroanatomical mapping systems has improved lesion formation and has facilitated substrate based ablation, which resulted in broadening of indications an increase use of RFCA for different types of arrhythmias.[27]

Radiofrequency catheter ablation has led to the reduction of VA episodes, and consequently to less appropriate ICD therapy, as it modifies the VA substrate.[28,29] At present, there is a I(B) indication for catheter ablation in patients with recurrent ICD shocks due to sustained scar related monomorphic VA.[1] However, long-term success is moderate, which may be partly due to substrates that cannot be fully abolished with current catheter ablation techniques.[28,30] Accordingly, in selected patients with recurrent VA refractory to anti-arrhythmic drug therapy and RFCA, surgical ablation may be still a valuable treatment option.

In contrast to VA occurring in patients with structural heart disease, monomorphic VA in the absence of structural heart disease are generally considered benign and are associated with a favorable prognosis. The most frequent presentation of these 'idiopathic' VA is premature ventricular complexes (PVC) but sustained monomorphic VTs may occur. The hemodynamic effect of frequent idiopathic VA on LV function is usually clinically nonsignificant.[31,32] Some patients however experience deterioration of LV function due to the arrhythmia. Importantly, this PVC-induced cardiomyopathy has been demonstrated to be reversible when the PVCs are eliminated.[32-35] In 1990 Morady and colleagues reported the use of catheter ablation with direct current shocks from 100-360J to successfully eliminate right ventricular outflow tract (RVOT) VA in patients without structural heart disease.[36] A few years later Klein et al demonstrated the use of RFCA to be effective and safe in a similar patient population.[37] From then on this technique developed and currently RFCA is a generally accepted and effective treatment in patients with VA causing symptoms or reduced LV function.[1]

Frequent idiopathic premature ventricular contractions

Idiopathic VA can cause severe and impeding symptoms including palpitations, (near)syncope and/or fatigue.[38-40] Approximately 10% of all patients referred for evaluation of any VA have idiopathic VA. Most commonly, idiopathic VA originate from the ventricular outflow tracts and in approximately 70% the focus is found in the RVOT.[1,41] If symptomatic or causing LV dysfunction, catheter ablation is the first choice therapy for RVOT idiopathic VA; it is associated with a high acute success rate of 95% and long-term recurrence rates look promising.[1,42-44] It is still unclear which patients with idiopathic VA are prone to develop LV dysfunction and will benefit most from catheter ablation. An observational study of patients without structural heart disease and frequent outflow tract VA reported a slight reduction in LV function after 5.6 years follow-up in 5%. Only a high PVC burden could be identified as determinant for LV dysfunction.[45] In other investigations long PVC-QRS widths, long lasting palpitations, but also the absence of symptoms have all been identified as risk factors for a reversible PVC-induced cardiomyopathy.[38,46] These parameters however were tested in comparable heterogeneous patient cohorts with already impaired LV function and none were validated in a large prospective cohort of patients. The potential relation between presenting symptoms and PVCs is difficult to determine in patients with normal LV function and non-specific complaints such as fatigue. Consequently, the potential benefit of PVC ablation in these patients is unclear. An adequate tool to identify patients who benefit from ablation is desirable.

B-type natriuretic peptide (BNP) and its precursor N-terminal-proBNP (NT-proBNP) have been used as a tool to monitor heart failure. They are synthesized in the ventricular myocardium in response to ventricular wall stress. In patients with heart failure due to LV dysfunction it has been demonstrated that a decrease in NT-proBNP value was associated with an improvement in invasively measured hemodynamic parameters.[47] Several investigations have demonstrated BNP to be elevated also in patients with frequent PVC.[33,48] Therefore, it has been suggested to use NT-proBNP as a marker for increased ventricular wall stress in patients with a preserved LV function undergoing PVC ablation for frequent PVCs. In **Chapter 2** the biomarker (NT-pro)BNP is used to analyze the hemodynamic benefit of a successful PVC ablation, independently of the presence of structural heart disease. **Chapter 3** evaluates NT-proBNP levels in idiopathic PVCs after PVC ablation thereby monitoring ventricular remodeling caused by frequent idiopathic PVC. Furthermore, the symptomatology of frequent idiopathic PVCs is analyzed and it is evaluated whether a non-specific symptom, like fatigue, is related to increased ventricular wall stress in patients without structural heart disease.

Electroanatomical mapping and local electrogram characteristics

To guide electroanatomical mapping of idiopathic focal PVC, conventional strategies are based on the earliest local activation time, a local unipolar QS-configuration and pace-mapping strategies to predict a successful ablation site.[49-54] Activation mapping is performed when the VA is hemodynamically well tolerated, like most focal idiopathic VA. At each mapping site unipolar

and bipolar electrograms can be recorded from the catheter tip electrodes and stored, allowing for the 3D reconstruction of the activation wavefront during the VA. With this approach the earliest site of activation, where the site of the focal source is located, can be identified.[49,50] Unipolar electrograms provide information about the direction of the wave front: an initial positive deflection of the unipolar electrogram indicates propagation towards the mapping catheter and has a high negative predictive value for a successful ablation site. When the electrode is located at the origin of the focal source the wave front propagates away producing a monophasic QS-configuration. However, a larger area around the focal source might produce a unipolar QS-configuration, which may therefore not be a sensitive marker for a successful ablation site.[51]

When activation mapping is not possible due to the infrequent nature of the arrhythmia pace-mapping can be used to identify the site of origin of the focal source. Pacing at any site in the ventricle results in a 12-lead surface QRS pattern specific for the ventricular activation sequence originating from that site. By comparing the paced 12-lead QRS while pacing from different sites with the spontaneous arrhythmia-QRS the site of origin can be approximated. However, the spatial resolution of a good pace-map with ≥11/12 matches has been found to be inferior to activation mapping.[53] Although these 3 criteria have demonstrated their practical value, each technique is associated with its own inherited limitations. Using the conventional mapping strategy, multiple RF applications (ranging from 3-8 in previous studies) are needed to eliminate idiopathic VA.[37,52,54,55] Radiofrequency catheter ablation may cause serious complications in up to 8% (i.e. thromboembolic, venous/arterial injury, cardiac tamponade, valve or coronary artery injury, damage to the conducting system).[1,41] Some of these complications are related to the application of RF energy. Therefore the number of RF applications should be limited, especially in patients without structural heart disease as most of these patients are young and healthy. A more accurate identification of the site of origin of the VA prior to RF ablation strategy is desirable.

The feasibility of guiding ablation by reversed polarity of adjacent bipolar electrograms has been demonstrated in pulmonary vein isolation.[56] The use of reversed polarity to guide RFCA is based on the hypothesis that rapid radial propagation from a focal source results in simultaneous deflection in opposite direction of the initial part of the bipolar electrograms. This method has not been applied to target idiopathic focal RVOT arrhythmias, but may be helpful to predict the successful ablation site more precisely. This may consequently limit the number of RF applications needed to terminate the VA. In **Chapter 4** the use of reversed polarity during ablation of idiopathic focal VA in the RVOT is examined and compared with the prior described electrogram characteristics to identify a successful ablation site.

Real-time image integration

As previously stated, electroanatomic mapping and ablation for VA is increasingly being performed and acutely highly effective in treating (scar-related) VA. However, recurrence rates

remain high and improvement of the mapping and ablation strategy is warranted. Careful patient selection is important as specific substrates require different approaches, which may be associated with serious complications.[1,41] Pre-procedural planning of the procedure is therefore of upmost importance to foresee any difficulties.[57] Cardiac multidetector computed tomography (MDCT) and/or contrast enhanced magnetic resonance imaging (CE-MRI) are modalities that can visualize the cardiac anatomy and/or give information about scar location and transmurality. Cardiac MDCT can visualize both coronary arteries and epicardial fat. CE-MRI can visualize and differentiate between endocardial, subendocardial and epicardial scar with its possible VA substrate.[57,58]

In post infarct patients most of the scar-related reentry circuits reside subendocardially and only a minority extends deep into the myocardium and even epicardially.[59] In other etiologies like arrhythmogenic cardiomyopathy and non-ischemic dilated cardiomyopathy the substrates are often located subepicardially.[60,61] In these cases endocardial catheter ablation may not be sufficient as the lesion of endocardial irrigated tip RF lesions reaches a depth of around 5.5mm and the local myocardial wall is often thicker.[62,63] Epicardial ablation is then necessary to successful target these VA. This approach is increasingly being performed, but the presence of coronary arteries and thick epicardial fat layers may impede an epicardial approach.[64,65] Thick epicardial fat can hinder the interpretation of voltages as it can exhibit reduced voltages and pace-mapping might be difficult due to a higher stimulation threshold.[66] Furthermore, ablation should be avoided in the vicinity of coronary arteries to prevent injury.[67] Especially in patients with non-ischemic cardiomyopathy, who have a substrate which is often located intramurally or at the subepicardium, this information is essential before starting ablation. **Chapters 5 and 6** further evaluate whether real-time integration of reformatted MDCT and/or CE-MRI images during electroanatomical mapping can provide complementary information during electroanatomical mapping and may help to prevent procedural complications.[57,65]

Surgical encircling cryoablation

The treatment of acute myocardial infarction has evolved over the years and survival increased tremendously after percutaneous coronary interventions have been introduced. Nevertheless, surviving patients still have an increased risk for sudden cardiac death and VA, which is even more prevalent when a LV anterior aneurysm is present.[68,69] Patients who develop heart failure are eligible for surgical ventricular reconstruction (SVR).[70] It was suggested by Di Donato and colleagues that in patients undergoing SVR hemodynamics would improve which would result in a risk reduction of VA.[71] Subsequently, the need of ICD implantation after surgery has been questioned in this patient population. However, until now VA occurrence rates after SVR have not been evaluated systematically.[13,14,72] Several studies have suggested that patients remain at high risk for VA after SVR.[69,73,74] Additional anti-arrhythmic treatment might therefore be needed. The former used surgical treatment for refractory VA, non-mapping guided encircling cryoablation, has been suggested as anti-arrhythmic therapy in patients with a history of

hemodynamic tolerated VA undergoing SVR.[14] Whether endocardial encircling cryoablation is effective to prevent VA during long-term follow-up is studied in **Chapter 7**.

A prior investigation reported a surgical endocardial cryoablation lesion depth of only 4.8mm in healthy myocardium.[75] This might not be sufficient to create a transmural lesion in the LV and thus will not electrically "isolate" the aneurysm scar from the remaining LV. Consequently, patients might still be at risk for aneurysm-related VA after SVR and endocardial cryoablation. A major concern for these patients is the possibility that the VA circuit may be located behind the patch material or in the excluded LV, where it is not amenable to endocardial catheter ablation.[76] It could be argued that combined endocardial-epicardial encircling cryoablation may generate a transmural lesion which would "isolate" the VA substrate from the remaining LV. Whether combined endo- and epicardial cryoablation results in a significant conduction delay or block over the ablation line is tested in **Chapter 8.**

Aim and outline of this thesis

Radiofrequency catheter ablation for VA is increasingly being performed in patients with and without structural heart disease, however long-term results are still disappointing. Furthermore, although overall complication rates are relatively low, remaining complications might be preventable. This reflects the urge for improvement in this field. The aim of the current thesis was to study new diagnostic tools for patient selection and novel mapping and ablation strategies for improved treatment of VA.

In **Part I,** new diagnostic tools for patient selection and treatment monitoring of patients with frequent PVCs are evaluated. In **Chapter 2** the biomarker (NT-pro)BNP is used to analyze the hemodynamic benefit of a successful PVC ablation, independently of the presence of structural heart disease. **Chapter 3** evaluates NT-proBNP levels in idiopathic PVCs after PVC ablation thereby monitoring ventricular remodeling caused by frequent idiopathic PVC. Furthermore, symptomatology of frequent idiopathic PVCs is analyzed and if a non-specific symptom like fatigue is related to increased ventricular wall stress in patients without structural heart disease.

The focus of **Part II** is on new mapping strategies to facilitate and improve VA ablation outcome. In **Chapter 4** a new PVC mapping strategy is analyzed, comparing the conventional mapping strategy which is guided by local activation time and unipolar QS-configuration, to a novel strategy guided by local activation time and the newly proposed electrocardiogram criterion of reversed polarity. The identification of an epicardial VA substrate by electroanatomic mapping and catheter ablation is limited by the presence coronary arteries and a thick epicardial fat layer. **Chapter 5** evaluates whether visualizing both, using cardiac MDCT facilitates the mapping procedure and could predict unsuccessful epicardial ablation sites. In **Chapter 6** CE-MRI and cardiac MDCT are integrated together with the 3D electroanatomical map to evaluate the effect of fat on electrogram characteristics in scar and non-scar areas. Additionally, an algorithm is developed to differentiate between scar, viable myocardium and fat during epicardial mapping.

Part III elucidates on a new strategy to treat and/or prevent VA in patients undergoing SVR. The incidence of VA after SVR has not been systematically studied. **Chapter 7** evaluates the incidence, type and timing of VAs after PES-guided EC concomitant to SVR for primary prevention of VA in ICD recipients. To enhance VA-free survival after SVR a randomized controlled trial was initiated which compared the standard used endocardial encircling cryoablation with a newly proposed therapy of combined endocardial-epicardial encircling cryoablation. This trial is discussed in **Chapter 8.** Finally, a summary and conclusions are provided in **Chapter 9.**

REFERENCES

1. Priori SG, Blomstrom-Lundqvist C, Mazzanti A, et al. 2015 ESC Guidelines for the management of patients with ventricular arrhythmias and the prevention of sudden cardiac death: The Task Force for the Management of Patients with Ventricular Arrhythmias and the Prevention of Sudden Cardiac Death of the European Society of Cardiology (ESC). Endorsed by: Association for European Paediatric and Congenital Cardiology (AEPC). *Eur Heart J*. 2015;36:2793-2867.
2. Moss AJ, Zareba W, Hall WJ, et al. Prophylactic implantation of a defibrillator in patients with myocardial infarction and reduced ejection fraction. *N Engl J Med*. 2002;346:877-883.
3. de Bakker JM, van Capelle FJ, Janse MJ, et al. Reentry as a cause of ventricular tachycardia in patients with chronic ischemic heart disease: electrophysiologic and anatomic correlation. *Circulation*. 1988;77:589-606.
4. Couch OA. Cardiac aneurysm with ventricular tachycardia and subsequent excision of aneurysm; case report. *Circulation*. 1959;20:251-253.
5. Mason JW, Stinson EB, Winkle RA, et al. Relative efficacy of blind left ventricular aneurysm resection for the treatment of recurrent ventricular tachycardia. *Am J Cardiol*. 1982;49:241-248.
6. Ecker RR, Mullins CB, Grammer JC, Rea WJ, Atkins JM. Control of intractable ventricular tachycardia by coronary revascularization. *Circulation*. 1971;44:666-670.
7. Nordstrom LA, Lillehei JP, Adicoff A, Sako Y, Gobel FL. Coronary artery surgery for recurrent ventricular arrhythmias in patients with variant angina. *Am Heart J*. 1975;89:236-241.
8. Graham AF, Miller DC, Stinson EB, et al. Surgical treatment of refractory life-threatening ventricular tachycardia. *Am J Cardiol*. 1973;32:909-912.
9. Josephson ME, Harken AH, Horowitz LN. Endocardial excision: a new surgical technique for the treatment of recurrent ventricular tachycardia. *Circulation*. 1979;60:1430-1439.
10. Horowitz LN, Harken AH, Kastor JA, Josephson ME. Ventricular resection guided by epicardial and endocardial mapping for treatment of recurrent ventricular tachycardia. *N Engl J Med*. 1980;302:589-593.
11. Harrison L, Gallagher JJ, Kasell J, et al. Cryosurgical ablation of the A-V node-His bundle: a new method for producing A-V block. *Circulation*. 1977;55:463-470.
12. Gallagher JJ. Surgical treatment of arrhythmias: current status and future directions. *Am J Cardiol*. 1978;41:1035-1044.
13. Frapier JM, Hubaut JJ, Pasquie JL, Chaptal PA. Large encircling cryoablation without mapping for ventricular tachycardia after anterior myocardial infarction: long-term outcome. *J Thorac Cardiovasc Surg*. 1998;116:578-583.
14. Guiraudon GM, Thakur RK, Klein GJ, et al. Encircling endocardial cryoablation for ventricular tachycardia after myocardial infarction: experience with 33 patients. *Am Heart J*. 1994;128:982-989.
15. Bardy GH, Lee KL, Mark DB, et al. Amiodarone or an implantable cardioverter-defibrillator for congestive heart failure. *N Engl J Med*. 2005;352:225-237.
16. Prystowsky EN, Nisam S. Prophylactic implantable cardioverter defibrillator trials: MUSTT, MADIT, and beyond. Multicenter Unsustained Tachycardia Trial. Multicenter Automatic Defibrillator Implantation Trial. *Am J Cardiol*. 2000;86:1214-5, A5.
17. Goldenberg I, Gillespie J, Moss AJ, et al. Long-term benefit of primary prevention with an implantable cardioverter-defibrillator: an extended 8-year follow-up study of the Multicenter Automatic Defibrillator Implantation Trial II. *Circulation*. 2010;122:1265-1271.

18. Buxton AE, Lee KL, Fisher JD, et al. A randomized study of the prevention of sudden death in patients with coronary artery disease. Multicenter Unsustained Tachycardia Trial Investigators. *N Engl J Med*. 1999;341:1882-1890.
19. Poole JE, Johnson GW, Hellkamp AS, et al. Prognostic importance of defibrillator shocks in patients with heart failure. *N Engl J Med*. 2008;359:1009-1017.
20. Schron EB, Exner DV, Yao Q, et al. Quality of life in the antiarrhythmics versus implantable defibrillators trial: impact of therapy and influence of adverse symptoms and defibrillator shocks. *Circulation*. 2002;105:589-594.
21. Kamphuis HC, de Leeuw JR, Derksen R, Hauer RN, Winnubst JA. Implantable cardioverter defibrillator recipients: quality of life in recipients with and without ICD shock delivery: a prospective study. *Europace*. 2003;5:381-389.
22. Gallagher JJ, Svenson RH, Kasell JH, et al. Catheter technique for closed-chest ablation of the atrioventricular conduction system. *N Engl J Med*. 1982;306:194-200.
23. Hartzler GO. Electrode catheter ablation of refractory focal ventricular tachycardia. *J Am Coll Cardiol*. 1983;2:1107-1113.
24. Borggrefe M, Breithardt G, Podczeck A, et al. Catheter ablation of ventricular tachycardia using defibrillator pulses: electrophysiological findings and long-term results. *Eur Heart J*. 1989;10:591-601.
25. Huang SK, Bharati S, Graham AR, et al. Closed chest catheter desiccation of the atrioventricular junction using radiofrequency energy--a new method of catheter ablation. *J Am Coll Cardiol*. 1987;9:349-358.
26. Morady F, Harvey M, Kalbfleisch SJ, et al. Radiofrequency catheter ablation of ventricular tachycardia in patients with coronary artery disease. *Circulation*. 1993;87:363-372.
27. Wijnmaalen AP, Zeppenfeld K. Ventricular tachycardia ablation: indications and techniques. *Minerva Cardioangiol*. 2011;59:149-169.
28. Kuck KH, Schaumann A, Eckardt L, et al. Catheter ablation of stable ventricular tachycardia before defibrillator implantation in patients with coronary heart disease (VTACH): a multicentre randomised controlled trial. *Lancet*. 2010;375:31-40.
29. Reddy VY, Reynolds MR, Neuzil P, et al. Prophylactic catheter ablation for the prevention of defibrillator therapy. *N Engl J Med*. 2007;357:2657-2665.
30. Sapp JL, Wells GA, Parkash R, et al. Ventricular Tachycardia Ablation versus Escalation of Antiarrhythmic Drugs. *N Engl J Med*. 2016;375:111-121.
31. Wijnmaalen AP, Delgado V, Schalij MJ, et al. Beneficial effects of catheter ablation on left ventricular and right ventricular function in patients with frequent premature ventricular contractions and preserved ejection fraction. *Heart*. 2010;96:1275-1280.
32. Takemoto M, Yoshimura H, Ohba Y, et al. Radiofrequency catheter ablation of premature ventricular complexes from right ventricular outflow tract improves left ventricular dilation and clinical status in patients without structural heart disease. *J Am Coll Cardiol*. 2005;45:1259-1265.
33. Sekiguchi Y, Aonuma K, Yamauchi Y, et al. Chronic hemodynamic effects after radiofrequency catheter ablation of frequent monomorphic ventricular premature beats. *J Cardiovasc Electrophysiol*. 2005;16:1057-1063.
34. Bogun F, Crawford T, Reich S, et al. Radiofrequency ablation of frequent, idiopathic premature ventricular complexes: comparison with a control group without intervention. *Heart Rhythm*. 2007;4:863-867.

35. Yarlagadda RK, Iwai S, Stein KM, et al. Reversal of cardiomyopathy in patients with repetitive monomorphic ventricular ectopy originating from the right ventricular outflow tract. *Circulation*. 2005;112:1092-1097.
36. Morady F, Kadish AH, DiCarlo L, et al. Long-term results of catheter ablation of idiopathic right ventricular tachycardia. *Circulation*. 1990;82:2093-2099.
37. Klein LS, Shih HT, Hackett FK, Zipes DP, Miles WM. Radiofrequency catheter ablation of ventricular tachycardia in patients without structural heart disease. *Circulation*. 1992;85:1666-1674.
38. Yokokawa M, Kim HM, Good E, et al. Relation of symptoms and symptom duration to premature ventricular complex-induced cardiomyopathy. *Heart Rhythm*. 2012;9:92-95.
39. Del Carpio Munoz F, Syed FF, Noheria A, et al. Characteristics of premature ventricular complexes as correlates of reduced left ventricular systolic function: study of the burden, duration, coupling interval, morphology and site of origin of PVCs. *J Cardiovasc Electrophysiol*. 2011;22:791-798.
40. Hasdemir C, Ulucan C, Yavuzgil O, et al. Tachycardia-induced cardiomyopathy in patients with idiopathic ventricular arrhythmias: the incidence, clinical and electrophysiologic characteristics, and the predictors. *J Cardiovasc Electrophysiol*. 2011;22:663-668.
41. Aliot EM, Stevenson WG, Almendral J, et al. EHRA/HRS Expert Consensus on Catheter Ablation of Ventricular Arrhythmias: developed in a partnership with the European Heart Rhythm Association (EHRA), a Registered Branch of the European Society of Cardiology (ESC), and the Heart Rhythm Society (HRS); in collaboration with the American College of Cardiology (ACC) and the American Heart Association (AHA). *Heart Rhythm*. 2009;6:886-933.
42. Borger van der Burg AE, de Groot NM, van Erven L, et al. Long-term follow-up after radiofrequency catheter ablation of ventricular tachycardia: a successful approach? *J Cardiovasc Electrophysiol*. 2002;13:417-423.
43. Chinushi M, Aizawa Y, Takahashi K, Kitazawa H, Shibata A. Radiofrequency catheter ablation for idiopathic right ventricular tachycardia with special reference to morphological variation and long-term outcome. *Heart*. 1997;78:255-261.
44. Calkins H, Kalbfleisch SJ, el-Atassi R, Langberg JJ, Morady F. Relation between efficacy of radiofrequency catheter ablation and site of origin of idiopathic ventricular tachycardia. *Am J Cardiol*. 1993;71:827-833.
45. Niwano S, Wakisaka Y, Niwano H, et al. Prognostic significance of frequent premature ventricular contractions originating from the ventricular outflow tract in patients with normal left ventricular function. *Heart*. 2009;95:1230-1237.
46. Yokokawa M, Kim HM, Good E, et al. Impact of QRS duration of frequent premature ventricular complexes on the development of cardiomyopathy. *Heart Rhythm*. 2012;9:1460-1464.
47. Knebel F, Schimke I, Pliet K, et al. NT-ProBNP in acute heart failure: correlation with invasively measured hemodynamic parameters during recompensation. *J Card Fail*. 2005;11:S38-S41.
48. Tada H, Ito S, Shinbo G, et al. Significance and utility of plasma brain natriuretic peptide concentrations in patients with idiopathic ventricular arrhythmias. *Pacing Clin Electrophysiol*. 2006;29:1395-1403.
49. Weiss C, Willems S, Rueppel R, Hoffmann M, Meinertz T. Electroanatomical Mapping (CARTO) of ectopic atrial tachycardia: impact of bipolar and unipolar local electrogram annotation for localization the focal origin. *J Interv Card Electrophysiol*. 2001;5:101-107.
50. Soejima Y, Aonuma K, Iesaka Y, Isobe M. Ventricular unipolar potential in radiofrequency catheter ablation of idiopathic non-reentrant ventricular outflow tachycardia. *Jpn Heart J*. 2004;45:749-760.

51. Barlow MA, Klein GJ, Simpson CS, et al. Unipolar electrogram characteristics predictive of successful radiofrequency catheter ablation of accessory pathways. *J Cardiovasc Electrophysiol*. 2000;11:146-154.
52. Ribbing M, Wasmer K, Monnig G, et al. Endocardial mapping of right ventricular outflow tract tachycardia using noncontact activation mapping. *J Cardiovasc Electrophysiol*. 2003;14:602-608.
53. Azegami K, Wilber DJ, Arruda M, Lin AC, Denman RA. Spatial resolution of pacemapping and activation mapping in patients with idiopathic right ventricular outflow tract tachycardia. *J Cardiovasc Electrophysiol*. 2005;16:823-829.
54. Bogun F, Taj M, Ting M, et al. Spatial resolution of pace mapping of idiopathic ventricular tachycardia/ectopy originating in the right ventricular outflow tract. *Heart Rhythm*. 2008;5:339-344.
55. Peeters HA, Sippens Groenewegen A, Wever EF, et al. Clinical application of an integrated 3-phase mapping technique for localization of the site of origin of idiopathic ventricular tachycardia. *Circulation*. 1999;99:1300-1311.
56. Yamane T, Shah DC, Jais P, et al. Electrogram polarity reversal as an additional indicator of breakthroughs from the left atrium to the pulmonary veins. *J Am Coll Cardiol*. 2002;39:1337-1344.
57. Wijnmaalen AP, van der Geest RJ, van Huls van Taxis CF, et al. Head-to-head comparison of contrast-enhanced magnetic resonance imaging and electroanatomical voltage mapping to assess post-infarct scar characteristics in patients with ventricular tachycardias: real-time image integration and reversed registration. *Eur Heart J*. 2011;32:104-114.
58. Heidary S, Patel H, Chung J, et al. Quantitative tissue characterization of infarct core and border zone in patients with ischemic cardiomyopathy by magnetic resonance is associated with future cardiovascular events. *J Am Coll Cardiol*. 2010;55:2762-2768.
59. Kaltenbrunner W, Cardinal R, Dubuc M, et al. Epicardial and endocardial mapping of ventricular tachycardia in patients with myocardial infarction. Is the origin of the tachycardia always subendocardially localized? *Circulation*. 1991;84:1058-1071.
60. Cano O, Hutchinson M, Lin D, et al. Electroanatomic substrate and ablation outcome for suspected epicardial ventricular tachycardia in left ventricular nonischemic cardiomyopathy. *J Am Coll Cardiol*. 2009;54:799-808.
61. Garcia FC, Bazan V, Zado ES, Ren JF, Marchlinski FE. Epicardial substrate and outcome with epicardial ablation of ventricular tachycardia in arrhythmogenic right ventricular cardiomyopathy/dysplasia. *Circulation*. 2009;120:366-375.
62. Wood MA, Goldberg SM, Parvez B, et al. Effect of electrode orientation on lesion sizes produced by irrigated radiofrequency ablation catheters. *J Cardiovasc Electrophysiol*. 2009;20:1262-1268.
63. Callans DJ, Ren JF, Narula N, et al. Effects of linear, irrigated-tip radiofrequency ablation in porcine healed anterior infarction. *J Cardiovasc Electrophysiol*. 2001;12:1037-1042.
64. Sacher F, Roberts-Thomson K, Maury P, et al. Epicardial ventricular tachycardia ablation a multicenter safety study. *J Am Coll Cardiol*. 2010;55:2366-2372.
65. Zeppenfeld K, Tops LF, Bax JJ, Schalij MJ. Images in cardiovascular medicine. Epicardial radiofrequency catheter ablation of ventricular tachycardia in the vicinity of coronary arteries is facilitated by fusion of 3-dimensional electroanatomical mapping with multislice computed tomography. *Circulation*. 2006;114:e51-e52.
66. d'Avila A. Epicardial catheter ablation of ventricular tachycardia. *Heart Rhythm*. 2008;5:S73-S75.
67. d'Avila A, Gutierrez P, Scanavacca M, et al. Effects of radiofrequency pulses delivered in the vicinity of the coronary arteries: implications for nonsurgical transthoracic epicardial catheter ablation to treat ventricular tachycardia. *Pacing Clin Electrophysiol*. 2002;25:1488-1495.

68. Di Donato M., Sabatier M, Menicanti L, Dor V. Incidence of ventricular arrhythmias after left ventricular reconstructive surgery. *J Thorac Cardiovasc Surg*. 2007;133:289-291.
69. Klein P, Bax JJ, Shaw LJ, et al. Early and late outcome of left ventricular reconstruction surgery in ischemic heart disease. *Eur J Cardiothorac Surg*. 2008;34:1149-1157.
70. Dor V, Saab M, Coste P, Kornaszewska M, Montiglio F. Left ventricular aneurysm: a new surgical approach. *Thorac Cardiovasc Surg*. 1989;37:11-19.
71. Di Donato M, Sabatier M, Dor V, Buckberg G. Ventricular arrhythmias after LV remodelling: surgical ventricular restoration or ICD? *Heart Fail Rev*. 2004;9:299-306.
72. Demaria RG, Mukaddirov M, Rouviere P, et al. Long-term outcomes after cryoablation for ventricular tachycardia during surgical treatment of anterior ventricular aneurysms. *Pacing Clin Electrophysiol*. 2005;28 Suppl 1:S168-S171.
73. Di Donato M, Sabatier M, Menicanti L, Dor V. Incidence of ventricular arrhythmias after left ventricular reconstructive surgery. *J Thorac Cardiovasc Surg*. 2007;133:289-291.
74. O'Neill JO, Starling RC, Khaykin Y, et al. Residual high incidence of ventricular arrhythmias after left ventricular reconstructive surgery. *J Thorac Cardiovasc Surg*. 2005;130:1250-1256.
75. d'Avila A, Aryana A, Thiagalingam A, et al. Focal and linear endocardial and epicardial catheter-based cryoablation of normal and infarcted ventricular tissue. *Pacing Clin Electrophysiol*. 2008;31:1322-1331.
76. Wijnmaalen AP, Roberts-Thomson KC, Steven D, et al. Catheter ablation of ventricular tachycardia after left ventricular reconstructive surgery for ischemic cardiomyopathy. *Heart Rhythm*. 2012;9:10-17.

Part I

New Developments in Radiofrequency Catheter Ablation of Idiopathic Ventricular Arrhythmias

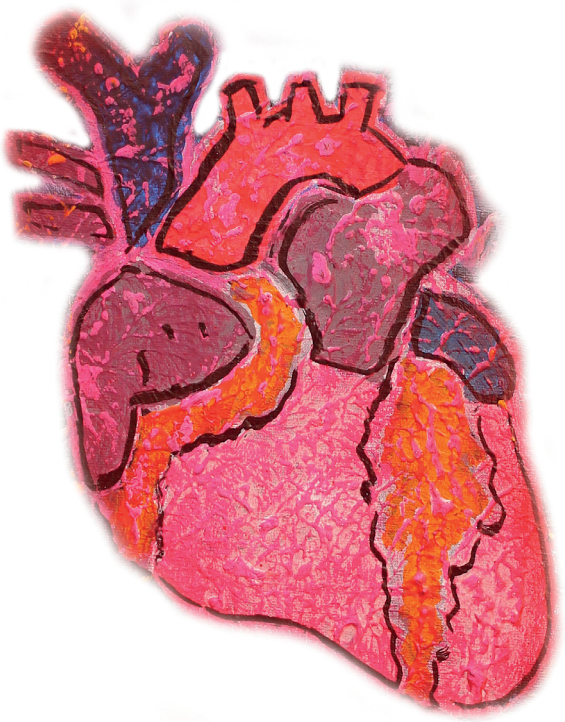

Chapter 2

The Neurohormonal, Structural and Functional Recovery Pattern after PVC Ablation is Independent of Structural Heart Disease Status in Patients with Depressed Left Ventricular Ejection Fraction; A Prospective Multicentre Study

Diego Penela[1], Carine van Huls van Taxis[2], Luis Aguinaga[3], Juan Fernández-Armenta[1], Lluis Mont[1], Maria Angels Castel[1], Jose María Tolosana[1], Marta Sitges[1], Augusto Ordóñez[4], Josep Brugada[1], Katja Zeppenfeld[2], Antonio Berruezo[1]

[1] Cardiology Department, Hospital Clínic and IDIBAPS (Institut d'Investigació Agustí Pi i Sunyer), Barcelona, Spain

[2] Department of Cardiology, Leiden University Medical Center, Leiden, The Netherlands.

[3] Private Cardiology Center, Tucuman, Argentina

[4] Cardiology Department, Hospital Sant Pau I Santa Tecla, Tarragona, Spain.

Journal of American College of Cardiology. 2013;62:1195-1202

ABSTRACT

Background

Ablation of premature ventricular complexes (PVC) in patients with left ventricular (LV) dysfunction is usually restricted to patients with suspected PVC-induced cardiomyopathy. To assess the benefit after PVC ablation in unselected patients with frequent PVC and LV dysfunction, regardless of the previous diagnosis of structural heart disease (SHD).

Methods

Consecutive patients with frequent PVC and LV dysfunction accepted for ablation at 4 centres were prospectively included. Eighty patients were included, 27 (34%) of them had a diagnosis of SHD.

Results

Successful sustained ablation (SSA) was achieved in 53 (66%) patients and their LV ejection fraction improved from 33.7±8% to 43.8±9.4% and 45.8±10.9% at 6 and 12 months, respectively ($p<0.05$), without differences related to previous diagnosis of SHD ($p=0.69$). BNP decreased from 140±115pg/mL to 64±76pg/mL, 41±48pg/mL and 40±51pg/mL at 1, 6 and 12 months, respectively ($p<0.05$). NYHA class improved from 2±0.7 to 1.69±0.5, 1.3±0.3 and 1.1±0.3 at 1, 6 and 12 months, respectively ($p <0.05$). A 13% baseline PVC burden had a 100% sensitivity and 85% specificity to predict an absolute increase ≥5% in LVEF after SSA. Twenty patients with >13% PVC and SSA had class I indication for cardioverter defibrillator implantation. All of them had no such indication 6 months post-ablation.

Conclusions

Independently of the presence of SHD, the SSA of frequent PVC in patients with depressed LVEF induced a progressive clinical and functional improvement. The improvement in heart failure parameters was related to the baseline PVC burden and the persistence of acute ablation success.

INTRODUCTION

There is increasing interest in identifying patients with frequent premature ventricular complexes (PVC) and left ventricular (LV) dysfunction who may benefit from catheter ablation. Small, single-centre observational studies have reported that radiofrequency catheter ablation (RFCA) of PVC can improve left ventricular ejection fraction (LVEF) in patients with a suspected PVC-induced cardiomyopathy.[1-6] The ablation of frequent PVC in a small series of 15 patients with ischemic heart disease (IHD) improved LVEF in comparison with a control group of patients without ablation.[7] Similarly, RFCA of PVC improved LVEF and NYHA class in non-responders to cardiac resynchronization therapy.[8] However, the relationship between the degree of clinical benefit and a diagnosis of SHD has not been studied. Moreover, patients with suspected PVC-induced cardiomyophathy are followed for 3 to 6 months after RFCA in most studies; the temporal pattern of improvement after ablation of frequent PVC has not been studied in depth.[9]

The aim of the study was to assess the clinical benefit and temporal recovery pattern after ablation of frequent PVC in an unselected group of consecutive patients with LV dysfunction, regardless of the PVC origin and SHD presence or etiology.

METHODS

This multicentre, prospective, observational study was conducted from February 2010 to January 2012. A total of 80 consecutive patients with LV dysfunction (defined as LVEF ≤50%) of any etiology and frequent and/or symptomatic PVC accepted for RFCA were included at four participating centers. Frequent PVC was defined as a burden of more than 4% at baseline 24-hour-Holter monitoring, which is the lowest reported PVC burden associated with tachycardiomyopathy in the literature.[10] No patient was excluded because of the number of PVC morphologies or the presumed site of origin (SOO) based on electrocardiographic (ECG) criteria.

Baseline evaluation

A detailed medical and drug history and a blood test, including neurohormonal evaluation (brain natriuretic peptide [BNP] in 3 centres and N-terminal pro brain natriuretic peptide [NT-proBNP in 1 center]) were obtained for all participants. All patients had a 12-lead surface ECG and Holter monitoring prior to the ablation procedure to evaluate the presence of multiple morphologies and to calculate the PVC burden. Baseline echocardiography was performed within the 4 months preceding the RFCA procedure. LVEF was calculated by the Simpson formula (i.e., 3 consecutive beats averaged to minimize measure distorsion generated by PVC). When logistically possible and in the absence of contraindication, a contrast-enhanced cardiac magnetic resonance (ce-MRI) was obtained and analysed to determine the presence of myocardial scar. Acquisition and post-processing methods are descrived in the online appendix.[11]

Ablation procedure

Before the ablation, antiarrhythmic drugs except amiodarone were withdrawn 5 half-lives. Ablation was guided by the CARTO navigation system (Biosense-Webster, Waterloo, Belgium). Intravenous infusion of isoproterenol was used if the patients had no spontaneous PVC at baseline. All PVC morphologies thought to contribute to the LV dysfunction, based on ≥4% burden in Holter monitoring and the operator's clinical judgement during the procedure, were targeted for ablation. A 3.5-mm tip, irrigated catheter (Navi-Star, Biosense Webster) was used for mapping and ablation. Radiofrequency application was guided by activation mapping in 44 patients, pace mapping in 2 patients and a combination of both techniques in 34 patients. Acute successful ablation was considered when targeted PVC were eliminated and were non-inducible after isoproterenol infusion. Patients were monitored for 30 minutes after the procedure to ensure complete PVC abolition. Programmed stimulation to induce ventricular arrhythmias was not part of the study protocol and was only performed in selected patients, at the operator's discretion. In case of acute successful ablation, amiodarone was discontinued. As the entire population of the study had LV dysfunction, therapy with beta-blocker (90%) and angiuotensin-converting enzyme inhibitor was maintained independently of the ablation success.

Follow-up

Patients were attended at an outpatient clinic. Scheduled visits at 1, 6 and 12 months post ablation included evaluation of functional class and a blood test with BNP determination. In one center NT-proBNP was obtained at 3 months.

A 24-hour Holter ECG was obtained at 6 and 12 months. Successful sustained ablation (SSA) was defined as the persistent elimination of at least 80% of PVC after a first ablation procedure with no recurrences after 12 months of follow-up. Echocardiography was repeated at 6 and 12 months. Echocardiographic response was defined as an absolute increase in LVEF of ≥5% after RFCA, as in clinical trials on CRT implantation and previous PVC ablation series.[10,12]

Statistical analysis

Continuous variables are presented as the mean value ± SD. BNP and NT-proBNP are presented as median and interquartile range due to their skewed distribution. Categorical variables are presented as total number and percentages. To compare means of 2 variables, Student *t* test was used (or Wilcoxon when necessary). Proportions were compared using Chi-squared or Fisher exact test as appropriate. Friedman analysis of variance by ranks was used for repeated measures. Logistic regression analysis was used to study the effects of baseline characteristics in predicting echocardiographic response, acute successful ablation and SSA. A P-value <0.10 was used to screen covariates for inclusion in the multivariate analysis model. A backward stepwise selection algorithm was applied to select covariates for inclusion in the multivariate regression model. At each step, the least significant variable was discarded from the model. Odds ratio (OR) and 95% confidence interval (CI) were calculated. Receiver operating curve (ROC) analysis

was used to evaluate the optimal cut-off value for predicting echocardiographic response. A P-value of <0.05 was considered statistically significant. Statistical analysis was performed using R software for Windows version 2.15.0 (R project for statistical computing, Vienna, Austria).

RESULTS

Eighty consecutive unselected patients (47 men, mean age 53±12 years) were included. Follow-up was not avaliable for 3 patients because of 1 non-cardiac death, 1 change of residence and 1 recent diagnosis of disabling neurological disease. Mean LVEF was 34.3±13%, with 22±13% mean PVC burden in the Holter monitoring (Table 1). Before the ablation, an attempt to suppress PVC was ineffective with beta-blocker in 56 patients, amiodarone in 1 patient and a combination of both in 16 patients.

Table 1. Baseline characteristics

	No SHD (n=53)	SHD (n=27)	All patients (n=80)	P-value
Age (years)	51.5±11.7	56.6±11.4	53±11.8	0.065
Gender (male)	25 (47%)	22 (82%)	47 (59%)	0.003
LVEF (%)	34.7±7.8	33.5±8.9	34.3±13	0.54
LVESD (mm)	44.5±6.8	45.7±7	44.9±6.9	0.48
LVEDD (mm)	59.3±6	61±6.9	59.9±6.3	0.21
Treatment (%)				
Beta-blocker	92	85	90	0.32
ACEI	81	85	83	0.66
Spironolactone	53	30	51	0.005
Amiodarone	23	19	21	0.67
PVC Holter				
%	18±12	29.8±13	22±13	<0.001
number/24h	17237±11109	27154±16971	20326±13863	0.009
NYHA				0.19
I	12 (23%)	9 (33%)	21 (26%)	
II	31 (58%)	10 (37%)	41 (51%)	
III	10 (19%)	8 (30%)	18 (23%)	
IV	0	0	0	
Hyperenhancement (%)	5.7%	33%	15%	<0.001
BNP, pg/mL	216±268	165±135	188±201	0.54
NT-proBNP, pg/mL	351±383 (n=10)	846±1033 (n=7)	536±711 (n=17)	0.19

ACEI: angiotensin-converting enzyme inhibitor; BNP: brain natriuretic peptide; LVEF: left ventricular ejection fraction; LVESD: left ventricular end-systolic diameter; LVEDD: left ventricular end-diastolic diameter; NT-proBNP: N-terminal pro brain natriuretic peptide; NYHA: New York Heart Association; PVC: premature ventricular complex; SHD: structural heart disease

Dyspnoe and palpitations were the dominant presentating symptom in 58 (74%) and 38 (48%) patients, respectively. Only 12 (15%) patients were asymptomatic at the time of ablation. Five patients with SHD had an implantable cardioverter-defibrillator (ICD) for secondary prevention at the time of ablation, 3 of them due to spontaneous sustained VT and 2 benause of syncope. Two patients had a pacemaker because of prior atrioventricular block. In all patients without previously diagnosed SHD, IHD was ruled out by coronary angiography or non-invasive stress test before the ablation procedure.

Twenty-seven patients (34%) had previously diagnosed SHD. Seventeen had IHD, 2 valvular heart disease, 4 non-compaction cardiomyopathy, and 1 case each of hypertensive cardiomyopathy, peripartum puerperal cardiomyopathy, tetralogy of Fallot and arrhythmogenic right and left ventricular dysplasia (Table 1). Most patients with previously diagnosed SHD had received that diagnosis before they were considered for PVC ablation, except 2 patients with noncompaction cardiomyopathy in whom the final diagnosis was established by the pre-procedural ce-CMR. Ten of the 17 (59%) ischemic patients had significant coronary artery disease and prior revascularization without myocardial infarction.

In total, 96 PVCs were targeted for RFCA. Twenty (25% patients had more than one PVC morphology in the baseline Holter monitoring. In 9 of them (4 ischemic and 5 without SHD), at least 2 different PVC morphologies were targeted for ablation; only the “dominant” PVC was targeted in the remaining 11 patients. Table 2 shows the SOO of targeted PVCs.

Acute successful ablation was achieved in 68 patients (85%). Complications occurred in 4 (5%) patients: 1 uncomplicated hematoma in the puncture site, 1 episode of pericarditis, 1 pulmonary thromboembolism and 1 episode of periprocedural tamponade resolved without further complications.

Follow-up

Mean follow-up was 11.2±2.4 months. PVC recurred in 15 of 68 patients (22%) with acute successful ablation, in 14 (93%) of them within 6 months. Therefore, SSA was achieved in 53 patients (66%).

Echocardiographic response

In patients with SSA, LVEF improved from 33.7±8% at baseline to 43.8±9.4% and 45.8±10.9 % at 6 and 12 months, respectively ($p<0.05$). Interestingly, most (84±39%) of the benefit was obtained in the first 6 months (Figure 1). Accordingly, left ventricular end diastolic diameter (LVEDD) decreased from 59.5±5.9mm to 56.3±5.3mm at 6 months and 54.9±6.1mm at 12 months ($p<0.05$). Left ventricular end systolic diameter (LVESD) decreased from 44.4±6.2mm to 39.9±5.3mm and 39 ±6.9mm at 6 and 12 months, respectively ($p<0.05$).

There was a close relationship between the percentage of PVC at baseline and the echocardiographic response (Figure 2). When SSA was achieved, a baseline PVC burden ≥13% had a sensitivity of 100% and a specificity of 85% (area under the curve 0.87 [CI 0.72-1]) to predict an

Table 2. Site of origin of the 96 PVCs targeted for ablation and the Number Involving Patients [SHD]

Left ventricle	Right ventricle	Epicardium
Outflow tract:	**Outflow tract:**	**Left ventricle summit:**
8 left coronary sinus of Valsalva [2]	24 septal [2]	5 [2]
8 right coronary sinus of valsalva [1]	15 lateral [2]	
3 subvalvular [2]		
Infarct scars:	**Parahisian:**	**Cardiac venous system:**
8 septal [8]	2 [1]	6 [2]
3 apical [3]		
3 lateral [3]		
Papillary muscle:	**Tricuspid annulus:**	**Epicardial scar:**
5 [5]	2 [0]	1 [1]
Mitral annulus:		**Right coronary sulcus groove:**
2 [2]		1 [1]

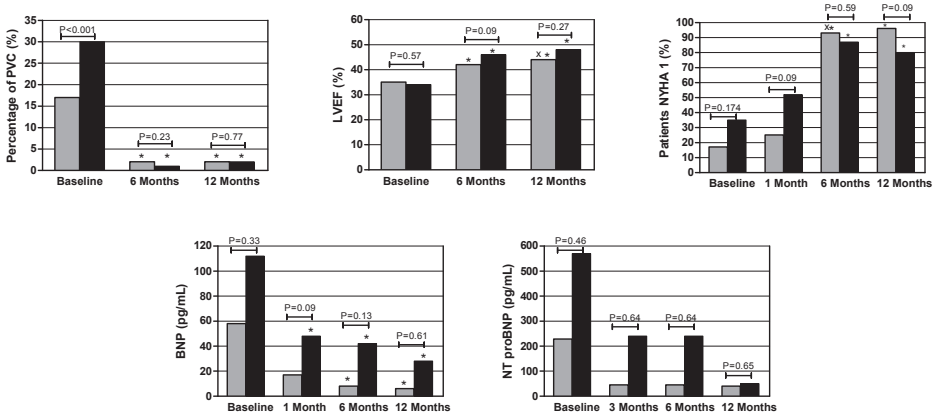

Figuur 1. Recovery pattern after radiofrequency ablation in patients with and without previously diagnosed SHD and with SSA.

The temporal recovery pattern of brain natriuretic peptide (BNP)/N-terminal pro brain natriuretic peptide (NT-proBNP) levels, left ventricular ejection fraction (LVEF), New York Heart Association (NYHA) functional class, and the reduction in premature ventricular complex (PVC) burden is shown. There were no significant differences at baseline except for the PVC burden. Most of the benefit was obtained in the first 6 months. Grey bars = no SHD; black bars = SHD. *p < 0.05 versus baseline. ^{x}p< 0.05 versus previous value during follow-up. SHD = structural heart disease; SSA = sustained successful ablation.

absolute increase of at least 5% of LVEF. Echocardiographic respons was observed in 88.3% of patients with ≥13% PVC and SSA. In these patients LVEF improved from 32.6±8.7% at baseline to 48.8±7.2% and 51.9±7.1% at 6 and 12 months, respectively (p<0.05) No patients with <13% PVC at baseline improved after ablation.

At baseline, 29 patients (36%) with ≥13% PVCs met the indication criteria for primary prevention ICD implantation.[13] In 20 patients (69%) SSA was achieved and at 6 months post-ablation none of whom had any ICD indication. In 5 addiditional patients, the PVC burden was

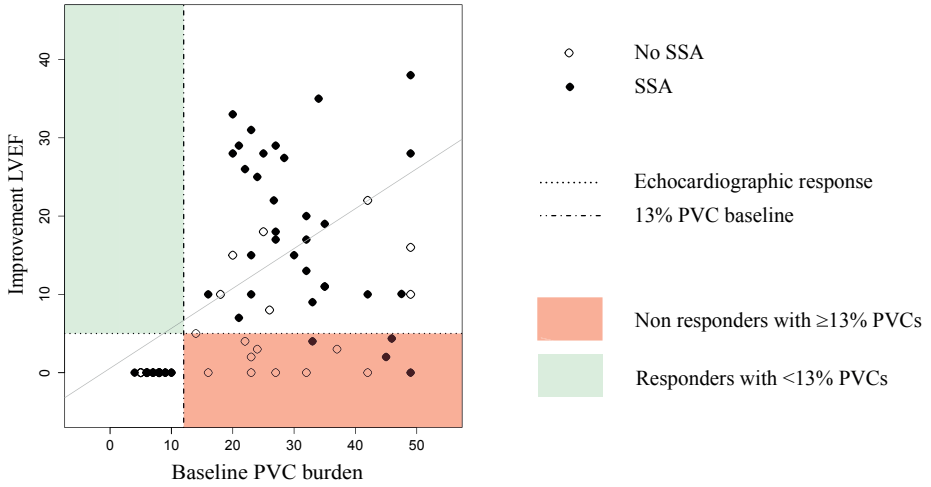

Figuur 2. Relationship between the percentage of PVCs at baseline Holter monitoring and left ventricular ejection fraction improvement during follow-up.
SSA: Successful sustained ablation. Other abbreviations as in Table 1.

reduced between 50-80% from baseline, LVEF improced and there were no indications for ICD implant at 6 months (n=3) and 12 months (n=2). Of the remaining 4 patients, 3 received an ICD and the fourth did not because of comorbidity criteria. No sudden death or life-threatening ventricular tachycardias occurred during the entire follow-up.

Neurohormonal response

In patients with SSA, there was a significant reduction in BNP levels from 109 (64 to 242)pg/mL at baseline to 60 (25 to 170)pg/mL, 50 (14 to 130)pg/mL, and 60 (19 to 81) pg/mL at 1, 6 and 12 months, respectively (p=0.004). NT-proBNP levels showed the same reduction pattern over time from 259 (90-907) pg/mL to 53 (29 to 337)pg/mL, 50 (28 to 330)pg/mL and 49 (29 to 708) pg/mL at 1, 6 and 12 months, respectively (n=17, p= 0.112) (Figure 1). Notebly, most of the reduction was obtained in the first month.

Clinical response

In patients with SSA, NYHA class improved during follow-up from only 12 patients (23%) with NYHA I at baseline to 15 (28%), 42 (79%) and 42 (79%) at 1, 6 and 12 months, respectively (p<0.001). Improvement in LVEF was directly related to the termporal pattern of functional recovery.

Ce-CMR

A ce-CMR study was available for 59 patients. Hyperenhancement was present in 11 (19%) of them. Eight (66%) of the 12 ischemic patients in whom a ce-CMR was available had hy-

perenhancement in the ce-CMR study. In patients with hyperenhancement, the mean scar mass was 9.23±8.4 grams. There was no significant difference in echocardiographic response rate between patients with or without hyperenhancement (LVEF improvement 12±7.6% and 9.6±12.3% respectively; p=0.56). Patients with hyperenhancement had a greater baseline PVC burden (30±13.7% versus 17.5±10.7%; p=0.001) and a greater absolute reduction of PVC percentage after SSA (29.8±11.9% versus 15.5±10.6%; p=0.003). Interestingly, the SOO was not related to the hyperenhancement areas in 7 (54%) of the 13 PVCs ablated in patients with scar in the ce-CMR.

Previously diagnosed SHD

There is an association between previously diagnosed SHD and LV origin (78% of the patients with previously diagnosed SHD had a LV site of PVC origin versus 26% in patients without; p<0.001). In patients with previously diagnosed SHD, the PVC burden was significantly higher at baseline (Figure 1) and the reduction of PVC after ablation more pronounced as compared to patients without SHD (absolute reduction of PVC percentage: 16±11% in patients without SHD, 28±13% in patients with SHD, p= 0.002). There was no difference in echocardiographic response between patients with known SHD and idiopathic LV dysfunction (mean absolute LVEF improvement during follow-up 13.5±11.8% vs 12±13%, respectively; p=0.691). Accordingly, there was no difference in neurohormonal response (mean improvement in BNP levels: 56 [5 to 143] pg/mL without SHD vs 87 [33 to 130] pg/mL SHD, p=0.79; mean improvement en NT-proBNP levels: 63 [36 to 240] pg/mL without SHD vs 183 [117 to 340] pg/mL SHD; p=0.655) or in clinical improvement during follow-up after SSA (Symptomatic patients with a decreae of at least 1 cotegory of NYHA class during follow-up; 27 (96%) without SHD versus 9 (90%) with SHD; p= 0.462).

Unsuccessful ablation

In 27 patients (34%) SSA was not achieved; the ablation attempt was unsuccessful in 12 patients (15%) and PVC recurred during follow-up in 15 (19%) additional patients. Recurrent PVC was different than that previously ablated in 2 patients (17%) wihtout SHD and in 2 patients (67%) with SHD.

Patients without SSA showed less improvement in LVEF, rate of clinical response and BNP/NT-proBNP reduction (Table 3). However, 7 patients with no SSA were clinical responders (Figure 2). In 5 of these patients, PVC recurred but the PVC burden was decreased by 50-80%. In the other two patients PVC elimination was obtained with antiarrhythmic drugs. In 4 patietns, a second ablation procedure was performed and 2 of them recurred.

Patients without SSA more frequently had nonsustained VT during follow-up Holter monitoring (48% vs 11%; p=0.001), although none of the patients had lifethreatening arrhythmias. Age, more than 1 PVC morphology at baseline, and epicardla origin were associated with failure to achieve SSA. In the multivariate analysis, only epicardial origin indepentently predicted fail-

Table 3. Echocardiographic response in patients according to baseline PVC burden on 24h-Holter-monitoring.

	No successful sustained ablation	Successful sustained ablation
≥13% PVC	N= 18 Responders: 38.8% Improvement LVEF: 6.8 ± 7.2%	N= 33 Responders: 88.3% Improvement LVEF: 18.4 ± 10.3%
<13% PVC	N= 8 Responders: 0 % Improvement LVEF: 1.1±3.1%	N=18 Responders: 0% Improvement LVEF: 0.67±2.7%

Abbreviations as in Table 1

ure in achieving SSA (OR 4.2; 95% CI 1.1 to 16,4; p=0.042). Age, more than 1 PVC morphology at baseline, and epicardial origin were associated with a failure to achieve acute ablation success. Only epicardial origin (OR 6.9; 95% CI 1.46 to 33.3; p=0.015) and the presence of more than 1 PVC morphology in the baseline Holter monitoring (OR 6.2; 95% CI 1.3 to 29.8; p=0.022) were independent predictors in the multivariate analysis.

Predictors of echocardiographic response

Table 4 shows the uni- and multivariate analysis for the prediction of echocardiographic response. Only SSA and baseline PVC percentage predicted response. The other variables analysed were suspected SOO (right vs left), epicardial origin, QRS width, SHD etiology and scar size in the ce-CMR. In addition, neither the epicardial origin (3 [9%] in responders versus 1 [5%] in nonresponders p=0.97) nor the QRS width (170±19ms in responders vs 175±19ms in nonresponders; p=0.41) were associated with the echocardiographic response in the subgroup of patients with SSA.

Table 4. Echocardiographic, neurohormonal and clinical response after ablation in patients with and without successful sustained ablation.

	Successful sustained ablation (n=53)	No successful sustained ablation (n=27)	P-value
LVEF improvement after RFCA (%)	12.6±12.4	5.1±6.7	0.007*
BNP reduction after RFCA (pg/mL)	-78±83	-21±116	0.16
NT-proBNP reduction after RFCA (pg/mL)	-272±374	+21±329	0.15
Mean NYHA functional class improvement after RFCA	1.1±0.53	0.67±0.59	0.008*

RFCA: radiofrequency catheter ablation; other abbreviations as in Table 1

Table 5. Predictors of echocardiographic response, uni- and multivariate Cox proportional hazards models.

	Response	No response	Univariate		Multivariate	
			OR (95% CI)	P-value	OR (95% CI)	P-value
Sex (male)	71.4%	42.8%	3.33 (1.29-8.92)	0.01		
Age	53.7 ± 12.3	52.6 ± 11.4	1.01 (0.97-1.05)	0.67		
Baseline PVC burden	29 ± 9.7	15.4 ± 13	1.11 (1.05-1.17)	<0.001	1.12 (1.06-1.18)	<0.001
QRS Width	170 ± 19	174 ± 18	0.99 (0.96-1.01)	0.33		
Location LV	44.7%	81.8%	1.02 (0.45-2.81)	0.81		
Location epicardial	20%	11.4%	1.68 (0.51-5.63)	0.4		
SSA	76.2%	57.1%	2.4 (0.9-6.4)	0.08	3.82 (1.09-13.32)	0.036
SHD	40.5%	28.6%	1.7 (0.65-4.43)	0.28		

Values are % or mean±SD. OR = odds ratio; other abbreviations as in Table 1 and 2

DISCUSSION

The present study describes the neurohormonal, echocardiographic and clinical benefit and the recovery pattern of consecutive patients with depressed LVEF and frequent PVCs submitted for ablation, regardless of the presence of previously diagnosed SHD. This is also the first series to describe in depth the influence of PVC recurrences in outcomes and its timing, 93% of recurrences occurring in the first 6 months. The ablation complexity of some PVCs, depending of SOO, probably explain why SSA was achieved in only two-thirds of patients, along with a perhaps higher recurrence rate in an unselected patient population with a large prportion of patients havind epicardial PVCs. As a similar benefit was obtained irrespective of known SHD, the distinction between a "PVC-induced" cardiomyopathy or a "PVC-worsened" cardiomyopathy seems not to be essential to select patients for PVC ablation. In contrast, a higher baseline PVC burden was associated with neurohormonal, echocardiographic and clinical benefit and may be used to select patients. An important finding of the study is the consistent temporal pattern of improvement for all heart failure parameters; an early improvement of BNP/NT-proBNP levels, functional class and LVEF was observed and persisted after 6 months of follow-up.

PVC-induced or PVC-worsened cardiomyopathy

Although there are several reports of reversible cardiomyopathy after PVC ablation in patients with frequent PVC,[1-8] most studies have included only patients with suspected PVC-induced cardiomyopathy; patients with known SHD have been systematically excluded. The present study was the first to assess PVC ablation outcomes in unselected patients with frequent PVCs and depressed LVEF. The findings are clinically important because PVCs are frequently observed in patients with SHD[14] and because a reversible "PVC-worsened" cardiomyopathy is a concept not yet deeply described and widely accepted. As result many of these patients are actually not considered candidates for RFCA. The present study suggests that they should be.

The improvement in LVEF observed in both groups, with and without known SHD, is comparable to that reported in previous studies[3,4] in selected patients with PVC-induced cardiomyopathy. One third of patients had previously diagnosed SHD and their LVEF improvement did not differ from that of patients with suspected PVC-induced cardiomyopathy. That finding is consistent with a report of significant LVEF improvement after ablation of frequent PVC in a series of 15 patients with previous myocardial infarction.[7] The authors suggested that the depressed LV function is at least partly due to a reversible cardiomyopathy in patients with more than 5% PVC at baseline, despite the presence of scar tissue. The present results support this hypothesis in a more heterogeneous group of patients with heart diseases of different etiologies. Interestingly, patients with previously diagnosed SHD as well as patients with hyper-enhancement in the CMR study had a signifiantly higher PVC burden at baseline and a greater reduction of PVC percentage after SSA. This phenomonon could be explained in part by referral bias (i.e. patients without a diagnosis of SHD are likely referred earlier for PVC treatment). As PVC burden is an independent predictor of response after ablation, this finding may explain a similar benefit after PVC ablation in patients with and without SHD as well as the lack of influence of the amount of scar in the response. On the other hand, the small percentage of patients with myocardial scar is in accordance with a previous report by Sarrazin et al[7] in which patients with myicardial infarction and frequent PVC had a smaller scar area in the ce-CMR than patients without PVC with similar LVEF. This finding suggest that a component of PVC-worsened LV dysfunction is present. Further studies with a higher number of patients having scar on ce-CMR are needed to establish its influence on response after frequent PVC ablation.

Predictors of response

In the present study baseline PVC percentage predicted response to RFCA. The PVC burden necessary to induce or worsen LV dysfunction is not clearly defined. A burden as low as 4% was found to be associated with cardiomyopathy.[10] However, the majority of patients with PVC-induced cardiomyopathy who improved after ablation had more than 10% PVC at baseline in another study.[15] In the present study, the optimal cutoff value in patients accepted for ablation was ≥13% PVCs at baseline to predict LVEF improvement of at least 5%. Importantly, no patient with less than 13% baseline PVCs improved after ablation. This is in line with the study of Baman et al,[15] who reported that the lowest PVC burden resulting in a reversible cardiomyopathy was 10% in patients with PVC-induced cardiomyopathy.

Previous studies showed that an epicardial PVC origin as well as the QRS width of the PVC were predictors of a reversible PVC-induced cardiomyopathy.[16] In the present study neither right versus left SOO, nor epicardial origin, nor QRS width were independent predictors of response. Although the SOO (epicardial origin) was associated to a lower rate of SSA, only the SSA was an independent predictor of response, suggesting that the lack of PVC burden reduction is the main variable to be taken into account, rather than the SOO. Therefore repeated Holter

monitoring could be reccomended to check for SSA and correctly interpret the response after ablation. Notebly, any recurrences are most likely to occur in the 6 months period.

Finally, despite ablation of only the "dominant" PVC in 11 of the 20 patients with multiple morphologies at baseline, this was not an independent predictor of SSA. This observation suggest that the elimination of all PVC morphologies may not be necessary.

ICD implantation

As a consequence of the improvement in heart failure parameters and the increase in LVEF, all patients with ≥13% baseline PVC burden meeting the indication criteria for primary prevention ICD implantation prior to RFCA, had no such indication 6 months after ablation. No sudden deaths or life-threatening ventricular arrhythmias occurred in these patients during the 6 months waiting period for re-evaluation nor during the entire follow-up. In view of these results, and taking into account that the 84±39% of the LVEF improvement was observed in the first 6 months after ablation, the 6 months re-evaluation interval after successful ablation seems to be a safe aproach. Whether an early evaluation for the presence of PVC recurrences should be done remains to be answered. Larger studies are needed to determine the length of the period for which ICD implantation can be withheld safely.

Study limitations

The main limitation of this study is the absence of a control group. A 24-h Holter monitoring may be insufficient to assess the exact PVC burden before and after ablation, due to the day-to-day variability of ectopy. Use of antiarrhythmic drugs in patients without acute successful ablation may affect the interpretation of the results, although only 2 patients reached ≥80% reduction of baseline PVC burden. The electrophysiological mechanism of ventricular arrhythmia was not systematically studied, but could influence the ablation strategy and recurrences if the PVC were related to scarring. Finally, although the presence of scar seems not to be essential in selecting patients for PVC ablation, it might influence the degree of reverse remodelling. We cannot exclude the possibility that LV dysfunction does not improve after PVC elimination in patients with significant SHD and a large myocardial scar. Further studies with higher number of patients having large scars on ce-CMR are needed to establish and influence on response after frequent PVC ablation.

Conclusion

Ablation of frequent PVC is associated with a progressive neurohormonal, structural and functional improvement in unselected patients with depressed LVEF, regardless of a potential PVC-induced or PVC-worsened cardiomyopathy. Improvement in LVEF was related to the baseline PVC burden and the persistence of acute ablation success. Given the magnitude of the obtained benefit and its consistency in unselected patients, all patients with depressed LVEF should be evaluated for the presence of frequent PVCs, especially those meeting criteria for primary prevention ICD implantation, as the benefit might modify the clinical decision making.

REFERENCES

1. Duffee DF, Shen WK, Smith HC. Suppression of frequent premature ventricular contractions and improvement of left ventricular function in patients with presumed idiopathic dilated cardiomyopathy. *Mayo Clin Proc*. 1998;73:430-433.
2. Chugh SS, Shen WK, Luria DM, Smith HC. First evidence of premature ventricular complex-induced cardiomyopathy: a potentially reversible cause of heart failure. *J Cardiovasc Electrophysiol*. 2000;11:328-329.
3. Takemoto M, Yoshimura H, Ohba Y, et al. Radiofrequency catheter ablation of premature ventricular complexes from right ventricular outflow tract improves left ventricular dilation and clinical status in patients without structural heart disease. *J Am Coll Cardiol*. 2005;45:1259-1265.
4. Yarlagadda RK, Iwai S, Stein KM, et al. Reversal of cardiomyopathy in patients with repetitive monomorphic ventricular ectopy originating from the right ventricular outflow tract. *Circulation*. 2005;112:1092-1097.
5. Bogun F, Crawford T, Reich S, et al. Radiofrequency ablation of frequent, idiopathic premature ventricular complexes: comparison with a control group without intervention. *Heart Rhythm*. 2007;4:863-867.
6. Taieb JM, Maury P, Shah D, et al. Reversal of dilated cardiomyopathy by the elimination of frequent left or right premature ventricular contractions. *J Interv Card Electrophysiol*. 2007;20:9-13.
7. Sarrazin JF, Labounty T, Kuhne M, et al. Impact of radiofrequency ablation of frequent post-infarction premature ventricular complexes on left ventricular ejection fraction. *Heart Rhythm*. 2009;6:1543-1549.
8. Lakkireddy D, Di Biase L, Ryschon K, et al. Radiofrequency ablation of premature ventricular ectopy improves the efficacy of cardiac resynchronization therapy in nonresponders. *J Am Coll Cardiol*. 2012;60:1531-1539.
9. Yokokawa M, Good E, Crawford T, et al. Recovery from left ventricular dysfunction after ablation of frequent premature ventricular complexes. *Heart Rhythm*. 2013;10:172-175.
10. Shanmugam N, Chua TP, Ward D. 'Frequent' ventricular bigeminy--a reversible cause of dilated cardiomyopathy. How frequent is 'frequent'? *Eur J Heart Fail*. 2006;8:869-873.
11. Fernandez-Armenta J, Berruezo A, Mont L, et al. Use of myocardial scar characterization to predict ventricular arrhythmia in cardiac resynchronization therapy. *Europace*. 2012;14:1578-1586.
12. Di Biase L, Auricchio A, Sorgente A, et al. The magnitude of reverse remodelling irrespective of aetiology predicts outcome of heart failure patients treated with cardiac resynchronization therapy. *Eur Heart J*. 2008;29:2497-2505.
13. Epstein AE, Di Marco JP, Ellenbogen KA, et al. ACC/AHA/HRS 2008 Guidelines for Device-Based Therapy of Cardiac Rhythm Abnormalities: a report of the American College of Cardiology/American Heart Association Task Force on Practice Guidelines (Writing Committee to Revise the ACC/AHA/NASPE 2002 Guideline Update for Implantation of Cardiac Pacemakers and Antiarrhythmia Devices) developed in collaboration with the American Association for Thoracic Surgery and Society of Thoracic Surgeons. *J Am Coll Cardiol*. 2008;51:e1-62.
14. Burkart F, Pfisterer M, Kiowski W, Follath F, Burckhardt D. Effect of antiarrhythmic therapy on mortality in survivors of myocardial infarction with asymptomatic complex ventricular arrhythmias: Basel Antiarrhythmic Study of Infarct Survival (BASIS). *J Am Coll Cardiol*. 1990;16:1711-1718.
15. Baman TS, Lange DC, Ilg KJ, et al. Relationship between burden of premature ventricular complexes and left ventricular function. *Heart Rhythm*. 2010;7:865-869.
16. Yokokawa M, Kim HM, Good E, et al. Impact of QRS duration of frequent premature ventricular complexes on the development of cardiomyopathy. *Heart Rhythm*. 2012;9:1460-1464.

Chapter 3

Fatigue as Presenting Symptom and a High Burden of Premature Ventricular Contractions are Independently Associated with Increased Ventricular Wall Stress in Patients with Normal Left Ventricular Function

Carine F.B. van Huls van Taxis, Sebastiaan R.D. Piers, Marta de Riva Silva, Olaf M. Dekkers, Daniël A. Pijnappels, Martin J. Schalij, Adrianus P. Wijnmaalen, Katja Zeppenfeld

Circulation: Arrhythmia and Electrophysiology. 2015 8;(6):1452-1459

ABSTRACT

Background

High idiopathic premature ventricular contractions (PVC) burden has been associated with PVC-induced cardiomyopathy. Patients may be symptomatic before left ventricular (LV) dysfunction develops. NT-proBNP and circumferential end-systolic wall stress (cESS) on echocardiography are markers for increased ventricular wall stress. This study aimed to evaluate the relation between presenting symptoms, PVC-burden and increased ventricular wall stress in patients with frequent PVCs and preserved LV function.

Methods

Eighty-three patients (41 male, 49±15yrs) with idiopathic PVCs and normal LV function referred for PVC-ablation, were included. Type of symptoms (palpitations, fatigue, [near-]syncope), PVC-burden on 24-hour Holter, NT-proBNP levels and cESS on echocardiography were assessed before and 3 months after ablation. Sustained successful ablation was defined as ≥80% PVC-burden reduction during follow-up.

Results

Patients were symptomatic for 24 months (Q1-Q3 16-60); 73% reported palpitations, 47% fatigue, and 30% (near-)syncope. Baseline PVC burden was 23±13%, median NT-proBNP 92pg/mL(Q1-Q3 50-156) and cESS 143±35kdyne/cm^2. Fatigue was associated with higher baseline NT-proBNP and cESS ($p<0.001$, $p=0.011$, respectively). After sustained successful ablation, achieved in 81%, NT-proBNP and cESS decreased significantly ($p<0.001$, $p=0.036$, respectively). Fatigue was independently associated with a significantly larger reduction in NT-proBNP. In patients with non-successful ablation NT-proBNP and cESS remained unchanged.

Conclusions

In patients with frequent PVCs and preserved LV function, fatigue was associated with higher baseline NT-proBNP and cESS, and with a significantly larger reduction in NT-proBNP after SSA. These findings support a link between fatigue and PVC-induced increased ventricular wall stress, despite preserved LV function.

INTRODUCTION

Premature ventricular contractions (PVCs) in the absence of structural heart disease are a common entity in the general population. While sporadic idiopathic PVCs are generally considered benign, a high PVC burden, a broad PVC-QRS, longstanding palpitations, but also the absence of symptoms, have been associated with PVC-induced cardiomyopathy.[1-4] Accepted indications for catheter ablation are frequent PVCs which are presumed to cause ventricular dysfunction[5] and the presence of severe symptoms, when antiarrhythmic drugs are not effective, tolerated or desired.[6] Notably, catheter ablation is considered contraindicated for asymptomatic patients with PVCs that are not suspected of causing and/or contributing to ventricular dysfunction.[5] The relation between presenting symptoms and PVCs may however be indefinite in patients with normal LV function and non-specific complaints such as fatigue and consequently, the potential benefit of PVC ablation in these patients is unclear.

B-type natriuretic peptide (BNP) and, more sensitive, N-terminal proBNP (NT-proBNP) have been used to monitor heart failure, and elevated BNP levels have been found in patients with symptomatic idiopathic PVCs.[7-9] The main stimulus for (NT-pro)BNP secretion is myocardial wall stress.[9,10] Prior studies suggest that BNP may serve as a sensitive marker to detect PVC-induced increased ventricular wall stress with unclear clinical relevance in the presence of normal LV function.[7,8] Circumferential end-systolic wall stress (cESS) on echocardiography has also been proposed as a marker for ventricular wall stress.[11] Increased ventricular wall stress may be related to fatigue as presenting symptom and perhaps to PVC-induced cardiomyopathy. The objectives of the current study were to evaluate the relation between presenting symptoms, PVC characteristics and markers of increased ventricular wall stress in patients with preserved LV function undergoing PVC ablation.

METHODS

Patients

The cohort consisted of consecutive patients with frequent idiopathic PVC and a normal LV function who underwent PVC ablation in the Leiden University Medical Center between July 2007 and June 2012. Reasons for referral were a high PVC burden, symptomatic frequent PVCs causing palpitations, (near-) syncope, or presumed symptomatic PVCs, if fatigue was the dominant presenting symptom. Fatigue was defined as reduced exercise tolerance or disproportionate tiredness interfering with normal daily affairs such as work, family matters, and/or social life.[12] Antiarrhythmic drugs were not effective, tolerated or desired in all patients to control the presenting symptoms.

Before ablation, a detailed medical history was obtained, which included careful evaluation of presenting symptoms, duration of symptoms and anti-arrhythmic drug usage. Presenting

symptoms were categorized as palpitations, (near-)syncope and fatigue. Effort was taken to review all prior ECGs and Holter monitoring to determine the time of first PVC documentation. Clinical evaluation was performed in all patients, including physical examination, a 12-lead ECG recording of the PVC, 24-hour Holter monitoring and transthoracic echocardiography. Coronary artery disease and structural heart disease were further excluded by exercise testing, coronary angiography, cardiac multi-detector computed tomography and/or magnetic resonance imaging if indicated. All patients were treated according to the routine clinical protocol and provided informed consent.

ECG and Holter analysis

PVC morphology, PVC-QRS duration and PVC coupling interval were derived from the 12-lead ECG and during the ablation procedure by using digital calipers at 200mm/s on the electrophysiology recording system (Prucka Engineering, Houston, TX, USA). The coupling interval was defined as the interval from the earliest onset of the preceding sinus beat QRS complex to the earliest onset of the PVC-QRS complex in any lead. A right bundle branch block (BBB)-like morphology was defined as a dominant positive deflection in V1 and a left BBB as a dominant negative deflection in V1. PVC burden was defined as the percentage PVCs of the total number of QRS complexes during 24 hours. In case of multiple PVC morphologies, the BBB and QRS duration of the dominant morphology was used for analyses.

Echocardiography

Two-dimensional echocardiography and color Doppler data were obtained in parasternal (short- and long-axis) and apical views using a commercially available ultrasound system (Vivid 7, General Electric Vingmed, Milwaukee, WI). All images were stored in cine-loop format for offline analyses with EchoPac 108.1.5 (General Electric Medical Systems, Horten, Norway). Echocardiographic measurements were performed on sinus beats, avoiding the first post-extrasystolic beat if feasible. LV end-diastolic and end-systolic volumes were obtained from the apical 2- and 4-chamber views and LV ejection fraction was calculated according to the biplane Simpson's method.

In addition, circumferential end-systolic wall stress was calculated using LV end-systolic dimension and posterior wall thickness at end-systole. Circumferential end-systolic wall stress was calculated according to the previously described formula:

$$\text{cESS} = \text{Systolic BP} \times a^2 \times (1+b^2/c^2) \times 1/(b^2-a^2)$$

where a = (LV end-systolic dimension/2), b = (LV end-systolic dimension/2) + (posterior wall thickness at end-systole), c = (LV end-systolic dimension/2) + (posterior wall thickness at end-systole/2).[11] All echocardiographic analyses were performed by an independent experienced observer, blinded to all clinical and procedural data.

NT-proBNP

Serum NT-proBNP level was measured before ablation using an automated immunoassay (Elecsys, Roche, Basel, Switzerland). NT-proBNP level ≥125pg/mL was considered abnormal.[13] The estimated Glomerular Filtration Rate (ml/min/1.73m^2) was calculated to exclude renal dysfunction as a cause for increased NT-proBNP concentrations.[14]

Mapping and radiofrequency catheter ablation

Anti-arrhythmic drugs were discontinued for at least 5 half-lives. Heparin was administered to maintain an activated clotting time of 250-300s. The right ventricle (RV) was accessed via the femoral vein and the aortic sinus cusps and the LV via a retrograde approach. Using a 3.5mm or 4mm irrigated-tip catheter (NaviStar ThermoCool, Biosense Webster; or Cool Path, St. Jude Medical) and a 3-D non-fluoroscopic mapping system (CARTO XP, Biosense Webster; or EnSite NavX, St. Jude Medical), limited electroanatomic mapping of the target area was performed to identify the site of origin of the PVC. If PVCs were not present at baseline, isoproterenol was administered (2-10μg/min) and programmed electrical stimulation was performed. The stimulation protocol consisted of 3 drive-cycle lengths (600, 500 and 400ms) with up to 3 ventricular extra stimuli and incremental burst pacing from 2 RV sites.

Ablation target sites were selected based on local activation time, unipolar QS-pattern and presence of reversed polarity.[15] Radiofrequency energy was applied at 20-45W depending on the location (maximum temperature 45ºC, flow 20-30ml/min, 60s). If the PVC was abolished by radiofrequency delivery without recurrence after 30 minutes monitoring this site was defined as site of origin and categorized as RV or LV site. The procedure was considered acutely successful when the targeted PVC did not recur spontaneously and could not be evoked by isoproterenol infusion or programmed electrical stimulation.

Follow-up

After the procedure patients were monitored for 24 hours to detect early PVC recurrence. All patients were re-evaluated at the outpatient clinic at 3 months. Additional follow-up was scheduled if clinically indicated. The re-evaluation consisted of careful history regarding the symptoms that were present before ablation, 12-lead ECGs, 24-hour Holter monitoring, transthoracic echocardiography and NT-proBNP measurement. Sustained successful ablation (SSA) was defined as a PVC burden reduction of ≥80% on 24-hour Holter monitoring during follow-up.[1-3,16]

Statistical analysis

Categorical variables are expressed as number (percentage) and continuous variables as mean ± standard deviation or median (quartiles 1-3 [Q1-Q3]) as appropriate. Differences between patient groups were analyzed using the chi-squared test, Fisher's exact test, student's t-test, or Mann-Whitney U test, as appropriate. For linear regression analysis, NT-proBNP levels were

log-transformed because of the skewed distribution. Parameters listed in Table 1 that were associated with NT-proBNP levels or cESS in univariate analysis (inclusion p<0.05) were included in a multivariate model (age, sex, hypertension, body mass index [BMI]). The percent increase in NT-proBNP per percent PVC burden was calculated by reversed transformation.

Differences between baseline and follow-up measurements were analyzed using the paired t-test or Wilcoxon signed rank test. In patients with SSA, the relation between the baseline variables, including previously described risk factors for PVC induced cardiomyopathy (provided in Table 1), and both NT-proBNP levels and cESS were analyzed by Mann-Whitney U tests or student's t-tests and linear regression analysis for dichotomous and continuous baseline variables, respectively. For paired data (for example pre- versus post procedure NT-proBNP values) no adjustment for confounding was deemed necessary given the paired design of the analysis. Statistical analysis was performed using SPSS, version 20.0 (IBM, Somers, New York, USA). P-values were all 2-sided and a p-value of <0.05 was considered statistically significant.

RESULTS

Patient characteristics

Eighty-three patients (41 male [49%], 49±15 years) with 24-hour Holter-derived PVC burden of 23±13% were included in the analyses. At first presentation sixty-one patients (73%) reported palpitations, 25 (30%) (near-)syncope and 39 (47%) fatigue. Eight patients (10%) were asymptomatic. In 73 patients 2±1 anti-arrhythmic drugs failed to control presenting symptoms and/or reduce PVC burden; 10 patients refused to take drugs.

Despite a normal LV function and volume indices, seventy-four patients (89%) had at least one clinical or PVC parameter that has been associated with PVC-induced cardiomyopathy in prior studies; 41 patients (49%) had a PVC burden ≥24%, 53 patients (64%) had a PVC-QRS duration ≥150ms and 40 patients (48%) had symptoms lasting ≥30 months. Table 1 summarizes baseline clinical parameters, PVC characteristics and echocardiographic results.

Median NT-proBNP was 92pg/mL (Q1-Q3 50-156pg/mL) before ablation. In 34 patients (41%) baseline NT-proBNP level was elevated (>125pg/mL).[13] Only one patient had reduced renal function (GFR 56ml/min). The average cESS on echocardiography was 143±35kdyne/cm^2.

Markers of ventricular wall stress, presenting symptoms and PVC characteristics

Patients presenting with symptoms of fatigue had significantly higher NT-proBNP concentrations compared to patients without fatigue (144pg/mL [Q1-Q3 107-359pg/mL] versus 52pg/mL [Q1-Q3 28-87pg/mL], p<0.001). This result remained significant after adjustment in a multivariate model for age, sex, hypertension and BMI (p<0.001). In addition, cESS was significantly higher in patients with fatigue compared to patients without fatigue (153±38kdyne/cm^2 versus 134±30kdyne/cm^2, p=0.011). After adjusting for age, sex, hypertension and BMI in a multi-

Table 1. Baseline characteristics

	All N=83	No fatigue N=44	Fatigue N=39	P-value*
Male, n (%)	41 (49)	24 (55)	17 (44)	0.382
Age, years	49±15	45±14	54±15	0.008
Body mass index, kg/m^2	27±5	26±4	28±5	0.011
Hypertension, n (%)	24 (29)	6 (14)	18 (46)	0.002
eGFR, ml/min/1.73m^2	81±22	83±22	79±22	0.380
Anti-arrhythmic drugs failed, n	2±1	2±1	2±1	0.873
β-blockade, n (%)	51 (61)	27 (61)	24 (62)	1.0
Calcium-antagonist, n (%)	17 (20)	9 (20)	8 (21)	1.0
Flecainide, n (%)	20 (24)	13 (30)	7 (20)	0.305
Amiodarone/Sotalol, n (%)	40 (48)	22 (50)	18 (46)	0.827
Symptom duration in months, median (Q1-Q3)	24 (16-60)	24 (12-48)	36 (19-61)	0.331
Presenting symptoms:				
Palpitations, n (%)	61 (73)	35 (80)	26 (67)	0.219
Fatigue, n (%)	39 (47)	0	39 (100)	-
(near) Syncope, n (%)	25 (31)	14 (32)	11 (28)	0.812
PVC burden, %	23±13	19±11	28±13	0.002
PVC characteristics				
PVC-QRS duration, ms	159±21	162±20	155±22	0.139
Coupling interval, ms	467±68	471±72	461±63	0.501
Left bundle branch block, n (%)	65 (78)	37 (84)	28 (72)	0.194
Echocardiography parameters				
LV ejection fraction, %	60±6	61±6	60±6	0.538
LVEDV-index, ml/m^2	58±15	60±15	55±14	0.171
LVESV-index, ml/m^2	23±8	24±8	22±7	0.322
cESS, kdyne/cm^2	143±35	134±30	153±38	0.011

cESS=circumferential end-systolic wall stress; EDV=end diastolic volume; ESV=end systolic volume; LV=left ventricle; PVC=premature ventricular contraction. *P-value calculated between groups

variate model this remained significant (p=0.010). No differences were observed in NT-proBNP concentration or in cESS between patients with or without palpitations, with or without (near-) syncope or with shorter or longer duration of symptoms (Figure 1). A multivariate model strengthened these results when correcting for age, sex, hypertension and BMI. A left-sided site of origin, a right BBB-like PVC morphology and in particular a PVC burden ≥24% were associated with higher NT-proBNP concentration. Only a left-sided origin of the PVC was associated with a higher cESS (Figure 1). A significant, although weak, correlation between PVC burden and log-transformed NT-proBNP could be demonstrated; 1% PVC burden increase resulted in 4% increase in NT-proBNP (Figure 2).

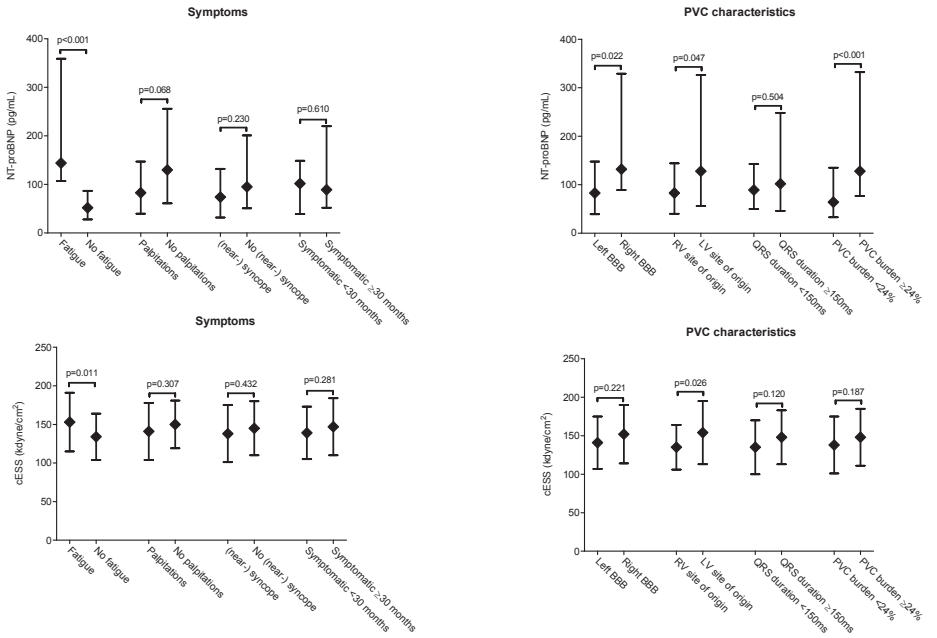

Figure 1. Top panels: Baseline NT-proBNP according to symptoms and PVC characteristics. Median and interquartile range are depicted. Bottom panels: Baseline circumferential end-systolic wall stress (cESS) according to symptoms and PVC characteristics. Mean with standard deviation are depicted.

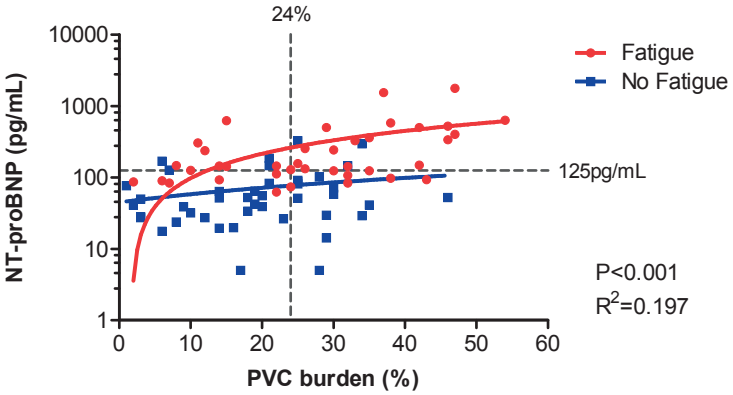

Figure 2. Correlation between NT-proBNP and PVC burden according to patients with and without fatigue.
Linear regression analyses for NT-proBNP and PVC burden. Red dots and line demonstrate patients with fatigue, blue squares and line patients without fatigue. Regression analysis was calculated for patients with versus without fatigue. The grey dotted lines illustrate the PVC-burden cut off value of 24% and NT-proBNP cut off value of 125pg/mL. The y-axis is log-scaled.

The following variables were associated with significantly higher baseline log-transformed NT-proBNP levels in univariate analysis and were therefore included in a multivariate model: age, hypertension, LV site of origin, PVC right BBB, PVC burden and fatigue. Fatigue, LV site of origin and PVC burden remained independently associated with baseline log-transformed NT-proBNP levels ($p<0.001$, $p=0.044$ and $p=0.015$, respectively).

Variables that were associated with high baseline cESS in univariate analysis were: fatigue, LV site of origin, LVEF, LVEDV-I and LVESV-I. These variables were included in a multivariate model and fatigue and LV site of origin remained independently associated with baseline cESS ($p=0.003$ and $p=0.017$, respectively).

Mapping and radiofrequency catheter ablation

Acute procedural success was achieved in 68 patients (82%). The site of origin was the RV in 49 patients (59%) and the LV in 34 patients (41%). In 13 patients (16%) catheter ablation was only temporarily successful or not effective likely due to an intramural/epicardial site of origin. In 2 patients (2%) radiofrequency delivery was withheld due to the proximity of the His-bundle and the ostium of the right coronary artery, respectively. Procedure and fluoroscopy times were 140±48 minutes and 16±11 minutes. There were no procedure-related complications and no early PVC recurrence was observed.

Follow-up

Re-evaluation after 3 months was completed in 80 patients (96%); 2 patients did not undergo 24-hour Holter monitoring and 1 did not undergo echocardiography. A sustained PVC burden reduction of ≥80% on 24-hour Holter monitoring was achieved in 67 patients (81%); all were asymptomatic for the presenting symptoms, including the pre-procedural complaints of fatigue. This included the 2 patients in which 24-hour Holter monitoring was not performed during follow-up, however both were highly symptomatic before and free of any symptoms after ablation and were therefore considered as having SSA. In one patient ablation was acutely not successful, but a sustained PVC reduction was achieved by flecainide. Patients with SSA demonstrated a small but significant reduction in LVEDV-I; from 57±14mL/m^2 to 54±15mL/m^2 ($p=0.039$), and LVESV-I; from 23±8mL/m^2 to 21±9mL/m^2 ($p=0.013$). LV ejection fraction did not change during follow-up (60±6% versus 61±8%, $p=0.341$).

In the 16 patients without SSA, presenting symptoms, LV ejection fraction and volume indices remained unchanged, although the average PVC burden was lower (from 21±14% to 13±12%, $p=0.002$). Six of these patients were on anti-arrhythmic drugs during follow-up.

Changes in NT-proBNP level and wall stress on echocardiography

In a total of 71 patients the NT-proBNP concentration was measured during follow-up. In the 59 patients with SSA in whom NT-proBNP was measured during follow-up, NT-proBNP decreased significantly from 93pg/mL (Q1-Q3 52-169pg/mL) to 53pg/mL (Q1-Q3 37-90pg/mL) ($p<0.001$)

resulting in a ΔNT-proBNP of 37pg/mL (Q1-Q3 6-108pg/mL). In 51 of 59 patients (86%) NT-proBNP normalized to <125pg/mL.

Among patients with SSA, those presenting with fatigue showed a significantly larger decrease in NT-proBNP levels than patients without fatigue (ΔNT-proBNP 73pg/mL [Q1-Q3 38-209pg/mL] versus 19pg/mL [Q1-Q3 -7-38pg/mL], p<0.001) (Figure 3). When corrected for age, sex, hypertension and BMI in a multivariate model it remained significant (p=0.034). Patients with a baseline PVC burden ≥24% before ablation also demonstrated a significantly larger decrease in NT-proBNP levels after SSA when compared to those with a burden of less than 24% (ΔNT-proBNP 68pg/mL [Q1-Q3 29-237pg/mL] versus 23pg/mL [Q1-Q3 -1-74pg/mL], p=0.015). When adjusting for age, sex, hypertension and BMI in multivariate analysis, ΔNT-proBNP remained significantly larger in the patients with a high burden (p=0.004). Other presenting symptoms or PVC characteristics did not correlate with an important decrease in NT-proBNP levels (Figure 4).

Circumferential end-systolic wall stress decreased after SSA from 144±35kdyne/cm^2 at baseline to 134±35kdyne/cm^2 during follow-up (p=0.036), resulting in a median ΔcESS of 11kdyne/cm^2 (Q1-3 -12-34kdyne/cm^2) in this group. No difference in ΔcESS was observed between patients with or without fatigue (p=0.955). Only a LV site of origin was associated with a larger decrease in cESS after SSA (Figure 4) which remained independently associated in multivariate regression analysis after adjusting for age, sex, hypertension and BMI (p=0.008). In patients without SSA, no significant changes in NT-proBNP or cESS were observed (from 84pg/mL [38-132pg/mL] to 67pg/mL [Q1-Q3 41-86pg/mL], p=0.272; from 142±45kdyne/cm^2 to 138±45kdyne/cm^2, p=0.778, respectively).

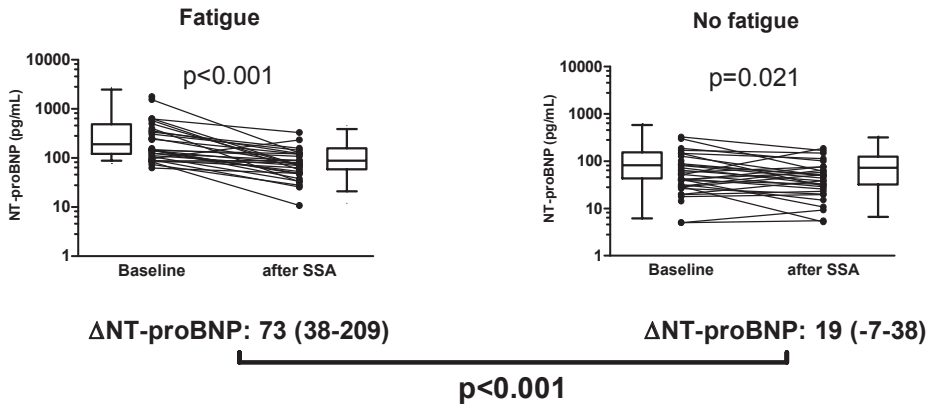

Figure 3. NT-proBNP levels before and after sustained successful ablation (SSA), in patients with and without fatigue.
The y-axis is log-scaled. The boxplots demonstrate the median, quartiles 1-3 and 95% confidence interval.

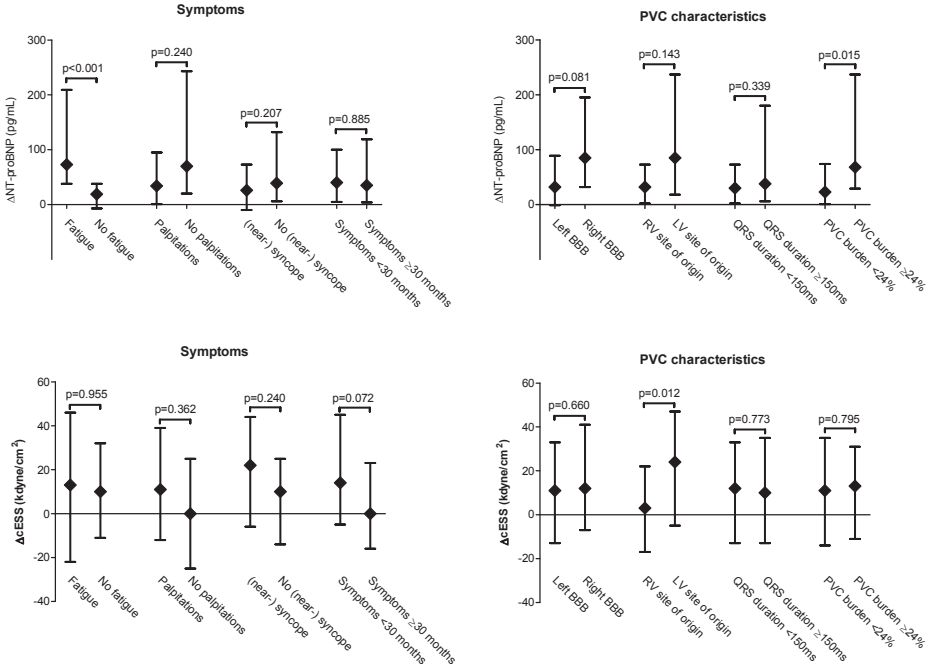

Figure 4. Sustained Successful Ablation.
Top panels: ΔNT-proBNP after sustained successful ablation according to symptoms and PVC characteristics. Median and quartiles 1-3 are depicted. Bottom panels: Δcircumferential end-systolic wall stress (ΔcESS) after sustained successful ablation according to symptoms and PVC characteristics. Median and quartiles 1-3 are depicted.

DISCUSSION

The main findings of the present study are that (1) NT-proBNP levels are elevated in 41% of patients with a preserved LV function who undergo catheter ablation for frequent PVCs. (2) Both NT-proBNP levels and cESS on echocardiography decreased after SSA, but not after non-SSA. (3) Symptoms of fatigue and a higher PVC burden are independently associated with higher NT-proBNP levels prior to ablation and were the only studied parameters associated with a significantly larger decrease of NT-proBNP levels after SSA. (4) Symptoms of fatigue were also associated with increased baseline cESS on echocardiography, but not with a significantly larger decrease after SSA.

Presenting symptoms, PVC characteristics and wall stress

Palpitations and (near) syncope are typical PVC-related symptoms whereas fatigue is often not reported or considered to be a nonspecific or atypical symptom.[4] In our cohort fatigue was present at baseline in 47% of the patients despite a normal LV function. Of importance, fatigue was independently associated with higher NT-proBNP levels and cESS at baseline and patients

with fatigue showed a significantly larger decrease in NT-proBNP levels after SSA compared to patients with only classical PVC related symptoms. In addition, compared to prior reported cESS values in patients with normal LV geometry, cESS was considerably higher in patients with fatigue, but not in patients without fatigue.[11] These data suggest that fatigue in patients with PVCs may be caused by PVC-induced wall stress in the absence of LV dysfunction, and that fatigue should therefore be considered as clinically relevant and PVC-related symptom.

An important number of patients with fatigue had elevated NT-proBNP levels despite a PVC-burden lower than 25%. The significant decrease in NT-proBNP level and cESS, accompanied by the relief of symptoms of fatigue after SSA, may therefore justify catheter ablation even if the PVC burden is below the currently suggested cut-off value.[1]

Marker of increased ventricular wall stress and risk factors for PVC induced cardiomyopathy

Longstanding palpitations, a high PVC burden, a broad PVC-QRS and a non-outflow tract (predominantly LV) site of origin are potential risk factors for a PVC-induced cardiomyopathy.[1-4] In addition, asymptomatic patients, in whom the duration of PVC cannot be evaluated, have been considered to be particularly prone to develop a cardiomyopathy.[4] Interestingly, we found that fatigue, which is not systematically reported as a PVC related symptom in prior studies, the LV site of origin and PVC burden were also all independently associated with increased NT-proBNP levels. In contrast, PVC-QRS and symptom duration were not. Of interest, although 40 patients of our cohort had already symptoms of more than 30 months, none had developed a PVC-induced cardiomyopathy before ablation. This finding does however not exclude that longstanding PVCs may remain a risk factor as 84% of our patients were successfully treated and PVC induced cardiomyopathy may develop over several years.[2,17]

Baseline cESS on echocardiography was associated with fatigue and a left-sided origin of PVCs, but not with any of the other parameters that have previously been associated with PVC-induced cardiomyopathy, including PVC burden. These findings suggest that cESS may perhaps be a less sensitive marker than NT-proBNP for detection of PVC induced increased ventricular wall stress.

Biomarker as a sensitive indicator for PVC induced wall stress

Two prior studies have reported elevated BNP levels in up to 64% of patients without LV dysfunction who underwent ablation for both idiopathic VTs and PVC.[7,8] Compared to the 41% of patients with elevated NT-proBNP levels in our study this percentage is remarkably high, in particular as prior published data have demonstrated that NT-proBNP is an even more sensitive marker to detect LV dysfunction.[18] The high BNP levels decreased to normal levels in around 61% after successful ablation.[8] Both prior reports found a correlation between BNP levels before ablation and PVC burden, which is in line with our data.

However, included patients were older and an independent predictor of elevated BNP levels was controlled hypertension. It is likely that LV hypertrophy and diastolic dysfunction due to aging and hypertension may contribute to the higher prevalence of increased BNP level in these prior reports.

In our patient cohort fatigue was associated with a higher PVC burden, NT-proBNP levels and cESS at baseline, and also with a significantly larger decrease in NT-proBNP levels after SSA, supporting the premise that increased wall stress may possibly cause fatigue. In the non-SSA group a trend towards a decrease in NT-proBNP was shown which may be explained by a significant (but less than the predefined 80%) PVC burden reduction in this group. NT-proBNP, which is likely a more sensitive marker for ventricular wall stress and widely applied, may also be preferable over cESS for detection of increased ventricular wall stress in patients with frequent PVCs and fatigue. Whether patients with fatigue and elevated NT-proBNP levels as biomarker for increased wall stress are also more likely to develop a PVC-induced cardiomyopathy requires further investigation.

Limitations

NT-proBNP levels and cESS were measured only twice, immediately prior to ablation and 3 months after ablation. The currently described patient cohort is unlikely to be representative for the general population of patients with PVCs as all patients were referred for ablation because of the PVC burden, symptoms or patient's preference. As we did not follow patients with frequent PVCs and fatigue without intervention we can only speculate about the potential relation between fatigue, PVC burden, PVC induced wall stress, and development of LV dysfunction. Furthermore, we recognize that fatigue is a nonspecific symptom and subjective to individual interpretation and therefore difficult to quantify.

Clinical implications

According to current recommendations, catheter ablation can be useful in patients with frequent symptomatic PVCs if antiarrhythmic drugs are not effective, tolerated or desired.[6] Ablation is not indicated for asymptomatic PVCs that are not suspected of causing or contributing to ventricular dysfunction.[5]

We could demonstrate for the first time that fatigue, which is often considered a nonspecific symptom and not typically related to PVCs, was associated with elevated NT-proBNP levels and cESS on echocardiography. NT-proBNP and cESS are markers for wall stress and both normalized after successful ablation accompanied by relief of symptoms of fatigue. Although we cannot prove causality, our findings suggest that fatigue may be associated with PVC-induced ventricular wall stress, which can be successfully treated by catheter ablation. In the light of the current findings, clinicians may therefore consider catheter ablation of PVCs in patients presenting only with fatigue, even in the absence of LV dysfunction, classical PVC related symptoms (such as palpitations or (near-)syncope), or a certain PVC burden. Whether elevated NT-proBNP level

and fatigue as presenting symptom identify patients at risk to develop PVC-induced cardiomyopathy requires further investigation.

Conclusion

In patients without LV dysfunction undergoing PVC ablation, fatigue was independently associated with higher NT-proBNP concentrations and cESS at baseline, and with a significantly larger reduction of NT-proBNP levels after SSA. These findings suggest that fatigue may be caused by PVC-induced increased ventricular wall stress, even in patients with a preserved LV function. Patients with fatigue and/or elevated NT-proBNP levels may benefit from ablation even in the absence of classical PVC related symptoms or LV dysfunction.

REFERENCES

1. Baman TS, Lange DC, Ilg KJ, et al. Relationship between burden of premature ventricular complexes and left ventricular function. *Heart Rhythm*. 2010;7:865-869.
2. Yokokawa M, Kim HM, Good E, et al. Relation of symptoms and symptom duration to premature ventricular complex-induced cardiomyopathy. *Heart Rhythm*. 2012;9:92-95.
3. Yokokawa M, Kim HM, Good E, et al. Impact of QRS duration of frequent premature ventricular complexes on the development of cardiomyopathy. *Heart Rhythm*. 2012;9:1460-1464.
4. Carballeira PL, Deyell MW, Frankel DS, et al. Ventricular premature depolarization QRS duration as a new marker of risk for the development of ventricular premature depolarization-induced cardiomyopathy. *Heart Rhythm*. 2014;11:299-306.
5. Aliot EM, Stevenson WG, Almendral J, et al. EHRA/HRS Expert Consensus on Catheter Ablation of Ventricular Arrhythmias: developed in a partnership with the European Heart Rhythm Association (EHRA), a Registered Branch of the European Society of Cardiology (ESC), and the Heart Rhythm Society (HRS); in collaboration with the American College of Cardiology (ACC) and the American Heart Association (AHA). *Heart Rhythm*. 2009;6:886-933.
6. Zipes DP, Camm AJ, Borggrefe M, et al. ACC/AHA/ESC 2006 guidelines for management of patients with ventricular arrhythmias and the prevention of sudden cardiac death: a report of the American College of Cardiology/American Heart Association Task Force and the European Society of Cardiology Committee for Practice Guidelines (Writing Committee to Develop Guidelines for Management of Patients With Ventricular Arrhythmias and the Prevention of Sudden Cardiac Death). *J Am Coll Cardiol*. 2006;48:e247-e346.
7. Sekiguchi Y, Aonuma K, Yamauchi Y, et al. Chronic hemodynamic effects after radiofrequency catheter ablation of frequent monomorphic ventricular premature beats. *J Cardiovasc Electrophysiol*. 2005;16:1057-1063.
8. Tada H, Ito S, Shinbo G, et al. Significance and utility of plasma brain natriuretic peptide concentrations in patients with idiopathic ventricular arrhythmias. *Pacing Clin Electrophysiol*. 2006;29:1395-1403.
9. Knebel F, Schimke I, Pliet K, et al. NT-ProBNP in acute heart failure: correlation with invasively measured hemodynamic parameters during recompensation. *J Card Fail*. 2005;11:S38-S41.
10. Krittayaphong R, Boonyasirinant T, Saiviroonporn P, et al. Correlation Between NT-pro BNP levels and left ventricular wall stress, sphericity index and extent of myocardial damage: a magnetic resonance imaging study. *J Card Fail*. 2008;14:687-694.
11. Yuda S, Khoury V, Marwick TH. Influence of wall stress and left ventricular geometry on the accuracy of dobutamine stress echocardiography. *J Am Coll Cardiol*. 2002;40:1311-1319.
12. Krupp LB, LaRocca NG, Muir-Nash J, Steinberg AD. The fatigue severity scale. Application to patients with multiple sclerosis and systemic lupus erythematosus. *Arch Neurol*. 1989;46:1121-1123.
13. Gustafsson F, Steensgaard-Hansen F, Badskjaer J, et al. Diagnostic and prognostic performance of N-terminal ProBNP in primary care patients with suspected heart failure. *J Card Fail*. 2005;11:S15-S20.
14. Vickery S, Price CP, John RI, et al. B-type natriuretic peptide (BNP) and amino-terminal proBNP in patients with CKD: relationship to renal function and left ventricular hypertrophy. *Am J Kidney Dis*. 2005;46:610-620.
15. van Huls van Taxis CF, Wijnmaalen AP, den Uijl DW, et al. Reversed polarity of bipolar electrograms for predicting a successful ablation site in focal idiopathic right ventricular outflow tract arrhythmias. *Heart Rhythm*. 2011;8:665-671.

16. Penela D, van Huls van Taxis CF, Aguinaga L, et al. Neurohormonal, structural, and functional recovery pattern after premature ventricular complex ablation is independent of structural heart disease status in patients with depressed left ventricular ejection fraction: a prospective multicenter study. *J Am Coll Cardiol*. 2013;62:1195-1202.
17. Niwano S, Wakisaka Y, Niwano H, et al. Prognostic significance of frequent premature ventricular contractions originating from the ventricular outflow tract in patients with normal left ventricular function. *Heart*. 2009;95:1230-1237.
18. Costello-Boerrigter LC, Boerrigter G, Redfield MM, et al. Amino-terminal pro-B-type natriuretic peptide and B-type natriuretic peptide in the general community: determinants and detection of left ventricular dysfunction. *J Am Coll Cardiol*. 2006;47:345-353.

Chapter 4

Reversed Polarity of Bipolar Electrograms to Predict a Successful Ablation Site in Focal Idiopathic Right Ventricular Outflow Tract Arrhythmias

Carine F.B. van Huls van Taxis, Adrianus P. Wijnmaalen, Dennis W. den Uijl, Marcin Gawrysiak, Hein Putter, Martin J. Schalij, Katja Zeppenfeld

Heart Rhythm. 2011;8:665-671

ABSTRACT

Background

Radiofrequency catheter ablation (RFCA) for idiopathic right ventricular outflow tract (RVOT) arrhythmias is typically guided by local activation time (LAT) mapping and unipolar electrogram morphology (QS-configuration). However, LAT mapping is limited by the large variation among patients and the area demonstrating a QS-configuration of the unipolar electrogram may be larger than the focal source. Reversed polarity has been proposed as criterion to guide RFCA. The aim of this study was to investigate the value of reversed polarity of adjacent bipolar electrograms to predict a successful ablation site in idiopathic RVOT arrhythmias.

Methods

Twenty-five consecutive patients (12 male [48%], 43±15 years) undergoing RFCA for RVOT arrhythmia were studied. Electrograms of ablation sites and of points within a 15mm radius to the successful site were evaluated for LAT, unipolar electrogram morphology and the presence of reversed polarity of adjacent bipolar electrograms. Electrogram characteristics of successful ablation sites were compared to non-successful ablation sites. The spatial distribution of each electrogram characteristic was studied.

Results

Successful ablation sites more often demonstrated reversed polarity and had an earlier LAT than non-successful sites. A wide spatial distribution was observed for unipolar electrograms with a QS-configuration around the successful ablation site. Mapping based on LAT and reversed polarity had a higher predictive value for a successful ablation site than mapping based on LAT and QS-configuration.

Conclusions

The presence of reversed polarity has a high predictive value for successful ablation sites in focal idiopathic RVOT arrhythmias and is likely to reduce the number of RFCA applications.

INTRODUCTION

Ventricular arrhythmias (VA) in the absence of structural heart disease are a common entity. Patients presenting with idiopathic VA account for 10% of patients referred for evaluation and treatment of VA and more than 70-80% of idiopathic VA originate from the right ventricular outflow tract (RVOT).[1] Although idiopathic VAs are generally considered benign, they can cause severe symptoms and may be associated with a VA induced cardiomyopathy.[2-6]

Current guidelines indicate anti-arrhythmic drugs as first choice therapy for symptomatic patients; however drugs are often ineffective or hampered by side effects.[1,7,8] Radiofrequency catheter ablation (RFCA) is a reasonable alternative and acutely highly effective with procedural success rates of more than 80%.[1,9-11] Although considered safe, serious complications may occur and the application of a limited number of radiofrequency lesions particular is preferred.[1,12-15]

To guide RFCA, conventional strategies are based on bipolar local activation time (LAT) mapping and the presence of a QS-configuration of the unipolar electrogram to predict a successful ablation site.[16-19] However, the use of LAT is limited by its large variation among patients and the area demonstrating a unipolar QS-configuration may be larger than the focal source.[18,20] A more specific electrogram characteristic to predict a successful ablation site in RVOT arrhythmias is therefore desirable.

The feasibility of guiding ablation by reversed polarity of adjacent bipolar electrograms has been demonstrated in pulmonary vein isolation based on the hypothesis that the excitation wavefront propagates radially from the breakthrough site of the left atrium to the pulmonary vein.[21] A similar reversal of the initial deflection of adjacent bipolar electrograms, indicative for wavefront propagation in opposite directions, has been demonstrated in patients with accessory pathways and focal atrial tachycardias.[22] This phenomenon however, has not been well documented in focal RVOT arrhythmias.

The aim of this study was to investigate the value of reversed polarity mapping to identify an arrhythmogenic focal source and to predict a successful ablation site in focal RVOT arrhythmias.

METHODS

Patient population

The patient population consisted of 25 consecutive patients undergoing RFCA of idiopathic focal VA originating from the RVOT. To rule out structural heart disease, a comprehensive clinical evaluation was performed including medical history, 12-lead electrocardiogram (ECG) and two-dimensional transthoracic echocardiography in all patients. If deemed necessary to exclude structural heart disease, exercise testing, coronary angiography, cardiac multi-detector computed tomography, magnetic resonance imaging and/or nuclear imaging were performed. Prior to RFCA, a 12-lead ECG recording of the VA and a 24-hour Holter registration were acquired in

all patients. Ventricular arrhythmias consisting of more than three consecutive monomorphic beats were classified as ventricular tachycardia (VT) and VA ≤3 consecutive monomorphic beats were classified as premature ventricular contraction (PVC).

After RFCA, all patients were monitored for 24 hours to detect early VA recurrence. All patients were evaluated on a regular basis at the outpatient clinic 3 months after discharge. Each visit included a clinical history, 12-lead ECG and 24-hour Holter registration.

Electrophysiological examination and catheter ablation

After informed consent was obtained electrophysiological evaluation was performed comprising electrical programmed stimulation (EPS) and right ventricular electroanatomical activation mapping to identify the site of origin within the RVOT. During mapping and ablation, conscious sedation was avoided whenever possible. Anti-arrhythmic drugs were discontinued for at least 5 half-lives. None of the patients were using amiodarone prior to the procedure. Heparin was administered to maintain an activated clotting time of 250-300s. Catheters were placed through a right femoral vein approach. A quadripolar electrophysiological catheter was inserted in the right ventricle and used for EPS. In the presence of a spontaneous clinical VA, activation mapping was performed using the surface VA QRS as a temporal reference. If no spontaneous VA occurred EPS was performed before and after intravenous isoprotenerol (2-8μg/min) infusion, if necessary. The EPS protocol consisted of 3 drive-cycle lengths (600, 500 and 400ms) with up to 3 ventricular extra stimuli and incremental burst pacing from 2 different right ventricular sites.

A 3.5mm irrigated-tip quadripolar mapping catheter (2-5-2mm inter-electrode spacing, Navistar ThermoCool, Biosense Webster Inc, Diamond Bar, CA, USA) was used to create an electroanatomical activation map. Electroanatomical mapping was performed using a 3-D non-fluoroscopic mapping system (CARTO XP™, Biosense Webster Inc, Diamond Bar, CA, USA).

Bipolar electrograms recorded from the distal (M1-M2) and proximal (M3-M4) electrode pair of the mapping catheter (filtered at 30-400Hz), the unipolar electrogram recorded from the distal electrode (M1; filtered at 1-240Hz, Wilson central terminal) and the 12-lead surface ECG were displayed simultaneously and stored on an electrophysiological recording system (Prucka Cardiolab, GE Healthcare, Piscataway, NJ, USA) and on the 3-D mapping system for off line analysis. Bipolar electrograms recorded from the mid electrode pair (M2-M3) were only displayed and stored on the electrophysiological recording system.

To guarantee accurate electroanatomical activation mapping and to avoid annotation of catheter induced PVCs, the VA QRS-morphology of each acquired mapping point was compared to a 12-lead QRS template of the clinical arrhythmia.

Target sites for RFCA were selected based on 1) LAT, 2) the presence of a unipolar QS-configuration and 3) the presence of reversed polarity. Local activation time was measured from the bipolar electrogram recorded from the distal electrode pair of the mapping catheter and was defined as the interval between the initial sharp peak of the electrogram and the onset of the VA QRS. Unipolar electrograms were recorded from the distal electrode of the map-

ping catheter. The presence of reversed polarity was evaluated from the bipolar electrograms recorded from the distal (M1-M2) and mid (M2-M3) electrode pairs of the mapping catheter and was defined as a rapid simultaneous deflection in opposite direction of the initial part of the bipolar electrograms occurring before the onset of the VA QRS. To record reversed polarity the mapping catheter was positioned parallel or in a shallow angel to the endocardial surface (Figure 1).

Radiofrequency energy was applied at 20-30W with a maximum temperature of 40°C and with external irrigation at 20ml/min to achieve an impedance-fall of 10 ohm. If the VA was abolished within 30s, the energy application was continued for 60s. If the VA was not abolished within 30s, the energy application was terminated, the site was tagged as non-successful ablation site on the map and mapping was continued. A successful ablation site was defined as the location where RFCA abolished the VA and was tagged on the map. The procedural endpoint was reached when the targeted VA did not occur spontaneously after a waiting period of 30 minutes after the last application and could not be induced by EPS before and after isoproterenol infusion.

Electrogram analysis

Electrogram characteristics at successful ablation sites, non-successful ablation sites and at mapping sites within close vicinity of the successful ablation site (area points) were analyzed. Area points were defined as mapping points acquired within a radius of 15mm from the successful ablation site. The distance between area points and non-successful ablation sites to the VA termination site was measured using the software provided by the CARTO XP system. Area points were further categorized according to the distance to the successful ablation site (1-5mm; 6-10mm; 11-15mm) to study the spatial distribution of the different electrogram characteristics with regard to the successful ablation site. For each analyzed mapping point (1) LAT, (2) unipolar electrogram morphology and (3) the presence of reversed polarity were evaluated. Local activation time, a unipolar QS-configuration and the presence of reversed polarity were compared for successful and non-successful ablation sites.

To further determine the accuracy of LAT, unipolar QS-configuration and the presence of reversed polarity to predict a successful ablation site, electrogram characteristics of successful sites were compared to the characteristics of area points. The cut-off value for LAT to predict a successful ablation site was determined based on the value with the highest combined sensitivity and specificity.

To study the impact of reversed polarity on the accuracy to predict successful ablation sites, two different electrophysiological mapping strategies were compared: (1) a conventional approach which was guided by LAT and unipolar QS-configuration and (2) a newly proposed approach guided by LAT and reversed polarity. Both approaches used LAT as a first selection criterion to delineate the area around the focal source within the RVOT. Next, within this area a unipolar QS-configuration or reversed polarity was used to identify the site of origin.

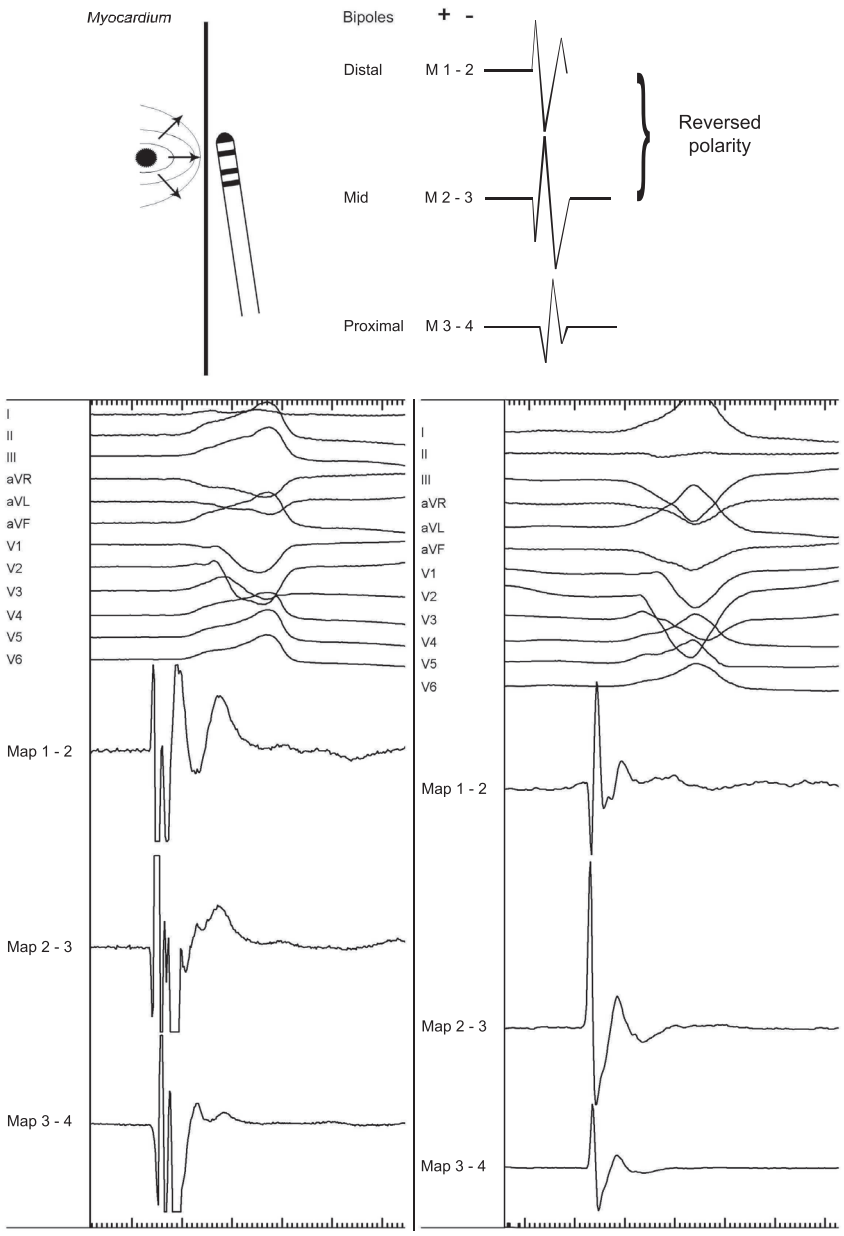

Figure 1.

Panel A. Schematic of an arrhythmogenic focal source within the RVOT with radial wavefront propagation and the position of the quadripolar mapping catheter. The distal (M1-M2) and mid (M2-M3) electrode pairs are simultaneously activated showing a rapid simultaneous deflection in opposite direction of the initial part of the bipolar electrograms defined as reversed polarity.

Panel B. Local bipolar electrograms recorded from the distal (M1-M2), mid (M2-M3) and proximal (M3-M4) electrode pairs of the ablation catheter and the12-lead surface ECG of idiopathic RVOT arrhythmias (sweep-speed 200mm/sec) in two patients. A single radiofrequency application at the recording site abolished the arrhythmia.

All electrograms were analyzed off-line by two independent observers blinded to the location of the mapping point and to the result of the ablation procedure. In case of discrepancy between the two observers, agreement was reached by consensus.

Statistical analysis

Statistical analysis was performed using SPSS, version 16.0 (SPSS Inc, Chicago, IL, USA). A p-value of <0.05 was considered statistically significant. Normality of distribution was tested using the Kolmogorov-Smirnoff test. Continuous variables are expressed as mean ± SD and were compared using the unpaired student's t-test. Categorical variables are expressed as number (%) and were analyzed using the chi-square test. In order to correct for correlations due to multiple measurements within the same patient, robust standard errors were calculated using Sandwich estimators.[23] Adjustment for multiple testing was performed using the Bonferroni correction. To determine the optimal cut-off value for LAT to predict a successful ablation site, a receiver operating characteristic curve was constructed. The cut-off value was based on the LAT value with the highest combined sensitivity and specificity. Finally, to test the clinical impact of electrophysiological mapping based on LAT and reversed polarity on the accuracy to identify a successful RFCA site, the net reclassification improvement compared to conventional mapping was calculated.[24]

RESULTS

Twenty-five consecutive patients (12 male, 43±15 years) with a total of 26 registered VA (22 PVC [85%]) were included in the study. All patients had been symptomatic for 38±40 months and were refractory to therapy with 1.3±1.3 anti-arrhythmic drugs. The VA burden on 24-hour Holter monitoring was 22±17%. All patients had a normal left and right ventricular function (mean left ventricular ejection fraction 58±5%) on echocardiography. To rule out structural heart disease additional diagnostic testing was performed and was normal in all patients. Twenty patients underwent exercise testing, coronary angiography was performed in 10 patients, cardiac multi-detector computed tomography in 1 patient, magnetic resonance imaging in 11 patients and nuclear imaging in 3 patients.

Electrophysiology study and radiofrequency catheter ablation

During electrophysiological study, the clinical VA occurred spontaneously in 22/25 (88%) patients. In 3 patients isoprotenerol infusion was required to induce the clinical VA, additional burst pacing was required to initiate the clinical VA in 1 patient. One patient presented with 2 spontaneous VA morphologies (both were targeted).

Electroanatomical activation mapping of the RVOT was performed prior to ablation in all patients (40±29 mapping points per VA). All VA were successfully abolished with a mean of

2.3±1.8 RF applications. Procedural time was 76±24 minutes (including a 30 minute waiting period after the last RF application) and a fluoroscopy time of 13±8 minutes. Procedural success was achieved in all patients. No procedure related complications occurred and all patients were discharged without in hospital VA recurrence.

After 8±7 months of follow-up all patients were free of symptoms without the use of anti-arrhythmic drugs. Twenty patients had a VA burden of <1% on 24-hour Holter monitoring. In 2 patients the VA burden was 2 en 6%, respectively, however the VA QRS-morphology differed from the VA QRS-morphology targeted during the index procedure. In 3 asymptomatic patients, who had disabling symptoms before ablation, 24-hour Holter monitoring was not available. None of the 4 patients with VT prior to ablation had VT recurrence.

Successful versus non-successful ablation sites

Electrogram characteristics from 26 successful and 33 non-successful ablation sites were compared. Local activation time was significantly earlier at successful ablation sites as compared to non-successful ablation sites (-28±7ms versus -22±8ms, p=0.002). However, there was a considerable overlap in LAT between both groups (Figure 2). Reversed polarity of adjacent bipolar electrograms was observed at 21 of 26 successful ablation sites (85%). In contrast, reversed polarity was absent at all non-successful ablation sites (p<0.001). The presence of a unipolar QS-configuration was similar between successful and non-successful ablation sites (22 [85%] versus 19 [83%], p=0.850).

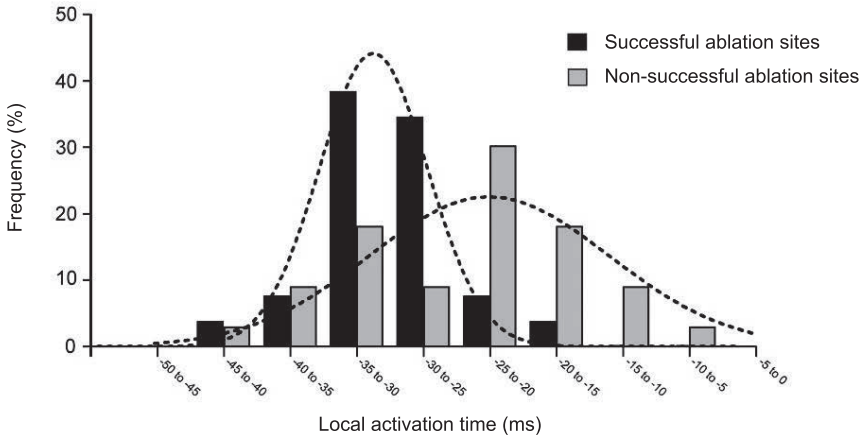

Figure 2. Frequency of local activation time (LAT) at successful ablation sites (black bars) versus non-successful ablation sites (grey bars). The dashed lines indicate the normal distribution of the LAT in the two groups. Please note the important overlap of LAT between successful and non-successful ablation sites.

Spatial distribution of electrogram characteristics

Local activation time, unipolar QS-configuration and the presence of reversed polarity were compared between 26 successful ablation sites and 139 area points within three different categories (Table 1). Local activation time was significantly earlier at successful ablation sites as compared to area points. The best cut-off value to discriminate between a successful ablation site and an area point was a LAT of -23ms. In addition, area points beyond a 5mm radius from the successful ablation site demonstrated less often a unipolar QS-configuration when compared to the successful ablation sites. However, no differences in unipolar electrogram morphology were found between successful ablation sites and area points within a 5mm radius. Moreover, the prevalence of a unipolar QS-configuration at distances between 6-10mm and 11-15mm remained high (63% and 53%, respectively) (Figure 3). Importantly, successful ablation sites showed significantly more often reversed polarity than area points across all categories. The sensitivity to discriminate between a successful ablation site and an area point was slightly higher for LAT (88%) as compared to a unipolar QS (85%) and the presence of reversed polarity (81%). However the specificity to identify a successful site was found to be significantly higher for reversed polarity (93%) as compared to LAT (71%) and a unipolar QS-configuration (35%) (Table 2).

Table 1. Spatial distribution of electrogram characteristics

	Successful ablation site	Area point		
		1 – 5mm	6 – 10mm	11 – 15mm
Number	26	43	51	45
LAT (ms)	-28±7	-21±8*	-18±8*	-18±8*
Unipolar QS-configuration, n (%)	22 (85)	37 (79)	32 (63) †	24 (53) ‡
Reversed polarity, n (%)	21 (81)	2 (5)*	3 (6)*	5 (11)*

LAT= Local activation time; * p<0.001 compared to successful ablation site; † p<0.05 compared to successful ablation site; ‡ p<0.02 compared to successful ablation site

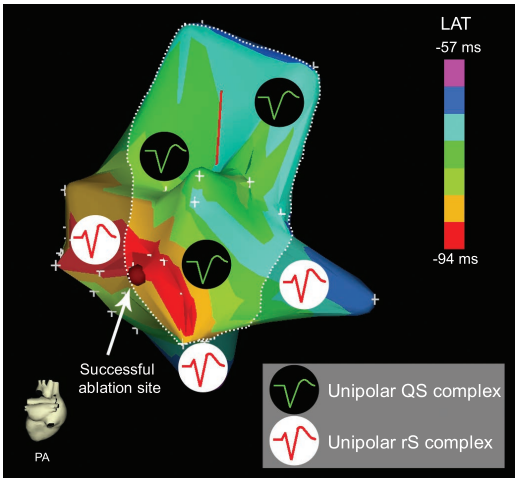

Figure 3. Electroanatomical activation map of a right ventricular outflow tract arrhythmia (posterior view)

Local activation time (LAT) is color coded with isochronal steps of 5ms according to the color bar. The white dotted line delineates the area around the successful ablation site (red tag) that demonstrated a unipolar QS-configuration. Black-with-green icons indicate areas demonstrating unipolar QS-configuration and white-with-red icons correspond to the area demonstrating a unipolar rS configuration.

Table 2. Electrogram characteristics

	Sensitivity	Specificity	NPV	PPV
LAT ≤-23ms	88	71	0.97	0.36
Unipolar QS-configuration	85	35	0.92	0.20
Reversed polarity	81	93	0.96	0.68

LAT= Local activation time; NPV= negative predictive value; PPV = positive predictive value

Comparison of two mapping strategies to predict a successful ablation site

To study the clinical impact of reversed polarity on the accuracy of electrophysiological mapping of idiopathic RVOT arrhythmias, a comparison was made between a conventional mapping strategy and a newly proposed mapping strategy including reversed polarity. For both strategies, LAT>-23ms was applied as the first criterion. If LAT was >-23ms, this mapping site could be excluded as a successful ablation site with a 97% likelihood. However, if LAT at a certain location was ≤-2ms, the accuracy to positively predict a successful ablation site was only 36%. After excluding mapping sites with LAT>-23ms the conventional mapping strategy used the presence of a unipolar QS-configuration as the second criterion to identify a successful ablation site whereas the new mapping strategy used the presence of reversed polarity. The presence of a unipolar QS-configuration identified the successful ablation site with 40% accuracy. In contrast, application of reversed polarity as the second criterion led to the identification of the successful ablation site with 86% accuracy (Figure 4). Moreover, mapping based on reversed polarity resulted in a net reclassification improvement of 0.189 (p=0.028). This index of reclassification illustrated that mapping based on LAT and reversed polarity resulted in a significant 'gain of certainty' to identify a successful RFCA site compared to conventional mapping based on LAT and unipolar QS-configuration.[24]

DISCUSSION

Key findings of the present study are: (1) the presence of reversed polarity was associated with a high likelihood for a successful RF application; and (2) mapping of idiopathic RVOT arrhythmia based on LAT and reversed polarity resulted in a higher predictive value for a successful ablation, compared to a conventional mapping strategy based on LAT and unipolar electrogram morphology.

Conventional mapping strategies

Several electrophysiological strategies have been described to guide RFCA of focal RVOT arrhythmias. Typically, mapping procedures are guided by unipolar and bipolar electrograms. Unipolar electrograms provide information about the direction of the wavefront: an initial positive deflection of the unipolar electrogram indicates propagation towards the mapping catheter

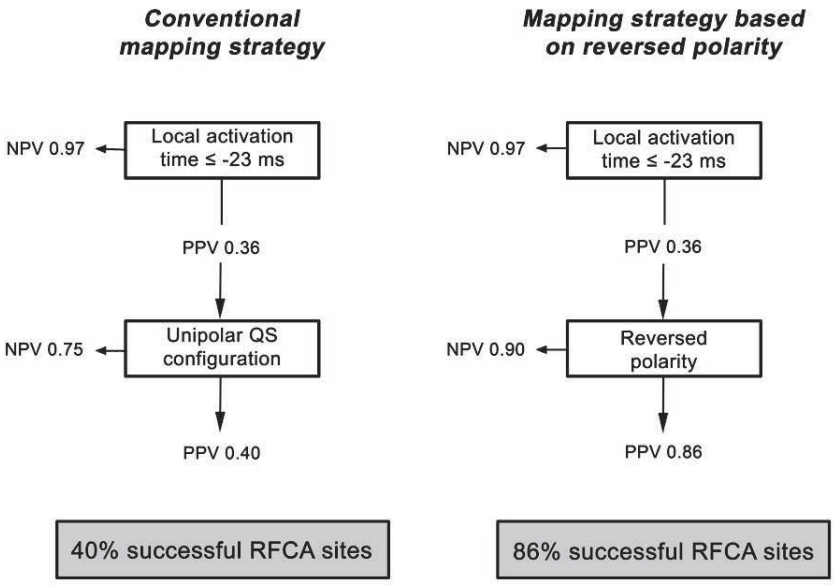

Figure 4. The predictive value of a new mapping strategy guided by local activation time (LAT) and reversed polarity was compared to a conventional mapping strategy guided by LAT and unipolar electrogram morphology. Both approaches use LAT as the primary selection criterion. The new approach uses reversed polarity as the second selection criterion whereas the conventional approach uses the unipolar electrogram morphology (i.e. presence of unipolar QS-configuration). NPV = negative predictive value; PPV = positive predictive value.

and has a high negative predictive value for a successful ablation site. As the wavefront reaches the electrode and propagates away, the deflection sweeps negative. When the electrode is located at the focal source the wavefront propagates away producing a monophasic QS complex. However, unipolar electrograms provide information about a large area and contain important far-filed signals. In contrast, in bipolar electrograms the far field signal is subtracted out thereby providing information about the local electrical activity, but do not contain information about the direction of the wavefront. Currently, most RFCA procedures for focal arrhythmias are guided by LAT defined by the initial peak of the bipolar electrogram and the rapid negative deflection of the unipolar electrogram, the unipolar electrogram morphology and pace-mapping. Although these criteria have demonstrated their practical value, each technique is associated with its own inherited limitations.[18,20,25,26] The spatial resolution of a good pace-map has been found to be 1.8±0.6 cm^2 and inferior to the spatial resolution of activation mapping. Based on this observation pace-mapping was not systematically investigated in our study.[26]

In the current study, LAT was significant earlier at successful ablation sites (-28±7ms) as compared to ablation sites that did not abolish the VA (22±8ms), which is in line with prior studies reporting LAT at effective sites between -24±7ms and -29±7ms.[3,26] However, we could demonstrate a significant overlap in LAT between successful and non-successful ablation sites. Although the best cut-off value for LAT (-23ms) to discriminate between a successful site and a

site in a proximity of less than 15mm provided a high negative predictive value, only a minority of successful sites could be identified correctly. This finding suggests that a cut-off value for LAT can be used to delineate the area of interest, but is not accurate enough to identify a site where RF energy should be applied. Furthermore, the current study confirms and extends prior observations that the area around a site of origin of a focal RVOT VA that exhibits a unipolar QS-configuration is considerably broad.[27] The wide spatial distribution of a unipolar QS is in line with the low additional value to predict a successful ablation site found in this study.

Reversed polarity

Reversed polarity of bipolar electrograms to guide ablation of focal RVOT arrhythmia was first suggested in a case report by Fisher et al using a custom-built orthogonal electrode array.[28] However, this method to target focal RVOT arrhythmias has not been applied in a large cohort of patients and using a standard quadripolar mapping catheter.

The use of reversed polarity to predict a successful ablation site is based on the hypothesis that rapid radial propagation from a focal source results in simultaneous deflection in opposite direction of the initial part of the bipolar electrograms. Provided that the bipoles are positioned orthogonally to the activation wavefront with the focal source ideally located between the bipoles. Due to the cylindrical anatomy of the RVOT it is possible to align a standard quadripolar mapping catheter orthogonally to the myocardial surface.

Indicating wavefront propagation in opposite direction, reversed polarity provides additional information to LAT. A focal source can be assumed if early local activation preceding the VA QRS is present and activation is observed in opposite directions. Combining these two electrogram characteristics is therefore likely to provide a reliable endpoint for catheter mapping. Accordingly, our suggested approach to map focal RVOT arrhythmias by combining LAT with reversed polarity resulted in a high negative predictive value, but importantly also in a high positive predictive value to identify a successful ablation site. In contrast, conventional mapping based on LAT and a unipolar QS-configuration had comparable negative predictive but poor positive predictive value.

Procedural aspects

Patients suffering from idiopathic focal RVOT arrhythmias are commonly young and healthy.[29] Therefore important goals when targeting focal RVOT arrhythmias are reduction of radiation exposure and number of RFCA applications needed to terminate the VA. Prior studies reported a mean fluoroscopy time up to 54 minutes targeting RVOT arrhythmias, whereas in the current study mean fluoroscopy time was only 13±8 minutes.[19,30] Moreover, the mean number of RFCA applications needed to terminate the VA ranged from 3 to 8 in previous studies, but could be reduced to only 2.3±1.8 RFCA applications in the current study.[19,26,30,31] These results indicate that implementation of reversed polarity is likely to reduce both radiation dose and number of RFCA applications.

Limitations

The present study comprised a relatively small number of patients. Therefore the results should be confirmed in a larger population. Furthermore, for statistical purposes LAT was dichotomized according to the cut-off value provided by the ROC-curve analysis, although this may not fully reflect clinical practice. In addition, during ablation target sites for RFCA were selected based on the combination of early LAT, the presence of a unipolar QS-configuration and the presence of reversed polarity. However, the decision to apply RF energy was made by the operator in a non-randomized fashion. The analyses of LAT, the presence of a unipolar QS-configuration and the presence of reversed polarity have been performed retrospectively. Ideally the newly proposed strategy, combining early LAT and reversed polarity presence, should have been validated prospectively. Finally, based on theoretical considerations the ablation catheter should be pulled back slightly when reversed polarity is recorded to ensure that the catheter tip is in the position of the second electrode. However, this was not systematically evaluated in the present study but seems to be unlikely to further reduce the number of RF applications needed.

Clinical implication

The presence of reversed polarity is easily to obtain and has a high predictive value to identify a successful ablation site in idiopathic focal RVOT arrhythmias. Combining LAT and reversed polarity can predict a successful ablation site with higher accuracy than conventional mapping based on LAT and unipolar QS-configuration. Its clinical application is likely to reduce the number of RFCA applications and radiation exposure to both patient and operator.

Conclusion

The presence of reversed polarity has a high predictive value for a successful ablation site in focal idiopathic RVOT arrhythmias. Combining local activation time and reversed polarity improves the accuracy of identifying the site of origin compared to conventional mapping strategies.

REFERENCES

1. Aliot EM, Stevenson WG, Almendral J, et al. EHRA/HRS Expert Consensus on Catheter Ablation of Ventricular Arrhythmias: developed in a partnership with the European Heart Rhythm Association (EHRA), a Registered Branch of the European Society of Cardiology (ESC), and the Heart Rhythm Society (HRS); in collaboration with the American College of Cardiology (ACC) and the American Heart Association (AHA). *Heart Rhythm*. 2009;6:886-933.
2. Takemoto M, Yoshimura H, Ohba Y, et al. Radiofrequency catheter ablation of premature ventricular complexes from right ventricular outflow tract improves left ventricular dilation and clinical status in patients without structural heart disease. *J Am Coll Cardiol*. 2005;45:1259-1265.
3. Sekiguchi Y, Aonuma K, Yamauchi Y, et al. Chronic hemodynamic effects after radiofrequency catheter ablation of frequent monomorphic ventricular premature beats. *J Cardiovasc Electrophysiol*. 2005;16:1057-1063.
4. Bogun F, Crawford T, Reich S, et al. Radiofrequency ablation of frequent, idiopathic premature ventricular complexes: comparison with a control group without intervention. *Heart Rhythm*. 2007;4:863-867.
5. Baman TS, Lange DC, Ilg KJ, et al. Relationship between burden of premature ventricular complexes and left ventricular function. *Heart Rhythm*. 2010;7:865-869.
6. Yarlagadda RK, Iwai S, Stein KM, et al. Reversal of cardiomyopathy in patients with repetitive monomorphic ventricular ectopy originating from the right ventricular outflow tract. *Circulation*. 2005;112:1092-1097.
7. Kobayashi Y, Miyata A, Tanno K, et al. Effects of nicorandil, a potassium channel opener, on idiopathic ventricular tachycardia. *J Am Coll Cardiol*. 1998;32:1377-1383.
8. Gill JS, Mehta D, Ward DE, Camm AJ. Efficacy of flecainide, sotalol, and verapamil in the treatment of right ventricular tachycardia in patients without overt cardiac abnormality. *Br Heart J*. 1992;68:392-397.
9. Borger van der Burg AE, de Groot NM, van Erven L, et al. Long-term follow-up after radiofrequency catheter ablation of ventricular tachycardia: a successful approach? *J Cardiovasc Electrophysiol*. 2002;13:417-423.
10. Calkins H, Kalbfleisch SJ, el-Atassi R, Langberg JJ, Morady F. Relation between efficacy of radiofrequency catheter ablation and site of origin of idiopathic ventricular tachycardia. *Am J Cardiol*. 1993;71:827-833.
11. Chinushi M, Aizawa Y, Takahashi K, Kitazawa H, Shibata A. Radiofrequency catheter ablation for idiopathic right ventricular tachycardia with special reference to morphological variation and long-term outcome. *Heart*. 1997;78:255-261.
12. Coggins DL, Lee RJ, Sweeney J, et al. Radiofrequency catheter ablation as a cure for idiopathic tachycardia of both left and right ventricular origin. *J Am Coll Cardiol*. 1994;23:1333-1341.
13. Zhou L, Keane D, Reed G, Ruskin J. Thromboembolic complications of cardiac radiofrequency catheter ablation: a review of the reported incidence, pathogenesis and current research directions. *J Cardiovasc Electrophysiol*. 1999;10:611-620.
14. Joung B, Lee M, Sung JH, et al. Pediatric radiofrequency catheter ablation: sedation methods and success, complication and recurrence rates. *Circ J*. 2006;70:278-284.
15. Morwood JG, Triedman JK, Berul CI, et al. Radiofrequency catheter ablation of ventricular tachycardia in children and young adults with congenital heart disease. *Heart Rhythm*. 2004;1:301-308.

16. Weiss C, Willems S, Rueppel R, Hoffmann M, Meinertz T. Electroanatomical Mapping (CARTO) of ectopic atrial tachycardia: impact of bipolar and unipolar local electrogram annotation for localization the focal origin. *J Interv Card Electrophysiol*. 2001;5:101-107.
17. Soejima Y, Aonuma K, Iesaka Y, Isobe M. Ventricular unipolar potential in radiofrequency catheter ablation of idiopathic non-reentrant ventricular outflow tachycardia. *Jpn Heart J*. 2004;45:749-760.
18. Barlow MA, Klein GJ, Simpson CS, et al. Unipolar electrogram characteristics predictive of successful radiofrequency catheter ablation of accessory pathways. *J Cardiovasc Electrophysiol*. 2000;11:146-154.
19. Ribbing M, Wasmer K, Monnig G, et al. Endocardial mapping of right ventricular outflow tract tachycardia using noncontact activation mapping. *J Cardiovasc Electrophysiol*. 2003;14:602-608.
20. Azegami K, Wilber DJ, Arruda M, Lin AC, Denman RA. Spatial resolution of pacemapping and activation mapping in patients with idiopathic right ventricular outflow tract tachycardia. *J Cardiovasc Electrophysiol*. 2005;16:823-829.
21. Yamane T, Shah DC, Jais P, et al. Electrogram polarity reversal as an additional indicator of breakthroughs from the left atrium to the pulmonary veins. *J Am Coll Cardiol*. 2002;39:1337-1344.
22. Damle RS, Choe W, Kanaan NM, et al. Atrial and accessory pathway activation direction in patients with orthodromic supraventricular tachycardia: insights from vector mapping. *J Am Coll Cardiol*. 1994;23:684-692.
23. Zeger SL, Liang KY. Longitudinal data analysis for discrete and continuous outcomes. *Biometrics*. 1986;42:121-130.
24. Pencina MJ, D'Agostino RB, Sr., D'Agostino RB, Jr., Vasan RS. Evaluating the added predictive ability of a new marker: from area under the ROC curve to reclassification and beyond. *Stat Med*. 2008;27:157-172.
25. Joshi S, Wilber DJ. Ablation of idiopathic right ventricular outflow tract tachycardia: current perspectives. *J Cardiovasc Electrophysiol*. 2005;16 Suppl 1:S52-S58.
26. Bogun F, Taj M, Ting M, et al. Spatial resolution of pace mapping of idiopathic ventricular tachycardia/ectopy originating in the right ventricular outflow tract. *Heart Rhythm*. 2008;5:339-344.
27. Man KC, Daoud EG, Knight BP, et al. Accuracy of the unipolar electrogram for identification of the site of origin of ventricular activation. *J Cardiovasc Electrophysiol*. 1997;8:974-979.
28. Fisher WG, Bacon ME, Swartz JF. Use of an orthogonal electrode array to identify the successful ablation site in right ventricular outflow tract tachycardia. *Pacing Clin Electrophysiol*. 1997;20:2188-2192.
29. Nakagawa M, Takahashi N, Nobe S, et al. Gender differences in various types of idiopathic ventricular tachycardia. *J Cardiovasc Electrophysiol*. 2002;13:633-638.
30. Peeters HA, Sippens Groenewegen A, Wever EF, et al. Clinical application of an integrated 3-phase mapping technique for localization of the site of origin of idiopathic ventricular tachycardia. *Circulation*. 1999;99:1300-1311.
31. Klein LS, Shih HT, Hackett FK, Zipes DP, Miles WM. Radiofrequency catheter ablation of ventricular tachycardia in patients without structural heart disease. *Circulation*. 1992;85:1666-1674.

Part II

New Developments in Real-Time Image Integration During Radiofrequency Catheter Ablation

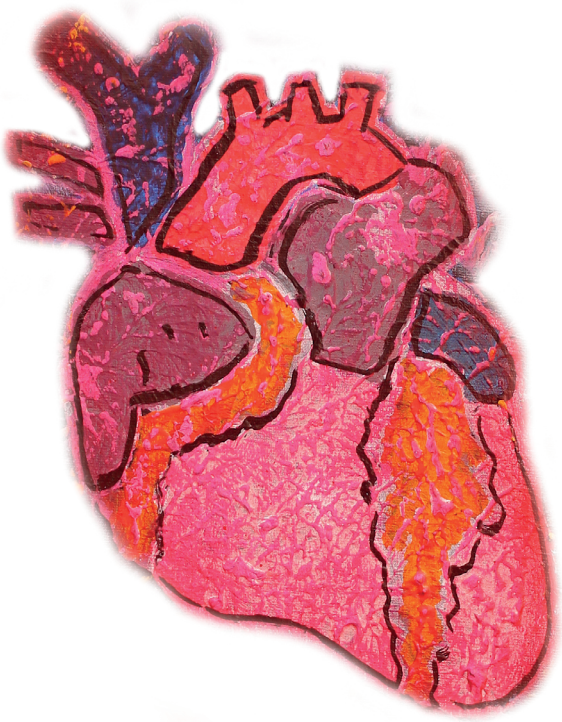

Chapter 5

Real-time integration of MDCT derived coronary anatomy and epicardial fat: Impact on epicardial electroanatomical mapping and ablation for ventricular arrhythmias

Carine F.B. van Huls van Taxis, Adrianus P. Wijnmaalen, Sebastiaan R.D. Piers, Rob J. van der Geest, Martin J. Schalij, Katja Zeppenfeld

JACC: Cardiovascular Imaging. 2013 Jan;6(1):42-52.

ABSTRACT

Objectives

This study aimed to evaluate the feasibility and accuracy of real-time integration of multi-detector computed tomography (MDCT) derived coronary anatomy and epicardial fat distribution and its impact on electroanatomical mapping and ablation.

Background

Epicardial catheter ablation for ventricular arrhythmias (VA) is an important therapeutic option in patients after endocardial ablation failure. However, epicardial mapping and ablation are limited by the presence of coronary arteries and epicardial fat.

Methods

Twenty-eight patients (21 male, age 59±16 years) underwent combined endo-epicardial electroanatomical mapping. Prior to the procedure, MDCT derived coronary anatomy and epicardial fat meshes were loaded into the mapping system (CARTO™). Real-time registration of MDCT data was performed after endocardial mapping. The distance between epicardial ablation sites and coronary arteries was assessed by registered MDCT and angiography. After the procedure, mapping and ablation points were superimposed on the MDCT using a reversed registration matrix for head-to-head comparison of mapping data and corresponding fat thickness.

Results

Image registration was successful and accurate in all patients (position error 2.8±1.3mm). At sites without evidence for scar epicardial bipolar voltage decreased significantly ($p<0.001$) with increasing fat thickness. Forty-six VA were targeted; 25 (54%) were abolished by catheter ablation, in 21 (46%) ablation failed. In 5 VA no target site was identified and in 3 adhesions prevented mapping. In 2 VA ablation was withheld due to His-bundle vicinity and in 7 due to proximity of coronary arteries. In 4 VA catheter ablation was ineffective. At ineffective ablation sites epicardial fat was significantly thicker compared to successful sites (16.9±6.8mm [range 7.3-22.2mm] and 1.5±2.1mm [range 0-6.1mm], $p=0.002$).

Conclusions

Real-time image integration of pre-acquired MDCT information is feasible and accurate. Epicardial fat of >7mm and the presence of coronary arteries are important reasons for epicardial ablation failure. Visualization of fat thickness during the procedure may facilitate interpretation of bipolar electrograms and identification of ineffective ablation sites.

INTRODUCTION

Epicardial electroanatomical mapping (EAM) followed by radiofrequency catheter ablation is an important therapeutic option in patients after endocardial ablation failure. However, despite the presence of a subepicardial substrate epicardial EAM and ablation may have important limitations. Bipolar voltage mapping might not be accurate to delineate subepicardial scar and can overestimate its extent as even thin layers of epicardial fat attenuate bipolar voltage.[1-3]

Once a potential ablation target site (TS) has been identified, ablation needs to be withheld in the vicinity of coronary arteries, usually visualized by repeated coronary injections, or may not be effective due to thick epicardial fat which presence can only be assumed when irrigated tip ablation is ineffective.[3,4] Cardiac multi-detector computed tomography (MDCT) can reliably visualize coronary arteries and epicardial fat.[5,6] Accurate real-time integration of MDCT derived coronary anatomy and fat distribution during the ablation procedure is therefore desirable.

The purpose of this study was (I) to evaluate epicardial fat distribution in patients undergoing combined endo-epicardial mapping and ablation, (II) to assess the feasibility and accuracy of real-time integration of MDCT derived coronary anatomy and fat distribution with EAM, (III) to determine the influence of fat thickness on epicardial bipolar and unipolar voltage and ablation outcome and (IV) to evaluate the potential use of integrated MDCT to identify inappropriate ablation sites.

METHODS

Patients and baseline evaluation

The study population consisted of 28 consecutive patients (21 male, 59±16 years) scheduled for combined endo-epicardial EAM and ablation.[7-9] Ethics committee approval was not necessary as all performed procedures were part of routine clinical protocol. Informed consent was obtained from all patients. Prior to the procedure patients underwent transthoracic echocardiography. When considered necessary, magnetic resonance imaging and/or nuclear imaging were performed for the presence of structural heart disease.

Pre-procedural MDCT acquisition and processing

Patients underwent cardiac MDCT prior to EAM using either a 64-detector row helical scanner (Aquillion 64; Toshiba multi-detector, Toshiba Medical Systems, Otawara, Japan) or a 320-detector row volumetric scanner (Aquillion ONE, Toshiba Medical Systems, Otawara, Japan). Patient's heart rate and blood pressure were monitored before the scan. In case of a heart rate ≥65bpm and in the absence of contra-indications beta-blocking medication was administered (metoprolol 50-100mg oral, or 5-10mg intravenous). Scan parameters depended on body posture. For the 64-row contrast-enhanced scan collimation was 64x0.5mm, tube voltage 100-135kV and a

tube current 250-350mA. For the 32-row contrast-enhanced scan, the heart was imaged in a single heartbeat using prospective triggering with exposure interval depending on the heart rate. Scan parameters were 350ms gantry rotation time, 100-135kV tube voltage and a tube current of 400-580mA. For both scans contrast material (lomeron 400, Bracco, Milan, Italy) was administered, 80-110mL or 60-90mL respectively, followed by saline flush.[5]

The MDCT data were analyzed using MASS software (V2009-EXP LKEB, Leiden, The Netherlands). The aortic, endocardial, pericardial and epicardial contours and the left main artery (LM) were traced (Figure 1A). The distance between the epicardial and pericardial contours was computed to assess epicardial fat thickness. A bull's eye reconstruction of the epicardial surface was created and divided into 3 equal long-axis segments (basal, mid and apical) and 8 equal short-axis segments A-H.[6] For each segment the mean epicardial fat thickness was calculated. The contours were converted into 3D meshes that could be imported into the EAM system (CARTO XP™, Biosense Webster Inc, Diamond Bar, CA, USA). The vertices of the epicardial surface mesh were color coded for fat thickness (Figure 1B). In addition, the original cardiac MDCT data were loaded into the CARTO system and cardiac structures were segmented. Prior to mapping all meshes and the segmented images were merged to a final fusion image (FFI) using CARTO-Merge (IPE) software enabling the registration and fusion of multiple datasets (Figure 1C). After the procedure all mapping and ablation points and registration matrix were exported from the CARTO system and superimposed on the corresponding short-axis MDCT slice using reversed registration (Figure 1D).

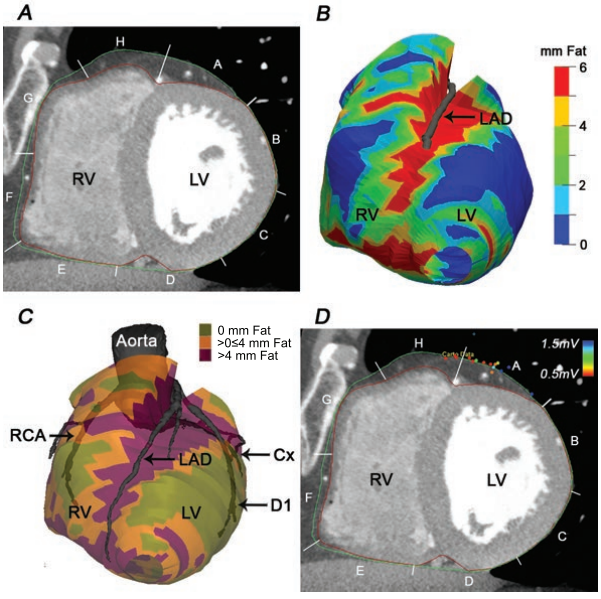

Figure 1.
Processing and integration of MDCT.
Panel A: Multi-detector computed tomography (MDCT) short axis slice with pericardial (green) and epicardial (red) contours divided into 8 segments A-H. Panel B: 3D epicardial surface mesh color coded for fat thickness. Panel C: MDCT derived aorta with coronary arteries merged with the epicardial fat meshes (color coded for fat thickness as indicated) into the final fusion image. Panel D: Same short axis slice as Panel A with reversed registration of epicardial mapping points projected on the corresponding MDCT location. Points are color coded for bipolar voltage (color bar). Cx=circumflex coronary artery; D1=first diagonal coronary artery; LAD=left anterior descending artery; LV=left ventricle; RCA=right coronary artery; RV=right ventricle"

Electrophysiological evaluation

Patients underwent programmed electrical stimulation and combined endo-epicardial EAM. Anti-arrhythmic drugs were discontinued for 5 half-lives, except for amiodarone (n=7). Stimulation consisted of 3 drive-cycle lengths, ≥3 ventricular extra stimuli and burstpacing at 2 right ventricular (RV) sites.

Electroanatomical mapping and real-time image integration

Pericardial access was obtained through a subxiphoid puncture (n=26) or by a surgical subxiphoidal window because of pericardial adhesions (n=2).[10] Limited EAM of the aortic root was performed with a 3.5mm, irrigated-tip catheter (NaviStar ThermoCool, Biosense Webster Inc, Diamond Bar, CA, USA). The mapping catheter was positioned in the ostium of the LM, confirmed by contrast injection through the catheter and the location was tagged on the map.[11] Secondly, an endocardial EAM of the left ventricle (LV) and/or RV was created. Electrograms were filtered at 30-400Hz (bipolar) and 1-240Hz (unipolar). Bipolar voltages <1.5mV were considered abnormal and <0.5mV dense scar.[12] The MDCT-derived images were aligned with the EAM using the LM location as a landmark for registration.[11] Subsequently, the surfaces of the LV or RV were aligned using CARTO-Merge software. Distances between the EAM and the FFI were calculated to evaluate registration accuracy.

Identification of target sites

In idiopathic ventricular arrhythmia (VA) LV, RV, aortic sinus and/or coronary venous system activation mapping was performed. If no TS could be identified, the potential epicardial TS was predicted based on the spatial distribution of earliest local activation time.[13] The local fat thickness and vicinity of coronary arteries was assessed prior to epicardial mapping (Figure 2A).

For scar-related VA, TS were selected based on activation and entrainment mapping for tolerated VA. For non-tolerated VA, TS were identified guided by pace-mapping (≥11/12 lead match between VA-QRS, stimulus-to-QRS interval >40ms) and the presence of late potentials (potentials separated by an isoelectric segment >20ms and inscribing after QRS).

Epicardial mapping and ablation

For idiopathic VA limited epicardial voltage mapping was performed, followed by activation mapping. In scar related VA, a regional epicardial voltage map was created of the target area.

Before epicardial ablation, the vicinity of coronary arteries was estimated on the FFI and categorized into 3 categories (<5mm, 5-15mm, >15mm). Subsequently, coronary angiography (LAO45°, RAO30°) was performed and the distance between catheter tip and coronary artery was evaluated on fluoroscopy using the length of the distal electrode pair (6.7mm) and tip-proximal-electrode distance (14.9mm) as a visual reference (Figure 3). The distances between the catheter tip and major coronary arteries on the FFI and fluoroscopy were compared to further evaluate the registration accuracy. If TS were in close proximity to a major branch ad-

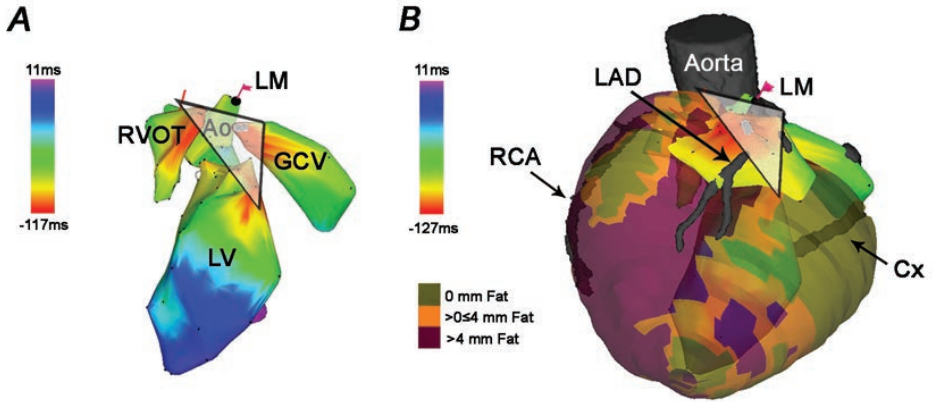

Figure 2.

Image integration: electroanatomical mapping and predicted target site in relation to MDCT derived epicardial fat thickness and coronary artery anatomy.

Panel A: Endocardial EAAM of the left ventricle (LV), right ventricle outflow tract (RVOT), aorta (Ao) and great cardiac vein (GCV). Similar activation time of the LV, RVOT and GCV was observed. The white triangle demonstrates the predicted epicardial target site in the vicinity of the left anterior descending artery (LAD), covered by >4mm fat. Panel B: The final fusion was registered with the endocardial EAAM, using the left main coronary artery landmark (LM). Limited epicardial EAAM confirmed the earliest activation within the predicted site not suitable for ablation.

Cx=Circumflex coronary artery; RCA=right coronary artery

ditional injections were performed to confirm the accuracy of spatial relation as measured on the FFI. Ablation was withheld when the estimated distance was <5mm. High output pacing was performed to determine the location of the phrenic nerve, if appropriate.

Radiofrequency energy was applied at 30-45W (maximum temperature 45ºC, flow 20-30ml/min, 60s) for endocardial TS and ≤50W (flow 20ml/min) for epicardial TS until pacing failed to capture and/or elimination of late potentials. Successful ablation sites were defined as sites where ablation terminated the VA and prevented re-inducibility. When short linear lesions were applied, non-inducibility after ablation regarded the ablation site as successful. In case the VA remained inducible after ablation, the site was considered non-successful. The endpoint of the procedure was non-inducibility of any VA, inability to identify TS or TS locations that prevented effective or did not allow radiofrequency delivery.

Follow-up

After discharge, patients were followed regularly at our outpatient clinic. Implantable cardioverter defibrillator interrogation was performed every 6 months. Therapy was regarded appropriate when delivered in response to any VA.

Post-procedural evaluation of the impact of epicardial fat

After the procedure, using the reversed registration, bipolar and unipolar voltages were correlated to epicardial fat thickness using only mapping points at sites with no evidence for scar

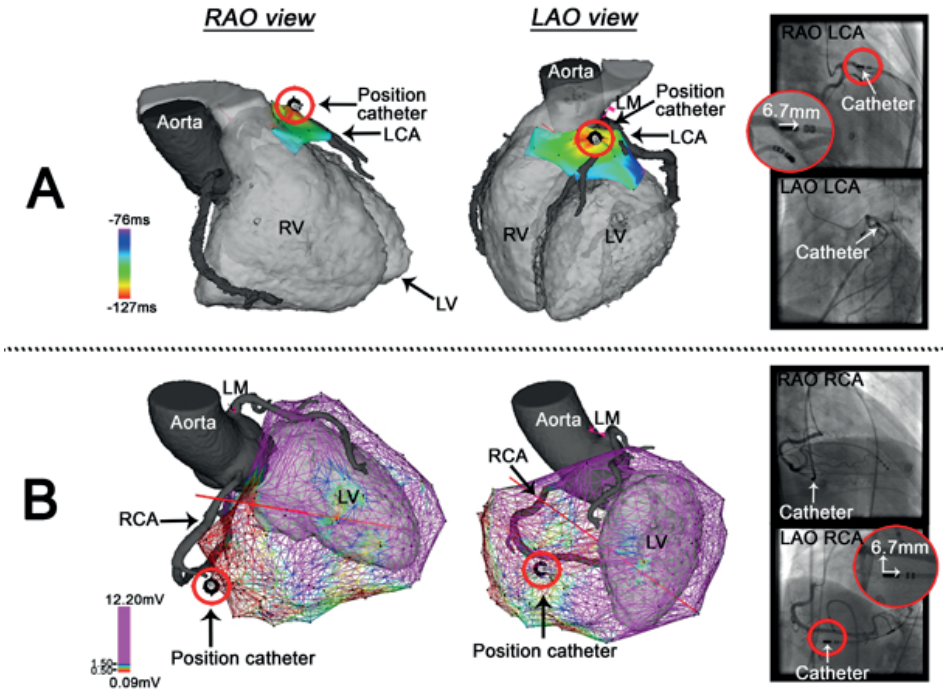

Figure 3.

Registration accuracy: comparing image integration with coronary angiography.

Registration accuracy in 2 patients comparing the distance between the catheter tip and coronary arteries on integrated multi-detector computed tomography (MDCT) images and coronary angiography in a right (RAO) and left (LAO) anterior oblique view. Upper panel: limited activation mapping identified a target site located on the left coronary artery (LCA) on both MDCT and angiography. Lower panel: the target site (based on pace-mapping) was located <7mm from the right coronary artery (RCA) confirmed by angiography.

LM=Left main artery; LV=Left ventricle; RV=Right ventricle

on imaging. Mapping points were grouped into 3 categories according to fat thickness (0mm, >0≤4mm and >4mm fat).[4] To investigate the impact of epicardial fat on ablation outcome, fat thickness at successful and non-successful ablation sites was compared.

Statistical analysis

Statistical analysis was performed using SPSS, version 18.0 (SPSS, Inc., Chicago, IL, USA). Continuous variables are expressed as mean±SD or median (interquartile range) when appropriate, and categorical variables as frequency (%). The Mann-Withney U-test was used to compare continuous variables between groups. Furthermore, the minimum and maximum value for epicardial fat thickness was noted at successful and non-successful target sites. All tests were two-tailed and a p-value <0.05 was considered statistically significant.

RESULTS

Baseline characteristics and pre-procedural MDCT processing

Baseline patient characteristics are summarized in Table 1. The epicardial surface covered by fat was 65±16%; 25±15% was covered by >4mm fat. The basal and apical anterior RV wall and the basal superior LV wall showed the thickest epicardial fat layer (5-6±3mm) (Online appendix Figure 1).

Table 1.

Patient characteristics	
Male gender (%)	21 (75)
Age, years	59±16
Body mass index, kg/m²	25±6
Diabetes mellitus (%)	5 (18)
LV ejection fraction,%	46±12
Etiology	
Idiopathic (%)	7 (25)
Ischemic (%)	2 (7)
ARVD/C (%)	3 (11)
LV-cardiomyopathy (%)	10 (36)
Biventricular-cardiomyopathy (%)	6 (21)

ARVD/C=Arrhythmogenic right ventricle dysplasia/cardiomyopathy; LV=left ventricle

Real-time image integration and registration accuracy

Endocardial voltage maps of the LV were obtained in 25 patients (structural heart disease 105±65 mapping points, idiopathic 50±25 mapping points) with an additional RV map in 9. In 3 patients only RV mapping was performed (67±23 points). Epicardial mapping was performed in all patients (structural heart disease 150±74 points, idiopathic 87±50 points). The MDCT derived images were successfully integrated with the aortic and LV and/or RV EAM with a surface registration error of 2.8±1.3mm.

Target sites and procedural outcome

In 22 patients 41 VA (cycle length 382±98ms) were induced; in 5 patients the clinical VA (idiopathic premature ventricular contractions) was present at baseline; in 1 patient no VA could be induced. All VA were targeted (Table 2). Seven VA (15%) in 5 patients were successfully ablated from the endocardium and 18 (39%) VA in 13 patients were successfully ablated from the epicardium (7.7±4.3 applications/VA). Ablation of 21 (46%) VA in 13 patients was non-successful, mainly due to ineffective ablation or proximity of the TS to coronary arteries.

Use of MDCT-derived coronary anatomy and epicardial fat distribution

To further evaluate the registration accuracy, the distances between 28 TS and coronary arteries on the FFI and coronary angiography were compared. In all cases the distance was confirmed by angiography (Figure 3, Table 2). In 2 patients ablation was successfully performed without acute complications despite the vicinity of coronary arteries; one patient had a TS near a functional occluded coronary artery, the other was in cardiogenic shock because of incessant VT. This patient died 6 weeks later due to progressive heart failure. No coronary artery lesion could be detected at autopsy (Online appendix Figure 2). Ineffective ablation sites were covered by >4mm fat (as delineated by the fat meshes) and located at the LV superior wall and RV anterior superior wall.

Procedural complications

In 1 patient epicardial bleeding (>80cm^3) occurred. There was no LM damage evaluated by angiography or procedure related death. Procedural time was 253±89 minutes and fluoroscopy time was 43±15 minutes.

Follow-up

During a mean follow-up of 27±15 months 5 patients died (4 heart failure; 1 cancer) and 1 patient underwent heart transplantation because of terminal heart failure. Of the remaining 22 patients, 11 patients experienced VA recurrence; all 7 patients with ablation failure (100%) and 4 (27%) who were non-inducible for any VA.

Post-procedural evaluation of the impact of epicardial fat

A total of 1046 epicardial mapping points was acquired at sites without evidence for scar. Twenty-two percent of these mapping points (n=232) were located at epicardium not covered by fat with a median bipolar voltage of 2.5mV (IQR 1.4-4.6mV) and median unipolar voltage of 7.5mV (IQR 5.4-12.0mV). Bipolar voltages decreased significantly with increasing fat thickness according to the predefined categories ($p<0.001$) (Figure 4A). However, 33% of mapping points at areas covered by >4mm fat showed bipolar voltages of >1.5mV (Figure 4B); using the previously suggested cut-off value of 2.8mm merely 37% of mapping points comprised bipolar voltage of >1.5mV.(3) Unipolar voltage was not influenced by fat (Figure 4C). Epicardial fat thickness was 19.0mm (IQR 9.7-21.9mm; minimum 7.3mm, maximum 22.2mm) at 4 non-successful ablation sites, as compared to 0.4mm (IQR 0.0-2.8mm; minimum 0.0mm, maximum 6.1mm) at 17 successful sites ($p=0.002$).

Predicted epicardial target sites in idiopathic VA

In the 7 idiopathic patients the earliest local activation was similar over a broad endocardial area (Δ local activation ≤10ms at ≥3 endocardial points >1.5cm apart) (n=2), at 2 remote endocardial sites (Δ local activation ≤10ms at 2 endocardial points >1.5cm apart) (n=1) or at both

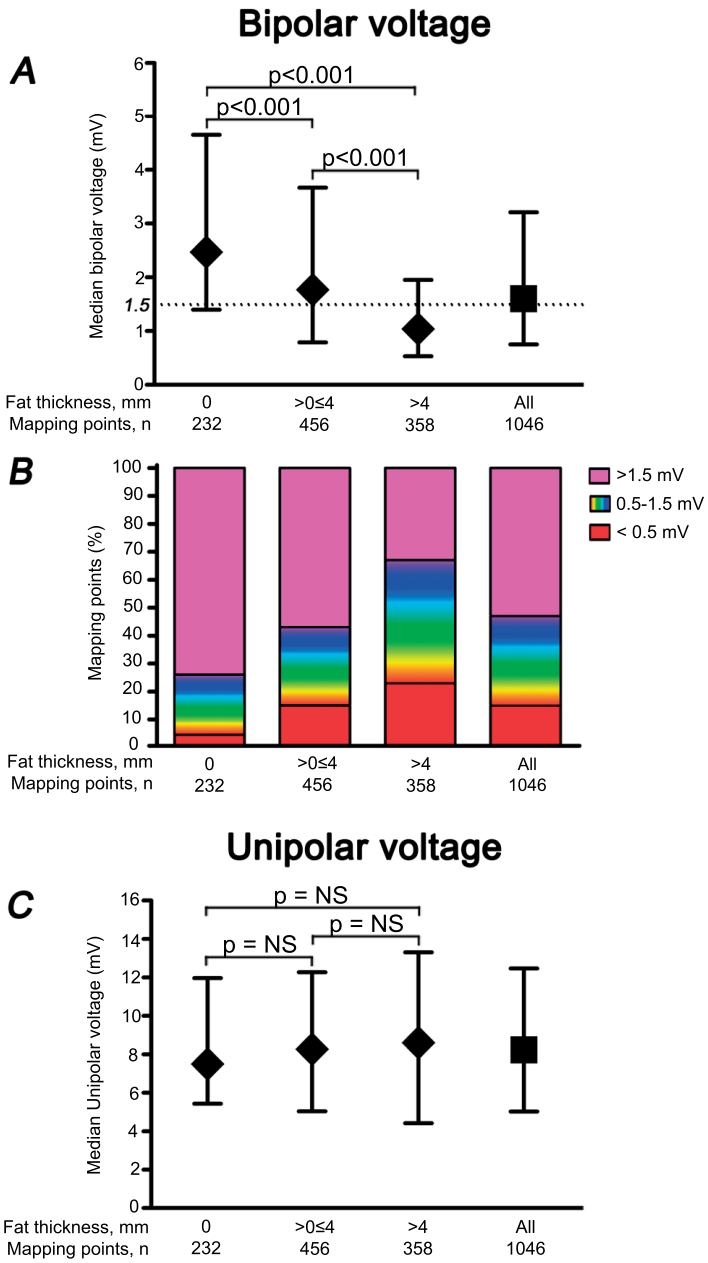

Figure 4.

Reversed registration: impact of epicardial fat on bipolar and unipolar voltages.

Panel A: Median bipolar voltage of epicardial mapping points according to the 3 epicardial fat thickness categories. Panel B: Distribution of epicardial mapping points for each epicardial fat thickness category according to the currently used cut-off values for bipolar voltage mapping. Panel C: Median unipolar voltage of epicardial mapping points according to the 3 epicardial fat thickness categories.

Table 2. Procedural characteristics

Pt no.	Age	Sex	BMI (kg/cm²)	Epi surface >4mm Fat(%)	Etiology	Epi mapping points	VA no.	VA CL	Mapping strategy	Target site	Mean fat thickness at TS(mm)	Acute ablation outcome	Failure reason	Vicinity to coronary artery
1	68	M	27.5	55	Idiopathic	106	1	PVC	A	LV sup	22.2±3.6	Failure	RF ineffective	LAD 5-15mm
2	76	M	19.9	13	LV-CMP	187	1	300	A+S	NI	NA	Failure	Unstable VA, no TS	NA
3	72	M	24.9	16	LV-CMP	173	1	270	A+S	LV inf-lat	2.2±2.1	Success		>15mm
							2	322	A+S	LV inf	1.3±0.7	Success		>15mm
4	57	F	19.8	17	Idiopathic	128	1	504	A	LV inf-lat	4.8±0.2	Success		RCA 5-15mm
5	59	M	24.9	18	ARVD/C	112	1	480	A+S	RV ant-sup	3.3±1.1	Success		RCA 5-15mm
6	62	M	34.7	37	LV-CMP	190	1	415	A+S	Septal	NA	Failure	TS near His	NA
							2	405	A+S	Septal	NA	Failure	TS near His	NA
7	18	M	20.9	4	Idiopathic	154	1	260	A	LV inf-lat	1.2±0.6	Success		RCA 5-15mm
8	22	M	18.8	12	ARVD/C	259	1	240	A+S	NI	NA	Failure	Unstable VA, no TS	NA
							2	190	A+S	NI	NA	Failure	Unstable VA, no TS	NA
9	40	M	19.9	13	Biv-CMP	246	0	-	S	NA	NA	-		NA
10	62	M	23.1	16	Ischemic	220	1	440	A+S	LV sup-lat	0.4±0.0	Success		>15mm
11	73	M	21.2	13	LV-CMP	189	1	458	A+S	LV inf	5.4±2.6	Failure	TS near RCA	RCA <5mm
12	74	M	23.3	30	Ischemic	182	1	310	A	RV diaphragmatic	6.1±3.4	Success		Functional occluded LAD <5mm
13	30	F	19.6	10	LV-CMP	172	1	243	S	LV sup-lat	0	Success		>15mm
							2	353	A+S	LV sup-lat	0	Success		>15mm

Table 2. Procedural characteristics (continued)

Pt no.	Age	Sex	BMI (kg/cm²)	Epi surface >4mm Fat(%)	Etiology	Epi mapping points	VA no.	VA CL	Mapping strategy	Target site	Mean fat thickness at TS(mm)	Acute ablation outcome	Failure reason	Vicinity to coronary artery
14	48	F	22.1	6	ARVD/C	97	1	253	A+S	RV sup	0	Success		>15mm
							2	250	A+S	RV sup	0	Success		>15mm
15	61	M	31.8	53	Biv-CMP	37	1	360	A+S	RV ant-inf	7.3±1.1	Failure	RF ineffective	RCA 5-15mm
							2	360	A+S	RV ant-inf-endo	NA	Success		NA
16	48	M	19.7	11	LV-CMP	176	1	520	A+S	LV sup-lat-endo	NA	Success		NA
							2	380	A+S	LV sup-lat-endo	NA	Success		NA
							3	430	A+S	LV inf-endo	NA	Success		NA
							4	430	A+S	LV inf-lat	0.4±1.0	Success		>15mm
17	65	M	29.7	36	Idiopathic	93	1	PVC	A	LV sup	10.8±5.8	Failure	TS near LAD	LAD <5mm
18	45	M	26.7	17	LV-CMP	92	1	340	S	LV sup-lat	0.3±0.3	Success		>15mm
							2	400	S	NI	NA	Failure	pericardial adhesions	NA
							3	440	S	NI	NA	Failure	pericardial adhesions	NA
							4	300	S	NI	NA	Failure	pericardial adhesions	NA
19	77	F	22.5	28	Biv-CMP	163	1	554	A+S	LV sup-lat	0	Success		Cx <5mm RF not withheld
20	70	M	23.1	48	Biv-CMP	18	1	230	S	RV ant-sup-endo	NA	Success		
21	71	M	34.3	21	LV-CMP	68	1	387	A+S	LV sup	1.3±1.2	Failure	TS near LAD	LAD <5mm
							2	621	A+S	LV sup	1.3±1.2	Failure	TS near LAD	LAD <5mm
							3	356	A+S	LV sup	1.3±1.2	Failure	TS near LAD	LAD <5mm
							4	387	A+S	LV sup	1.3±1.2	Failure	TS near LAD	LAD <5mm

Table 2. Procedural characteristics (continued)

Pt no.	Age	Sex	BMI (kg/cm²)	Epi surface >4mm Fat(%)	Etiology	Epi mapping points	VA no.	VA CL	Mapping strategy	Target site	Mean fat thickness at TS(mm)	Acute ablation outcome	Failure reason	Vicinity to coronary artery
22	54	M	26.8	23	Idiopathic	61	1	PVC	A	LV sup	21.0±5.0	Failure	RF ineffective	RCA 5-15mm
23	69	M	28.4	45	Biv-CMP	80	1	350	A+S	RV ant-inf-endo	NA	Success		
24	71	M	38.7	53	LV-CMP	50	1	375	A+S	LV sup	17.1±2.0	Failure	RF ineffective	LAD 5-15mm
25	66	F	24.2	21	Biv-CMP	273	1	500	A+S	LV inf	0.1±0.3	Success		>15mm
							2	430	A+S	RV sup	0.7±1.4	Success		>15mm
26	69	M	24.0	19	Idiopathic	33	1	PVC	A	LV sup	5.5±0.3	Success		LAD 5-15mm
27	59	F	25.5	11	LV-CMP	159	1	430	S	LV sup-lat-endo	NA	Success		NA
							2	360	S	LV inf-lat-endo	NA	Success		NA
							3	350	S	NI	NA	Failure	Unstable VA, no TS	NA
							4	280	S	NI	NA	Failure	Unstable VA, no TS	NA
28	57	F	36.8	43	Idiopathic	32	1	PVC	A	LV sup	20.2±7.6	Failure	TS near LAD	LAD <5mm

A = Activation mapping; Ant = Anterior; ARVD/C = Arrhythmogenic right ventricular dysplasia/cardiomyopathy; Biv = Biventricular; CL = Cycle length; CMP = Cardiomyopathy; Cx = Circumflex artery; EF = Ejection fraction; Endo = endocardial; Epi = epicardial; F = Female; Inf = Inferior; LAD = Left anterior descending coronary artery; Lat = Lateral; LV = Left ventricle; M = Male; NA = Not applicable; NI = Not identified; PVC = Premature ventricular complex; RCA = Right coronary artery; RF = Radiofrequency energy; S = Substrate mapping; Sup = Superior; VT = Ventricular arrhythmia

an endocardial and aortic sinus/cardiac venous site (n=4) suggesting an epicardial TS. The predicted potential epicardial TS after endocardial/aortic/cardiac venous system-mapping and its distance to the coronary arteries and fat thickness was confirmed after epicardial EAM and reversed registration in all patients. The area was located near (<5mm) a coronary artery in 2 patients (no ablation) (Figure 2B). In 2 patients the TS was covered by 21.0-22.2mm fat and ablation was ineffective. In 3 patients the TS was located remote (range 7.3-11.5mm) from a coronary artery and covered by 3.8±2.3mm fat. Ablation at these sites abolished the VA.

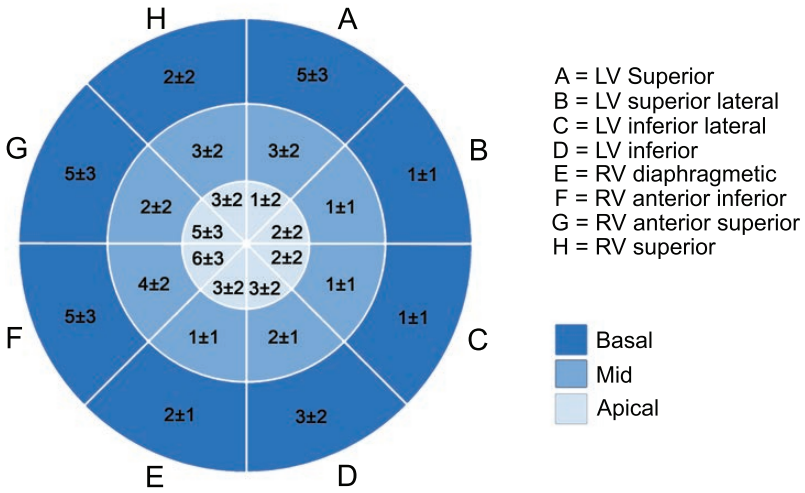

Figure 5
The 24 segments bull's eye reconstruction with 8 short axis segments and 3 long axis segments. For each segment the mean epicardial fat thickness (mm) is indicated.

DISCUSSION

The distribution of epicardial fat and coronary anatomy varies between patients. Both are of key relevance during epicardial mapping and ablation. This study is the first to demonstrate the feasibility and accuracy of real-time integration of MDCT derived images to visualize both, the coronary anatomy and fat distribution even before epicardial mapping. In 62% of patients with epicardial ablation failure, lack of success was related to the proximity of a coronary artery or thick fat correctly identified using image integration.

Accuracy of real-time image integration

Image integration was performed using the LM as a single landmark and the surface registration tool provided by the CARTO system after limited endocardial mapping. This approach resulted in highly accurate integration of MDCT data, verified with surface registration statistics with a

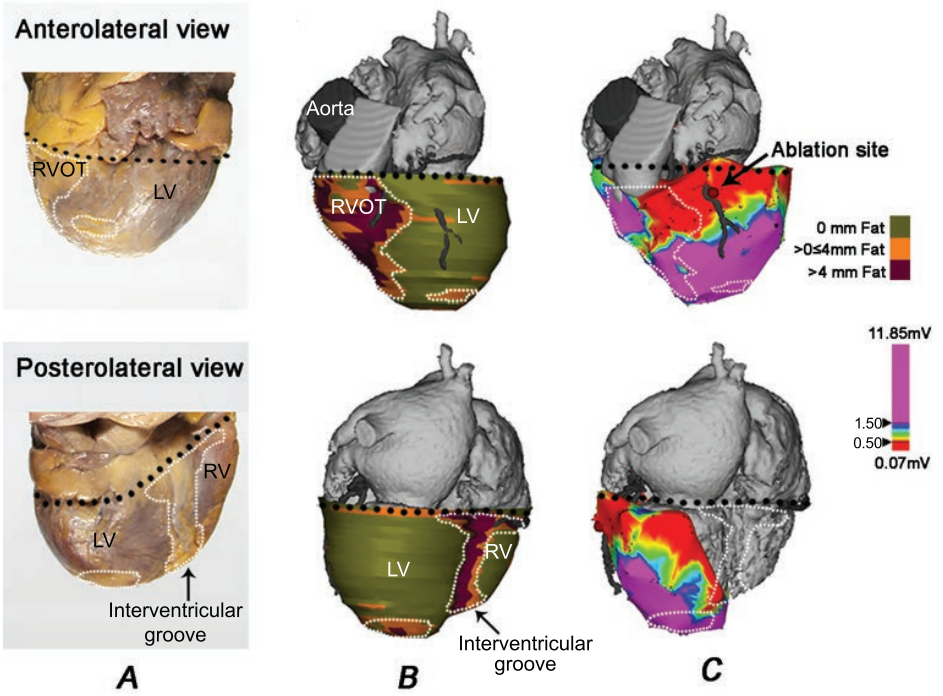

Figure 6.
Panel A: Gross pathology of the heart of the patient who died 4 weeks after ablation. Panel B: Final fusion image. Panel C: Fusion of the multi-detector computed tomography (MDCT) anatomy with the epicardial electroanatomical voltage map in a modified anterolateral (top) and posterolateral (bottom) view. The ablation site in the vicinity of the circumflex coronary artery is indicated. Comparison of panel A and B shows a good correlation between epicardial fat distribution by pathology and the MDCT derived epicardial fat mesh (white dotted lines). The black line indicates the atrioventricular groove; the anterolateral low voltage area (color coded as indicated) is compatible with subepicardial scar in the absence of epicardial fat. LV = left ventricle, RV = right ventricle, RVOT = right ventricle outflow tract.

mean surface registration error of only 2.8mm. After confirmation of the registration accuracy by a single coronary injection, the distance between TS and coronary arteries can be accurately assessed on integrated MDCT. In all 14 patients in whom the TS was located in the proximity of a coronary artery, the distance was estimated correctly. Therefore in most cases, the decision to perform ablation can be solely based on the MDCT image integration. However, when MDCT image integration demonstrate the TS to be in close proximity to a relevant coronary artery branch, additional limited coronary injections may still be necessary.

The demonstrated correspondence of the distance between catheter position and coronary arteries on integrated MDCT and angiography has important practical implications. After confirmation of the registration accuracy by a single coronary injection, the distance between TS and coronary arteries can be evaluated by integrated MDCT only. Although additional limited contrast injection may still be necessary in case of a TS in close proximity to a major branch, or when small arteries, such as diagonal and obtuse marginal branches are not accurately visual-

ized on MDCT, in most cases image integration is likely to prevent multiple coronary injections in different angulations. It may even enable more accurate assessment of the proximity of a coronary artery if angiography in some angulations is limited by the location triangle of the EAM system.

Epicardial fat and voltage mapping

Up to 64% of the epicardial surface was covered with fat and 25% with >4mm. Epicardial fat was not restricted to the atrio- and interventricular groove as assumed by others.[1-3] It can attenuate bipolar voltages thereby preventing accurate delineation of subepicardial scar by bipolar voltage mapping. A fat layer ≥2.8mm was suggested to best separate low voltage (<1.5mV) from normal voltage in a prior study.[3] However, our newly proposed technique of reversed registration allowed a head-to-head comparison of local voltage data and fat thickness. Although we could confirm a decrease in bipolar voltages with increasing fat thickness, up to 60% of mapping points acquired in areas with fat and >37% of points acquired in areas with ≥2.8mm fat showed normal bipolar voltages. These findings underline the importance of accurate MDCT derived fat information to avoid underestimation of the presence of a significant epicardial fat layer.

In contrast to prior observations this study demonstrates that unipolar voltage is not influenced by epicardial fat which may be caused by the larger field of view.[3,14,15] Therefore, unipolar voltage mapping may be useful for identification of subepicardial or intramural scar even when thick fat is present.

Epicardial fat and impact on ablation

Epicardial fat was thickest at the LV superior and RV anterior wall, which is in line with prior investigations.[6] Of interest, all ineffective ablation lesions were located in these areas. In a prior study epicardial cooled tip ablation was unable to produce lesions when applied at sites covered by a fat layer >3.5mm.[4] However, this was tested for only 3 applications in an animal model. In humans, Desjardins et al. compared fat thickness of 12 effective and 4 ineffective epicardial cooled-tip ablation sites; all ineffective ablation sites were covered by 10.8-14.6mm fat while effective ablation sites were all located at sites covered by <1.8mm fat.[3] Therefore, a cut-off value for epicardial fat thickness precluding effective ablation remained undetermined.

In the current study, ablation was performed at 21 epicardial sites covered by 0-22.2mm fat, including 6 sites covered by 3.0-10.0mm fat. Fat thickness at ineffective ablation sites ranged from 7.3-22.2mm. In contrast, all effective ablation sites were covered by 0-6.1mm fat. These findings suggest that epicardial fat up to 7mm allows for effective irrigated tip ablation in humans.

Predicted epicardial target sites in idiopathic VA

Real-time visualization of coronary anatomy and epicardial fat before obtaining epicardial access might be particularly important in patients with idiopathic focal arrhythmias. Based

on local activation times we could not only correctly predict the epicardial TS but also, using the integrated MDCT, the proximity of coronary arteries and fat thickness at these TS before epicardial access. Consequently, image integration may predict potential ablation failure and may thereby prevent unnecessary epicardial access in selected patients.

Limitations

The comparison of successful and non-successful ablation sites was performed retrospectively. The validation of a cut-off value of >7mm for epicardial fat preventing effective ablation should be performed in a prospective manner in a larger group of patients. Although MDCT derived fat distribution cannot directly be verified using fluoroscopy, the 3D coordinates for fat meshes and coronary anatomy were derived from the same MDCT suggesting an identical accuracy to delineate fat thickness.

The additional value of electrogram characteristics for delineation of scar was not analyzed, since the current gold standard to delineate scar (contrast-enhanced magnetic resonance imaging) was not available during the procedure in all patients. However, the objective of this study was to demonstrate the clinical value of real-time image integration of MDCT derived data and to determine the influence of epicardial fat thickness on bipolar and unipolar electrogram voltages. Therefore, only areas without evidence for scar were evaluated.

Conclusion

Real-time image integration of pre-acquired MDCT data on coronary anatomy and epicardial fat using the LM as a single landmark with EAM is safe, accurate and feasible and available before epicardial access. One fourth of the epicardial surface is covered by >4mm fat which is predominantly present at the LV superior wall and RV anterior wall. Although bipolar voltages decrease with increasing fat thickness the exact delineation of fat based on bipolar voltage is poor and may even be worse if subepicardial scar is present. In contrast, unipolar voltages are not influenced by fat and might therefore be superior to identify scar covered by fat.

Epicardial fat of >7mm and the presence of coronary arteries are important reasons for epicardial ablation failure. The distance between ablation target sites and main coronary artery branches can be assessed by visualization of the MDCT-derived coronary anatomy. Visualization of fat thickness may facilitate interpretation of bipolar electrograms and identification of ineffective ablation sites. Finally, accurate image integration after endocardial ablation failure for focal VA may even prevent unnecessary pericardial access and thereby potential complications in selected patients.

REFERENCES

1. Saba MM, Akella J, Gammie J, et al. The influence of fat thickness on the human epicardial bipolar electrogram characteristics: measurements on patients undergoing open-heart surgery. *Europace*. 2009;11:949-953.
2. Tung R, Nakahara S, Ramirez R, et al. Distinguishing epicardial fat from scar: analysis of electrograms using high-density electroanatomic mapping in a novel porcine infarct model. *Heart Rhythm*. 2010;7:389-395.
3. Desjardins B, Morady F, Bogun F. Effect of epicardial fat on electroanatomical mapping and epicardial catheter ablation. *J Am Coll Cardiol*. 2010;56:1320-1327.
4. d'Avila A, Houghtaling C, Gutierrez P, et al. Catheter ablation of ventricular epicardial tissue: a comparison of standard and cooled-tip radiofrequency energy. *Circulation*. 2004;109:2363-2369.
5. van Velzen JE, Schuijf JD, de Graaf FR, et al. Diagnostic performance of non-invasive multidetector computed tomography coronary angiography to detect coronary artery disease using different endpoints: detection of significant stenosis vs. detection of atherosclerosis. *Eur Heart J*. 2011;32:637-645.
6. Abbara S, Desai JC, Cury RC, et al. Mapping epicardial fat with multi-detector computed tomography to facilitate percutaneous transepicardial arrhythmia ablation. *Eur J Radiol*. 2006;57:417-422.
7. Berruezo A, Mont L, Nava S, et al. Electrocardiographic recognition of the epicardial origin of ventricular tachycardias. *Circulation*. 2004;109:1842-1847.
8. Daniels DV, Lu YY, Morton JB, et al. Idiopathic epicardial left ventricular tachycardia originating remote from the sinus of Valsalva: electrophysiological characteristics, catheter ablation, and identification from the 12-lead electrocardiogram. *Circulation*. 2006;113:1659-1666.
9. Valles E, Bazan V, Marchlinski FE. ECG criteria to identify epicardial ventricular tachycardia in nonischemic cardiomyopathy. *Circ Arrhythm Electrophysiol*. 2010;3:63-71.
10. Sosa E, Scanavacca M, d'Avila A, Pilleggi F. A new technique to perform epicardial mapping in the electrophysiology laboratory. *J Cardiovasc Electrophysiol*. 1996;7:531-536.
11. Wijnmaalen AP, van der Geest RJ, van Huls van Taxis CF, et al. Head-to-head comparison of contrast-enhanced magnetic resonance imaging and electroanatomical voltage mapping to assess post-infarct scar characteristics in patients with ventricular tachycardias: real-time image integration and reversed registration. *Eur Heart J*. 2011;32:104-114.
12. Marchlinski FE, Callans DJ, Gottlieb CD, Zado E. Linear ablation lesions for control of unmappable ventricular tachycardia in patients with ischemic and nonischemic cardiomyopathy. *Circulation*. 2000;101:1288-1296.
13. van Huls van Taxis CF, Wijnmaalen AP, den Uijl DW, et al. Reversed polarity of bipolar electrograms for predicting a successful ablation site in focal idiopathic right ventricular outflow tract arrhythmias. *Heart Rhythm*. 2011;8:665-671.
14. Hutchinson MD, Gerstenfeld EP, Desjardins B, et al. Endocardial unipolar voltage mapping to detect epicardial ventricular tachycardia substrate in patients with nonischemic left ventricular cardiomyopathy. *Circ Arrhythm Electrophysiol*. 2011;4:49-55.
15. Polin GM, Haqqani H, Tzou W, et al. Endocardial unipolar voltage mapping to identify epicardial substrate in arrhythmogenic right ventricular cardiomyopathy/dysplasia. *Heart Rhythm*. 2011;8:76-83.

Chapter 6

Epicardial Substrate Mapping for Ventricular Tachycardia Ablation in Patients with Nonischemic Cardiomyopathy: A New Algorithm to Differentiate Between Scar and Viable Myocardium Developed by Simultaneous Integration of CT and Contrast-Enhanced MRI

Sebastiaan R.D. Piers, Carine F.B. van Huls van Taxis, Qian Tao, Rob J. van der Geest, Said F. Askar, Hans-Marc J. Siebelink, Martin J. Schalij, Katja Zeppenfeld

European Heart Journal. 2013;34:586-596

ABSTRACT

Background

During epicardial electroanatomical mapping (EAM) it is difficult to differentiate between fibrosis and fat, as both exhibit attenuated bipolar voltage (BV). The purpose of this study was to assess whether unipolar voltage (UV), BV and electrogram characteristics (EC) can distinguish fibrosis from viable myocardium and fat during epicardial EAM for ventricular tachycardia (VT) ablation in nonischemic cardiomyopathy (NICM).

Methods and Results

Ten NICM patients (7 males, 56±13 years) with VT underwent epicardial EAM with real-time integration of CT-derived epicardial fat and contrast-enhanced MRI-derived scar. BV (filtered 30-400Hz), UV (filtered 1-240Hz) and EC (duration and morphology) were correlated with the presence of fat and scar. At sites devoid of fat, the optimal cutoff values to differentiate between scar and myocardium were 1.81mV for BV and 7.95mV for UV. BV, UV and electrogram duration >50ms distinguished scar from myocardium in areas covered with <2.8mm fat (all $p<0.001$), but not ≥2.8mm fat. In contrast, electrogram morphology-characteristics could also detect scar covered with ≥2.8mm fat ($p=0.001$). A newly developed 3-step algorithm combining electrogram morphology, duration and UV could correctly identify scar with a sensitivity of 75%. UV but not BV could detect intramural scar in the absence of fat.

Conclusions

Both BV ≤1.81mV and UV ≤7.95mV are useful for detection of scar during epicardial EAM, in the absence of ≥2.8mm fat. However, EC can be used to detect scar covered with fat. A newly developed algorithm combining UV and EC can differentiate between scar and viable myocardium. UV but not BV could detect intramural scar.

INTRODUCTION

The substrate for ventricular tachycardia (VT) in patients with left ventricular (LV) nonischemic cardiomyopathy (NICM) is frequently located intramurally or epicardially and may require an epicardial ablation approach.[1,2] Since the majority of induced VTs are haemodynamically unstable,[3] substrate mapping is indispensable for successful ablation. Epicardial substrate mapping is however challenging. Firstly, it may be difficult to differentiate between scar and epicardial fat, since both exhibit attenuated bipolar electrogram amplitudes.[4,5] Secondly, even in the absence of epicardial fat, scar may be difficult to detect if located intramural.

Electrogram characteristics have been proposed to distinguish scar from epicardial fat[4] since long electrogram duration, fragmented electrograms and late potentials indicate slow conduction typical for inhomogeneous scar.[6] However, subtle bipolar electrogram abnormalities such as low-amplitude late potentials may be reduced to noise level by the interposition of epicardial fat. Unipolar voltage has been demonstrated to have a larger field of view,[7] which may allow detection of scar covered by fat and intramural scar.

Computed tomography (CT) and contrast-enhanced magnetic resonance imaging (CE-MRI) are considered gold standards for delineation of fat and fibrosis. Prior studies have demonstrated the feasibility and accuracy of integration of CT-derived epicardial fat[5] and CE-MRI-derived fibrosis[8,9] with electroanatomical maps (EAM). By integrating both CT- and CE-MRI-derived data during substrate mapping, gold standards for the presence of fat and fibrosis become available.

The purpose of this study was to (1) establish bipolar and unipolar voltage cutoff values for scar detection during epicardial EAM, (2) assess whether voltages and electrogram characteristics can distinguish scar from viable myocardium in the presence of fat, (3) develop an algorithm that differentiates between scar and viable myocardium and (4) to determine whether the epicardial area of interest containing ablation target sites can be delineated using voltage or electrogram characteristics.

METHODS

Patients

The study population consisted of 10 out of 11 consecutive patients with NICM referred for combined endocardial and epicardial VT ablation, with integration of both CT-derived epicardial fat and CE-MRI-derived scar information. One patient was excluded because of imaging artifacts causing non-interpretable CE-MRI image data. Coronary artery disease was excluded by coronary angiography in all patients. Seven patients underwent combined endocardial and epicardial VT ablation after endocardial ablation failure which was presumed to be due to an epicardial VT exit site based on the lack of early endocardial activation during VT and/or an en-

docardial substrate for VT. In the remaining 3 patients, an epicardial VT exit site was suspected based on the 12-lead ECG morphology of the clinical VT.[10]

Six patients with idiopathic ventricular arrhythmias (VA) who underwent endocardial and epicardial EAM with CT integration served as controls for voltages and electrogram characteristics. Structural heart disease was excluded by echocardiography and CT in 6 patients (100%), by coronary angiography in 5 patients (83%) and by MRI in 4 patients (67%). All 6 patients underwent combined endocardial and epicardial ablation after endocardial ablation failure and an endocardial activation pattern consistent with an epicardial site of origin. All patients were treated according to the clinical protocol and provided informed consent.

CT acquisition and processing

Before the procedure, electrocardiogram-gated cardiac CT imaging was performed with intravenous iodinated contrast agent either on a 64-detector row helical scanner or a 320-detector row volumetric scanner (Toshiba Medical Systems, Otawara, Japan). Using in-house developed software (Mass, V2009-EXP LKEB, Leiden, The Netherlands) the endocardial, epicardial and pericardial contours were manually traced on short-axis reformatted CT slices (0.5x0.5mm resolution, 2mm thickness, 2mm inter-slice gap) to create 3D meshes (Figure 1). Fat thickness was computed by calculating the distance between epicardial and pericardial contours and the vertices of the epicardial 3D mesh were color-coded for fat thickness. Subsequently, the original CT data and the meshes were imported into the mapping system (CARTO XP™, Biosense Webster Inc, Diamond Bar, CA, USA). Using CARTOMerge (IPE) software, which enables integration of multiple datasets, the ventricles, aorta and coronary arteries were segmented and merged with the 3D meshes.

CE-MRI acquisition and processing

Contrast-enhanced MRI was performed on a 1.5 T Gyroscan ACS-NT/Intera MR system (Philips Medical Systems, Best, The Netherlands). A standardized protocol was followed, including a black-blood turbo spin-echo sequence for the proximal aorta.[9] Contrast- enhanced images were acquired 15min after bolus injection of gadolinium. The heart was imaged in one breath-hold with 20–24 imaging levels (dependent on heart size) in short-axis views.

The images were post-processed as described previously.[9] The centerline of the proximal coronary arteries was manually defined in the black-blood spin-echo image data and the aortic, endocardial and epicardial contours were semi-automatically detected on the short axis views. The contours were converted into 3D meshes (Mass research software, Figure 1). Myocardial tissue with ≥35% of maximal signal intensity was considered scar. The vertices of the LV endocardial and epicardial meshes were color-coded with scar transmurality for the inner and outer half of the wall, respectively. All meshes were imported into the CARTO system using CARTOMerge (IPE) software.

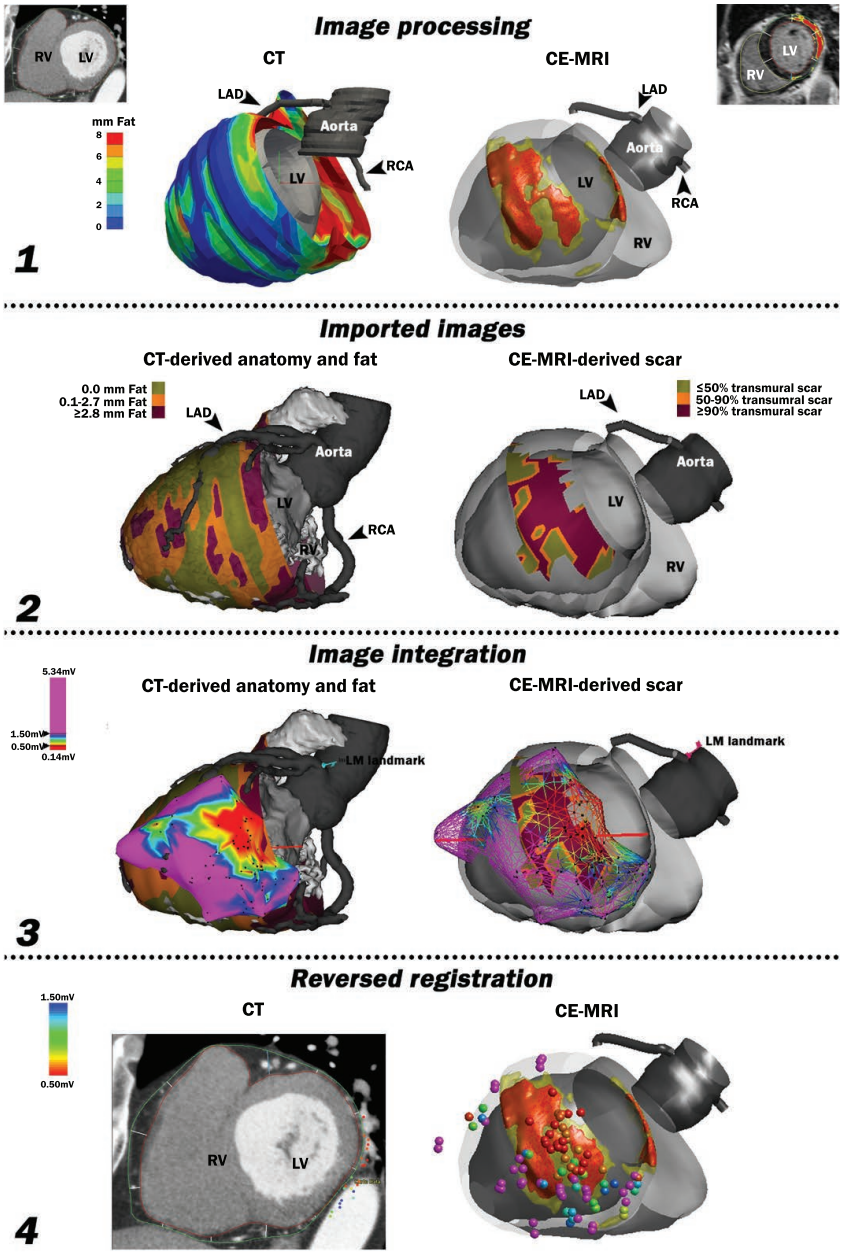

Figure 1. Processing and integration of CT and contrast-enhanced MRI

Step 1. Epicardial fat meshes and 3D scar reconstructions were created from the short-axis CT and CE-MRI slices. Step 2. Before the procedure, the CT was segmented and all meshes were imported into the mapping system. Step 3. During the procedure, CT- and CE-MRI-derived images were integrated with the electroanatomical map (displayed as a mesh to better visualize the scar distribution [right]) Step 4. After the procedure, points were projected on the corresponding short-axis CT slices and the 3D scar reconstruction to determine fat thickness and the presence of underlying scar.

CE-MRI denotes contrast-enhanced MRI; LAD, left anterior descending; LM, left main; LV, left ventricle; RCA, right coronary artery; RV, right ventricle.

Electrophysiological evaluation

Anti-arrhythmic drugs were discontinued for ≥5 half-lives with the exception of amiodarone (n=1). Programmed electrical stimulation was performed under conscious sedation (3 drive cycle lengths [600, 500 and 400ms], 1-3 ventricular extrastimuli [≥200ms] from 2 right ventricular (RV) sites and burst pacing (CL≥200ms), repeated with isoproterenol (2-10μg/min) when necessary). A positive endpoint for stimulation was the induction of sustained monomorphic VT lasting >30s or requiring termination because of hemodynamic compromise.

Electroanatomical mapping, real-time image integration and ablation

Pericardial access was obtained through a subxyphoid puncture followed by intravenous heparin administration. Electroanatomical mapping was performed using a 3.5mm irrigated-tip catheter with a 2mm ring electrode and a 1mm interelectrode spacing (NaviStar ThermoCool, Biosense Webster Inc, Diamond Bar, CA, USA) and the CARTO^{XP} system. Electrograms were filtered at 30-400Hz (bipolar) and 1-240Hz (unipolar). Limited EAM of the aortic root was performed and the left main coronary artery position, confirmed by undiluted contrast injection through the mapping catheter, was tagged on the map. Secondly, an endocardial map of the LV was created using a retrograde approach via the aorta. An RV map was created if indicated. CT-derived images were visually aligned with the EAM using the left main landmark to overcome rotation errors. The LV surfaces were automatically aligned using CARTOMerge software and the mean surface registration error was calculated. CE-MRI-derived images were visually aligned with the EAM using the left main landmark. Then, the LV surfaces were aligned with the translation tool until the lowest mean surface registration error was reached.

After image registration, epicardial EAM of the target area was performed. Endocardial and epicardial ablation target sites were identified based on activation mapping and entrainment mapping for stable VT, and substrate mapping (electrogram characteristics and pace-mapping) for unstable VT. Radiofrequency energy was applied at 30-45W (maximum temperature 45ºC, flow 20-30ml/min, 60s) for endocardial sites and up to 50W (flow 20ml/min) for epicardial sites.

Electrogram analysis

All bipolar electrograms were displayed at the same gain (reference caliper 0.20mV, Figure 2) and categorized as normal (≤4 sharp spikes) or abnormal (>4 sharp spikes).[11] The latter were subdivided into the following morphologies: double potentials (amplitude ratio ≤1.5), continuously fragmented electrograms (amplitude/duration [mV/msec] ratio ≤0.05), late potentials (inscribing after QRS and separated by an isoelectric segment >20ms) or other abnormal morphologies (>4 spikes but none of the previous; Figure 2). In addition, electrogram duration was measured from the first to the last sharp spike[11] and categorized into 4 predefined categories: ≤50ms, 51-60ms, 61-70ms or >70ms.

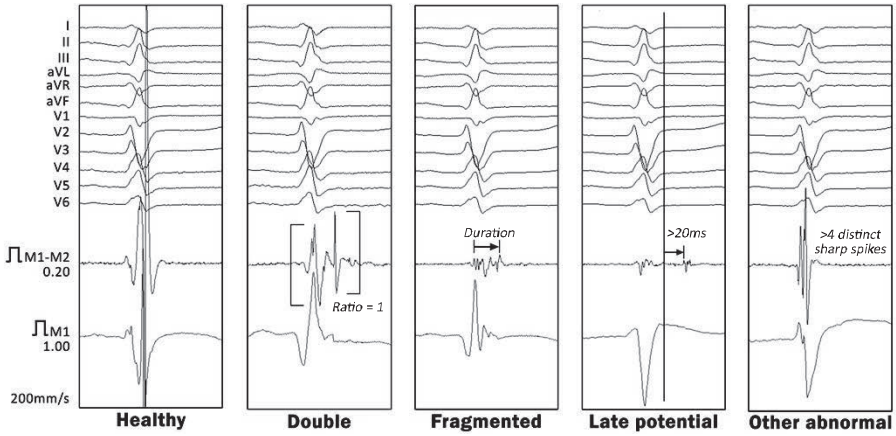

Figure 2. Electrogram morphology categories.

Post-procedural reverse registration of electroanatomical maps with both CT and CE-MRI

After the procedure, all points were superimposed on the corresponding short-axis CT slice using the reversed registration matrix and point coordinates (Mass research software). The epicardial fat thickness was calculated for each point and categorized as 0.0mm, 0.1-2.7mm or ≥2.8mm. Sites with 0.0mm fat were analyzed separately to assess the impact of scar on electroanatomical mapping parameters in the absence of fat. The 2.8mm cutoff has been demonstrated to separate low (<1.5mV) from normal bipolar voltage.[5]

All points were also superimposed on a 3D reconstruction of the CE-MRI, which was created using the short-axis slices (MATLAB software, version 2009b). Centered around each mapping point that was projected on the LV epicardial surface, a 5mm-diameter transmural cylinder was created and divided into three layers of equal thickness. Points with late enhancement (LE) in the endocardial 1/3 or 2/3 were categorized as endocardial scar, those with LE only in the intramural layer as intramural scar, those with LE in the epicardial 1/3 or 2/3 as epicardial scar and points with LE in all 3 layers as transmural scar. All LV epicardial ablation target sites with a ≥11/12 pacemap were evaluated for voltages, electrogram characteristics and the presence of LE.

Endomyocardial biopsy

After ablation, when indicated by current guidelines[12] endomyocardial biopsy was performed (6 patients, interventricular septum [n=4] and/or apicolateral LV [n=3]). Tissue was fixed in 4% formaldehyde. After embedding the tissue in paraffin, cross-sections were cut at 4µm and stained for collagen content by Picro-sirius Red staining. Nuclei were counterstained with Mayer's hematoxylin. High resolution images were taken by microscopy and collagen content was quantified as a percentage of the total biopsy surface using dedicated software (ImageJ, National Institutes of Health, USA). The amount and pattern of fibrosis (compact and/or interstitial) were compared with CE-MRI and EAM findings.

Statistical analysis

Categorical variables are displayed as number (percentage) and continuous variables as mean±SD or median (interquartile range). Data were analyzed using the χ^2 test, Fisher's exact test, Mann-Whitney U test or Kruskal-Wallis test when appropriate. Receiver-operating characteristic curve analysis was performed to determine the optimal cutoff values of bipolar and unipolar voltage for detection of scar, which were defined as the values maximizing the sum of sensitivity and specificity. The area under the curve (AUC) was calculated to evaluate the accuracy of the mapping parameters. To create an algorithm for differentiation between scar and viable myocardium, independent predictors of scar were identified using multivariable logistic regression analysis and backward stepwise selection (inclusion $p<0.10$, exclusion $p>0.20$). The algorithm outcome was positive for scar if any of the incorporated parameters was abnormal. McNemar's test was used to compare the sensitivity and specificity for the different steps of the algorithm. All analyses were performed with SPSS v18.0 (SPSS Inc., Chicago, Illinois). All p-values were two-sided and a p-value of <0.05 was considered significant.

RESULTS

Patients

Ten patients with NICM (7 males, 56±13 years) and 6 patients with idiopathic VA (5 males, 55±19 years) were studied. Baseline characteristics are summarized in Table 1. Mapping of the LV (NICM mean 110±66 points [median 102, min 33 – max 254], idiopathic mean 50±27 points [median 50, min 21 – max 90]) and epicardium (NICM mean 137±78 points [median 138, min 55 – max 247], idiopathic mean 80±51 points [median 81, min 28 – max 164]) was performed focusing on the area of interest based on the 12-lead ECG of spontaneous and induced VA.

Image integration was successfully performed in all patients (CT surface registration error 2.0±0.3mm in NICM patients and 3.5±1.8mm in patients with idiopathic VA; CE-MRI surface registration error 3.2±0.4mm) (figure 3).

Fat and epicardial voltages

Of 1374 epicardial mapping points acquired in patients with NICM, 476 (35%) points were projected on the RV and excluded. Epicardial fat thickness was 0.0mm at 423 (47%) epicardial LV sites, 0.1-2.7mm at 296 (33%) sites and ≥2.8mm at 179 (20%) sites. LE on MRI was present at 558 (62%) points and no LE at 340 (38%). In patients with idiopathic VA, 268 points were analyzed. Epicardial fat thickness was 0.0mm fat at 37 (14%) epicardial LV sites, 0.1-2.7mm at 48 (18%) sites and ≥2.8mm at 183 (68%) sites. Both bipolar and unipolar electrogram amplitudes at sites without LE were attenuated by fat in NICM ($p<0.001$, Figure 4A-B) and controls ($p<0.001$, data not shown).

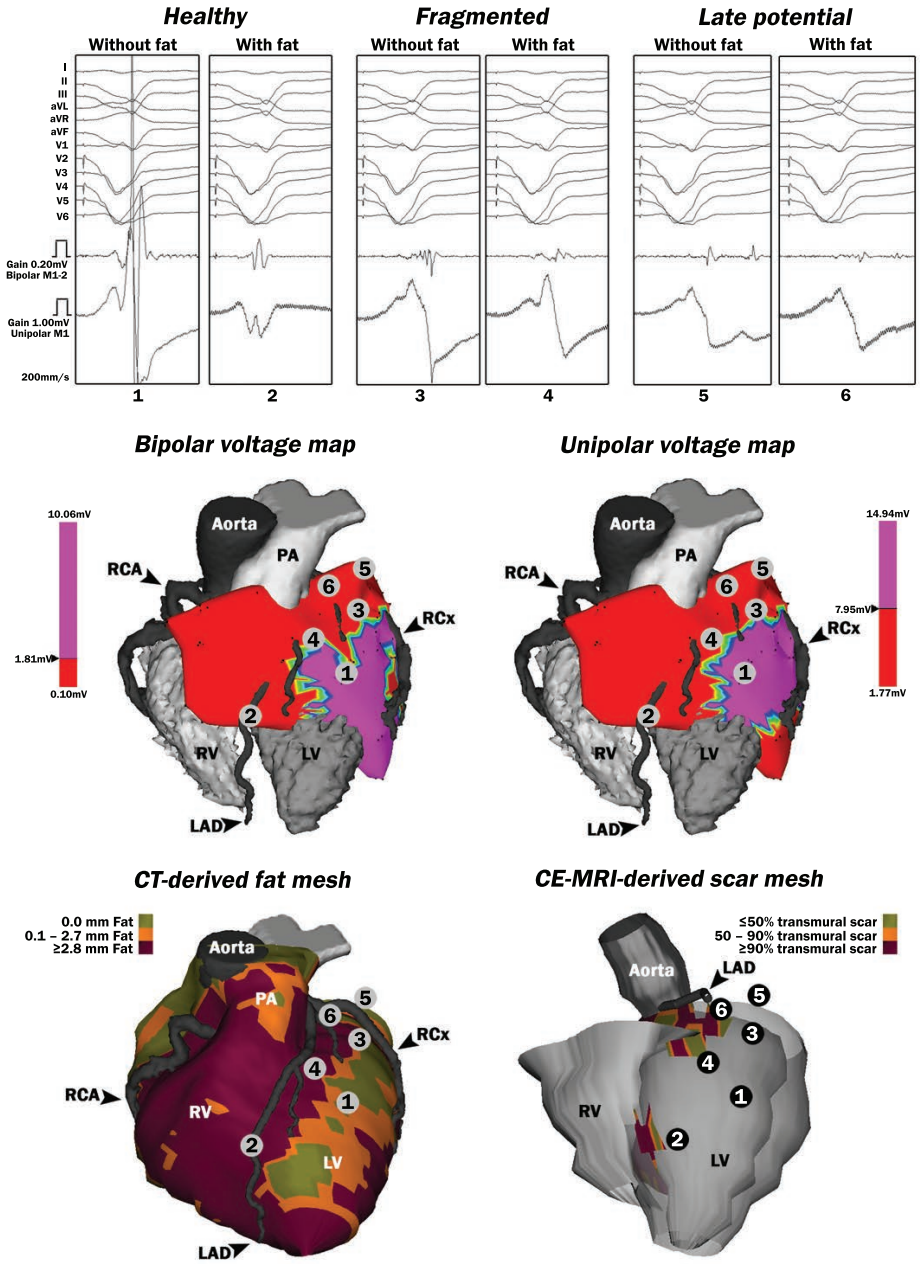

Figure 3. Example of simultaneous CT and contrast-enhanced MRI integration during epicardial electroanatomical mapping.

Substrate mapping demonstrates low voltage areas consistent with epicardial fat, scar or both. Late potentials were detected at the basal LV low voltage area, while an apparently healthy but attenuated electrogram was found at the interventricular groove. Integrated CT-derived fat meshes demonstrate that the interventricular groove and the RV are covered by thick fat layers, possibly explaining the attenuated electrogram amplitudes. The late potentials were caused by a basal scar, which was identified by the integrated CE-MRI-derived scar mesh. RVOT=RV outflow tract. Other abbreviations as in Figure 1.

Table 1. Baseline characteristics.

	Patients with NICM	Patients without SHD
	(n=10)	(n=6)
Male gender (%)	7 (70%)	5 (83%)
Age, years	56±13	55±19
Body mass index, kg/m²	25±4	28±5
LV ejection fraction, %	39±13	56±7
LV end-diastolic volume, mL	243±99	112±33
Hypertension (%)	3 (30%)	3 (30%)
Diabetes Mellitus (%)	1 (10%)	3 (50%)
Creatinin clearance < 60 mL/min	2 (20%)	2 (33%)
Atrial flutter / fibrillation (%)	1 (10%)	0
PVC (%)	0	5 (83%)
VT (%)	10 (100%)	2 (33%)

LV = left ventricular, NICM = nonischemic cardiomyopathy, PVC = premature ventricular contraction, SHD = structural heart disease, VT = ventricular tachycardia

Bipolar and unipolar voltages: scar vs. viable myocardium

Bipolar and unipolar voltages in areas without scar on CE-MRI or fat on CT were similar in NICM patients and controls (Figure 4A-B). In patients with NICM, cutoff values of 1.81mV for bipolar voltage (AUC 0.73, sensitivity 59% and specificity 78%) and 7.95mV for unipolar voltage (AUC 0.79, sensitivity 80% and specificity 72%) could best differentiate between the absence and presence of scar in areas devoid of fat. In areas covered by ≥2.8mm fat neither bipolar nor unipolar voltage could differentiate between the absence or presence of scar. A summary of the value of EAM parameters for identification of scar is provided in Table 2.

Electrogram characteristics: scar vs. viable myocardium

In NICM patients electrograms were prolonged (>50ms) at 263 (47%) sites with scar, as compared to only 45 (13%) sites without evidence of scar on CE-MRI (p<0.001). Electrograms at scar sites with <2.8mm fat were more often prolonged (>50ms) than electrograms at scar sites with ≥2.8mm fat (50% vs. 36%, p=0.02, Figure 5A-B).

The electrogram morphology at sites with scar was categorized as normal in 173 (31%), double-equal in 61 (11%), fragmented in 57 (10%), late potential in 22 (4%) and other abnormal morphologies in 245 (44%) points. The double-equal, fragmented and late potential morphologies were unaffected by fat thickness (p=0.90), while the other abnormal electrogram morphologies were affected by fat thickness (p<0.001, Figure 5A-B, Table 2).

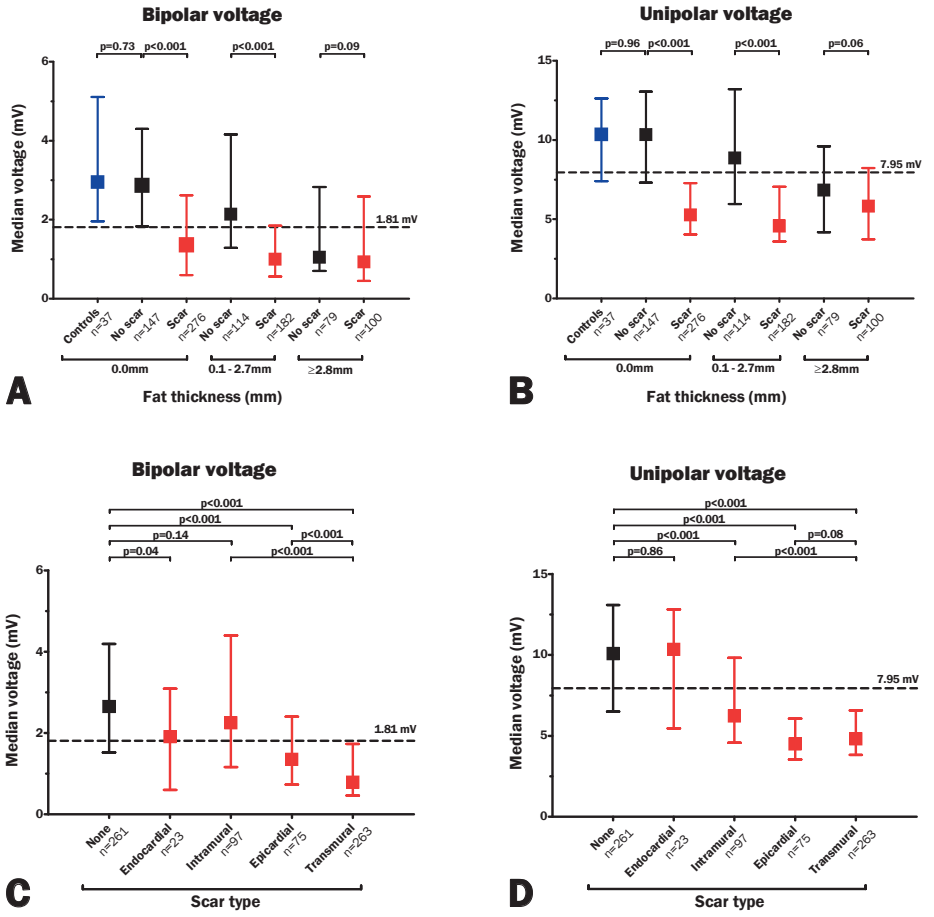

Figure 4. Scar, fat and bipolar & unipolar voltages.
Median and interquartile range of bipolar and unipolar voltage at scar and non-scar sites for different fat thicknesses (Panel A-B) and scar types (Panel C-D).

Algorithm for differentiation between scar and viable myocardium (Table 2, Figure 6)

The variables that were independently associated with scar by multivariable logistic regression analysis were electrogram morphology, electrogram duration and unipolar voltage, but not bipolar voltage. The 3 independently associated variables were used to create a 3-step algorithm, which is displayed in Figure 6.

Table 2. Diagnostic performance of electroanatomical mapping parameters to detect scar for areas with <2.8mm fat and ≥2.8mm fat.

	AUC*		PPV		NPV		Sensitivity		Specificity	
Fat thickness (mm)	<2.8	≥2.8	<2.8	≥2.8	<2.8	≥2.8	<2.8	≥2.8	<2.8	≥2.8
Mapping parameters										
Bipolar voltage ≤1.8mV	0.73	0.57	78%	58%	53%	48%	65%	69%	68%	35%
Unipolar voltage ≤7.95mV	0.78	0.58	80%	60%	64%	52%	79%	71%	66%	39%
Electrogram duration >50ms	0.70	0.58	89%	69%	50%	50%	50%	36%	89%	80%
Electrogram morphology - any abnormal	-	-	80%	69%	58%	55%	72%	56%	68%	68%
Algorithm										
STEP 1: Electrogram morphology - only double, fragmented, late potential	-	-	91%	92%	42%	50%	25%	24%	96%	98%
STEP 1+2: As above, *OR* duration >50ms †	-	-	88%	70%	54%	51%	58%	42%	86%	77%
STEP 1+2+3: As above, *OR* unipolar voltage ≤7.95mV †	-	-	78%	70%	66%	51%	83%	42%	60%	77%

* Parameters are analyzed as a continuous variable.

† Overall sensitivity and specificity compared to previous step by McNemar's test, p<0.001.

AUC denotes area under the curve; NPV, negative predictive value; PPV, positive predictive value.

The complete algorithm had an overall sensitivity of 75%. The sensitivity was 83% in areas covered with <2.8mm fat, which decreased to 42% in the presence of ≥2.8mm fat (Table 2). However, in contrast to bipolar and unipolar voltage, the algorithm maintained a high specificity in areas covered with ≥2.8mm fat. Using the complete algorithm 84% of transmural, 73% of epicardial and 64% of intramural scar sites could be identified, as compared to only 36% of endocardial scar sites.

Bipolar & unipolar voltage, electrogram characteristics and scar type

To determine the accuracy of bipolar and unipolar voltage for detection of different types of scar, sites covered by ≥2.8mm fat were excluded. Both bipolar and unipolar voltage were reduced in the presence of epicardial and transmural scar (all p<0.001, Figure 4C-D), but only unipolar voltage was affected by intramural scar (p<0.001). Sites with transmural scar more often had prolonged (>50ms) and morphologically abnormal electrograms than sites with epicardial, intramural or endocardial scar (all p<0.001, Figure 5C-D). Epicardial scar in turn resulted in more prolonged (>50ms) electrograms than intramural (p=0.007) or endocardial scar (p=0.046). Late potentials were only observed at sites with transmural scar.

Ablation target sites

A total of 40 VTs was induced (cycle length 310±77ms). A ≥11/12 pacemap could be produced for 17 VTs (43%). At 9 of these 17 sites (53%), diastolic potentials were identified during VT and at 4 (24%) VT slowed and terminated during ablation. Eight (47%) target sites were located at

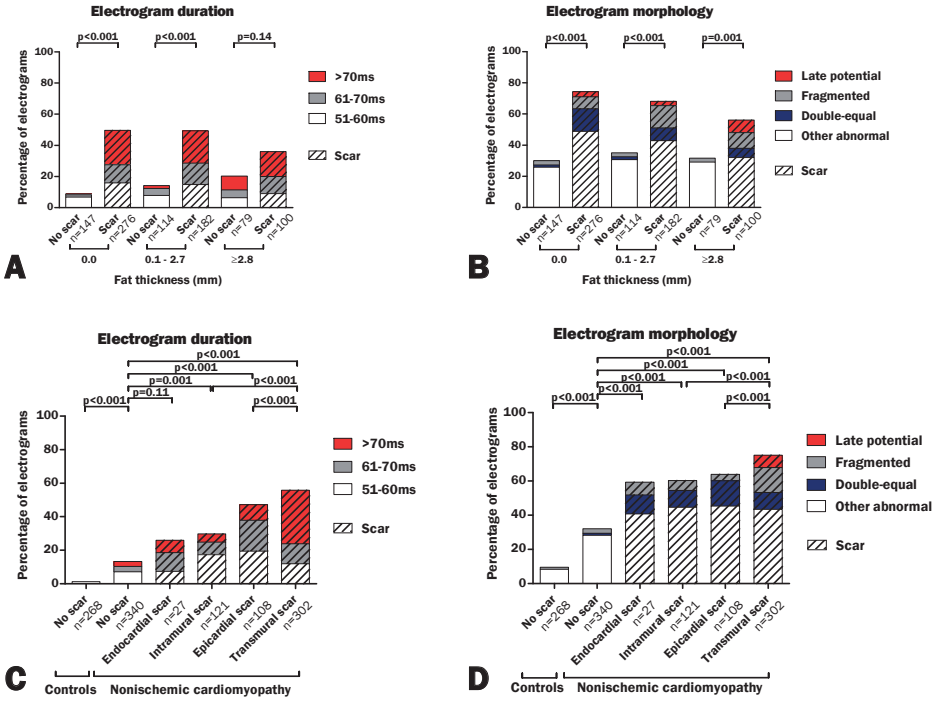

Figure 5. Scar, fat and electrogram characteristics.

Electrogram duration and electrogram morphology at scar and non-scar sites for different fat thicknesses in nonischemic cardiomyopathy (Panel A-B) and for different scar types in nonischemic cardiomyopathy and controls (Panel C-D).

the LV epicardium, 3 (18%) in the LV, 3 (18%) in the aortic root, 2 (12%) at the epicardial RV outflow tract and 1 (6%) at the RV side of the interventricular septum. At all LV epicardial target sites bipolar voltage was ≤1.81mV, unipolar voltage ≤7.95mV, electrogram duration >50ms and electrogram morphology abnormal (5 late potential, 1 fragmented, 2 other abnormal). Late enhancement was present at all LV epicardial target sites (6 transmural, 1 subepicardial, 1 intramural). Six of 8 VTs (75%) were not inducible after ablation. One VT could not be abolished presumably due to a deep intramural circuit (intramural LE on MRI) and another due to interposition of a coronary artery and >10mm epicardial fat.

Histology

Endomyocardial biopsy from the interventricular septum was performed in 4 patients (3 specimens each) distant from areas with LE on MRI. In 3 patients, voltages and electrograms were normal at the biopsy site, although both interstitial and limited compact fibrosis was identified in 2 of 3 patients (both 8% of surface, Supplemental figure). In the fourth patient, bipolar voltage was 1.40mV, unipolar voltage 4.46mV, electrogram duration 65ms and electrogram morphology 'other abnormal'. Histology revealed more severe compact and interstitial fibrosis (46% of surface).

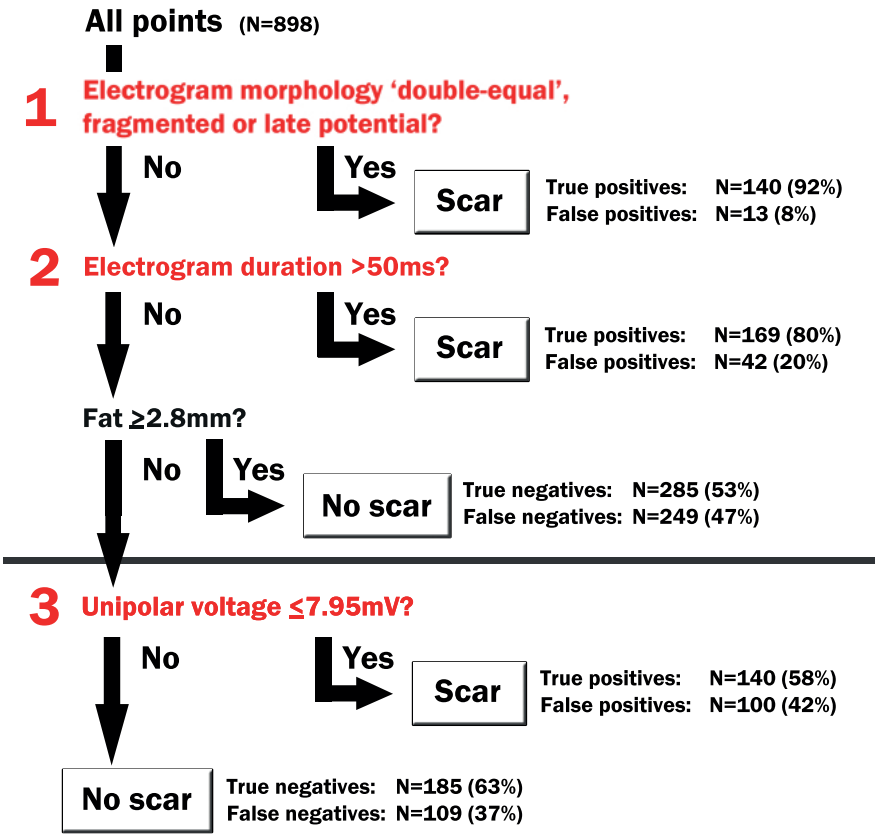

Figure 6. Algorithm for differentiation between scar and viable myocardium.

Endomyocardial biopsy from the apicolateral LV was performed in 3 patients (3 specimens each). Voltages and electrograms were normal at the biopsy site, while both interstitial and limited compact fibrosis were found in all 3 patients (2, 13 and 16% of surface). None of the biopsy sites corresponded to an area of LE.

DISCUSSION

The present study is the first to compare voltage maps, electrogram characteristics, fat and scar by integration of both CT and CE-MRI with epicardial EAM. In addition, the distribution and amount of fibrosis as identified by histology, were also compared with EAM and CE-MRI. The main findings can be summarized as follows: (1) bipolar voltage ≤1.81mV and unipolar voltage ≤7.95mV are the optimal cutoff values for identification of scar during epicardial EAM of areas devoid of fat, (2) electrogram characteristics, but not bipolar or unipolar voltages, can detect

scar covered by fat, (3) the proposed algorithm can be applied to differentiate between scar and viable myocardium and (4) unipolar voltage can be used to identify intramural scar.

Bipolar and unipolar voltage, scar and fat

In the current study, epicardial bipolar and unipolar cutoff values for detection of scar were determined based on CT and CE-MRI. In a prior study by Cano et al.[2], normal epicardial bipolar voltage values were assessed by excluding a 1.5cm wide area along the course of the coronary arteries and the atrioventricular groove. Thick fat layers often found in other areas[13] may explain the reported lower bipolar voltage cutoff value of 1.0mV. In another study, CT-derived fat was integrated with EAM, but a gold standard for the presence of scar was lacking.[5] The currently presented cutoff values of 1.81mV for bipolar voltage and 7.95mV for unipolar voltage are likely to be more accurate since detailed information on fat and scar was available.

It has been postulated that having a larger 'field of view', unipolar voltage could detect scar covered by fat, thereby compensating for the limitation of bipolar voltage mapping. However, in the NICM population unipolar voltage could not differentiate between presence or absence of scar at sites with ≥2.8mm fat, suggesting a limited field of view.

Electrogram characteristics, scar and fat

Prolonged bipolar electrograms with an abnormal morphology are likely to indicate slow conduction in inhomogeneous scar, perhaps related to VT. Since bipolar electrogram amplitudes are attenuated by epicardial fat, low amplitude components such as late potentials may be reduced to noise level. In this study, both CT-derived fat and CE-MRI-derived scar information were integrated, which for the first time allowed evaluation of the value of different EAM parameters. Electrograms were prolonged at only 47% of sites with LE, suggesting that CE-MRI and EAM may provide complementary information, with CE-MRI more accurately delineating (intramural) fibrosis and EAM providing functional information. Importantly, double-equal, fragmented and late potentials were not affected by fat and almost exclusively detected in scar areas, whereas other (more subtle) abnormal electrogram morphologies were affected by fat and also frequently found in non-scar areas. Subtle electrogram abnormalities may be caused by small amounts of fibrosis not detected by CE-MRI, as was found in the biopsy specimens. Late potentials may indicate the presence of slow conduction caused by large amounts of scar, which is supported by the presence of transmural scar at all sites with late potentials.

Algorithm

If CE-MRI is not available, the proposed easy-to-apply 3-step algorithm may be used to improve the accuracy of scar delineation during epicardial EAM. In areas with ≥2.8mm fat (as delineated by CT, which can be acquired irrespective of prior device implantation) only the first and second step should be used to maintain specificity, whereas the third step may be used for sites with <2.8mm fat (on average 80% of mapping sites). When CT scans are not available, step 1 and

2 of the algorithm can be used, although with lower sensitivity. When only the electrogram morphology (any abnormal) is applied, the sensitivity is acceptable and the specificity is unaffected by fat thickness.

Voltage mapping and scar type

In the current study, for the first time it is demonstrated that epicardial unipolar voltage can be used to identify intramural scar. However, due to the limited field of view unipolar voltages cannot be used to detect subendocardial scar. Previously, Hutchinson et al. demonstrated that 61% of endocardial low unipolar voltage areas (≤8.27mV) overlapped with epicardial low bipolar voltage areas.[7] This may however also be explained by epicardial scar extending towards the endocardium. Further studies are needed to assess the exact 'field of view'.

Ablation target sites

Since extensive epicardial EAM is time-consuming, it may be preferable to map the area of interest only. Importantly, all target sites were projected on areas with transmural LE on MRI, suggesting that CE-MRI may be used to delineate the area of interest. The combination of all EAM parameters may be used when CE-MRI is not available.

Histology

Histology is the true gold standard to detect, quantify and characterize fibrosis, but its results, unlike CE-MRI, are not readily available during the procedure. Biopsy specimens revealed both interstitial and compact fibrosis in the majority of cases, although LE on MRI was only found remote from these areas. These findings may explain why electrogram characteristics were frequently abnormal even in the absence of LE on MRI. Interstitial fibrosis and small amounts of compact fibrosis not detected by CE-MRI may cause electrogram abnormalities, as activation fronts curve around lines of block created by such strands of fibrosis.[14] This is an important finding when considering CE-MRI as a gold standard for detection of fibrosis in NICM. Whether areas of fibrosis not detectable on CE-MRI are related to VT needs further evaluation.

Limitations

This study only analyzed mapping points that were projected on the LV epicardium and therefore, our findings do not apply to the RV epicardium. In addition, our findings only apply to the commonly used 3.5mm-tip catheters with a 2mm ring electrode and a 1mm interelectrode spacing. Although low voltage may have been caused by poor contact, this was unlikely as pericardial effusions were absent and the irrigant was removed frequently. One patient with an electroanatomical small basolateral scar not clearly visible on CE-MRI due to imaging artifacts, was excluded illustrating that CE-MRI and EAM may still be used in a complementary manner.

It should be noted that obtaining pre-procedural CT scans requires pre-procedural planning and is associated with radiation exposure. However, CT-derived coronary anatomy may also

reduce the number of contrast injections before epicardial ablation and thus, reduce the radiation exposure during the procedure.

The relatively small number of mapping points, particularly in patients with idiopathic VA, may have limited the accuracy of the maps. The number of controls was small due to the fact that epicardial ablation is not required in the majority of patients with idiopathic VA. The number of NICM patients studied was also small because implanted devices frequently impeded CE-MRI acquisition. For patients in whom CE-MRI is not available during the procedure, we provide tools to distinguish scar from viable myocardium and fat.[9]

Clinical implications

Substrate mapping is of key importance during epicardial VT ablation since activation mapping cannot be performed in the majority of VTs. However, during epicardial EAM it may be difficult to distinguish scar from fat, as both are associated with attenuated bipolar electrogram amplitudes. Moreover, even in the absence of epicardial fat, scars may be difficult to detect if located intramurally. The current study provides insight into the value of different epicardial EAM parameters for detection of scar in patients with NICM. Our findings have important implications when EAM is performed at areas covered by ≥2.8mm fat, such as the basal LV[13] which is often affected in patients with NICM[3,15]. In addition, epicardial unipolar voltage mapping may be particularly useful for detection of intramural scars, which are common in patients with NICM[1] and cannot reliably be detected based on bipolar voltage and electrogram characteristics alone.

Magnetic resonance imaging is limited by the presence of devices and even if safe, it is significantly hampered by artifacts.[8] Computed tomography is however available in all patients and may be important not only to prove, but also to exclude the presence of epicardial fat. The combination of CT, unipolar voltage mapping and electrogram characteristics is likely to improve the accuracy of epicardial substrate mapping, which is important for successful catheter ablation of VT.

Conclusion

Bipolar voltage ≤1.81mV and unipolar voltage ≤7.95mV are the optimal cutoff values to differentiate between scar and viable myocardium during epicardial EAM, but both are attenuated by epicardial fat. Specific electrogram morphologies are not affected by fat, but can identify only one quarter of all scar sites. The proposed easy-to-use algorithm allows more accurate differentiation between scar and viable myocardium during epicardial EAM. Unipolar voltage, but not bipolar voltage can be used to identify intramural scar.

REFERENCES

1. Bogun FM, Desjardins B, Good E, et al. Delayed-enhanced magnetic resonance imaging in nonischemic cardiomyopathy: utility for identifying the ventricular arrhythmia substrate. *J Am Coll Cardiol*. 2009;53:1138-1145.
2. Cano O, Hutchinson M, Lin D, et al. Electroanatomic substrate and ablation outcome for suspected epicardial ventricular tachycardia in left ventricular nonischemic cardiomyopathy. *J Am Coll Cardiol*. 2009;54:799-808.
3. Nakahara S, Tung R, Ramirez RJ, et al. Characterization of the arrhythmogenic substrate in ischemic and nonischemic cardiomyopathy implications for catheter ablation of hemodynamically unstable ventricular tachycardia. *J Am Coll Cardiol*. 2010;55:2355-2365.
4. Tung R, Nakahara S, Ramirez R, et al. Distinguishing epicardial fat from scar: analysis of electrograms using high-density electroanatomic mapping in a novel porcine infarct model. *Heart Rhythm*. 2010;7:389-395.
5. Desjardins B, Morady F, Bogun F. Effect of epicardial fat on electroanatomical mapping and epicardial catheter ablation. *J Am Coll Cardiol*. 2010;56:1320-1327.
6. de Bakker JM, van Capelle FJ, Janse MJ, et al. Slow conduction in the infarcted human heart. 'Zigzag' course of activation. *Circulation*. 1993;88:915-926.
7. Hutchinson MD, Gerstenfeld EP, Desjardins B, et al. Endocardial unipolar voltage mapping to detect epicardial ventricular tachycardia substrate in patients with nonischemic left ventricular cardiomyopathy. *Circ Arrhythm Electrophysiol*. 2011;4:49-55.
8. Dickfeld T, Tian J, Ahmad G, et al. MRI-Guided ventricular tachycardia ablation: integration of late gadolinium-enhanced 3D scar in patients with implantable cardioverter-defibrillators. *Circ Arrhythm Electrophysiol*. 2011;4:172-184.
9. Wijnmaalen AP, van der Geest RJ, van Huls van Taxis CF, et al. Head-to-head comparison of contrast-enhanced magnetic resonance imaging and electroanatomical voltage mapping to assess post-infarct scar characteristics in patients with ventricular tachycardias: real-time image integration and reversed registration. *Eur Heart J*. 2011;32:104-114.
10. Valles E, Bazan V, Marchlinski FE. ECG criteria to identify epicardial ventricular tachycardia in nonischemic cardiomyopathy. *Circ Arrhythm Electrophysiol*. 2010;3:63-71.
11. Zeppenfeld K, Kies P, Wijffels MC, et al. Identification of successful catheter ablation sites in patients with ventricular tachycardia based on electrogram characteristics during sinus rhythm. *Heart Rhythm*. 2005;2:940-950.
12. Cooper LT, Baughman KL, Feldman AM, et al. The role of endomyocardial biopsy in the management of cardiovascular disease: a scientific statement from the American Heart Association, the American College of Cardiology, and the European Society of Cardiology. Endorsed by the Heart Failure Society of America and the Heart Failure Association of the European Society of Cardiology. *J Am Coll Cardiol*. 2007;50:1914-1931.
13. Abbara S, Desai JC, Cury RC, et al. Mapping epicardial fat with multi-detector computed tomography to facilitate percutaneous transepicardial arrhythmia ablation. *Eur J Radiol*. 2006;57:417-422.
14. de Bakker JM, van Capelle FJ, Janse MJ, et al. Fractionated electrograms in dilated cardiomyopathy: origin and relation to abnormal conduction. *J Am Coll Cardiol*. 1996;27:1071-1078.
15. Hsia HH, Callans DJ, Marchlinski FE. Characterization of endocardial electrophysiological substrate in patients with nonischemic cardiomyopathy and monomorphic ventricular tachycardia. *Circulation*. 2003;108:704-710.

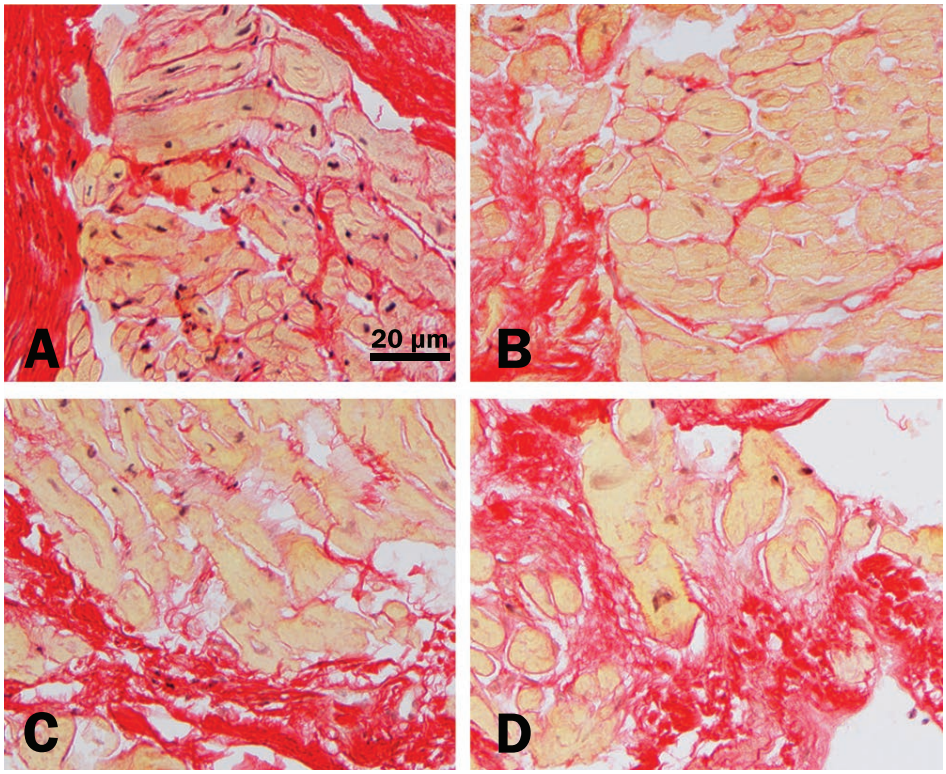

Supplemental figure. Histologic examination of scar architecture in biopsy specimens.
Endomyocardial biopsy specimens from the right ventricular septum (upper panels) and from the apicolateral left ventricle (lower panels) distant from areas with late enhancement on MRI. All reveal both compact and interstitial fibrosis.

Part III

New Developments in Surgical Cryoablation of Ventricular Arrhythmias

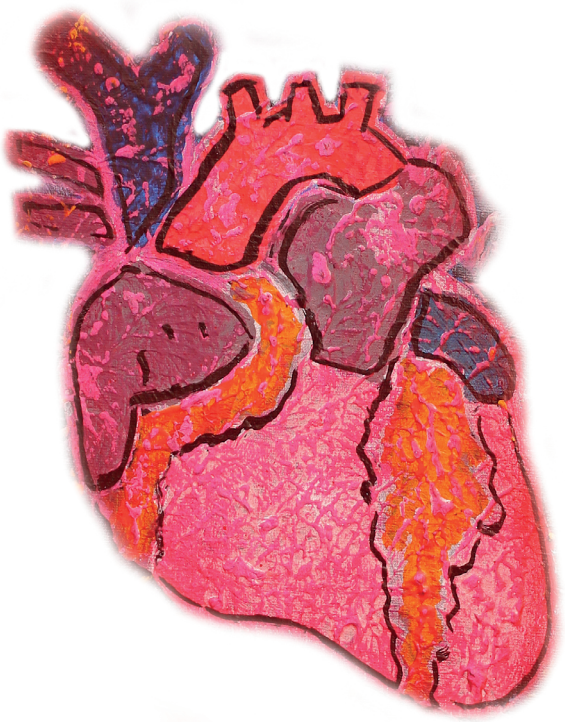

Chapter 7

Programmed Electrical Stimulation Guided Encircling Cryoablation Concomitant to Surgical Ventricular Reconstruction for Primary Prevention of Ventricular Arrhythmias

Carine F.B. van Huls van Taxis, Adrianus P. Wijnmaalen, Patrick Klein, Olaf M. Dekkers, Jerry Braun, Harriette F. Verwey, Martin J. Schalij, Robert J.M. Klautz, Katja Zeppenfeld

European Journal of Cardiothoracic Surgery. 2018;54:98-105

ABSTRACT

Background

Surgical ventricular reconstruction (SVR) is an effective treatment to improve left ventricular (LV) function in patients with ischemic heart failure and a LV anterior-apical aneurysm. Ventricular arrhythmia (VA) is an important cause for morbidity and mortality in these patients. Encircling cryoablation (EC) targeting the VA-substrate may therefore be required. Programmed electrical stimulation (PES) can identify patients at risk for VA. The objective of this study was to evaluate the incidence and type of VA during long-term follow-up after PES-guided EC concomitant to SVR for primary prevention of VA.

Methods

Thirty-eight patients without spontaneous VA referred for SVR who underwent pre-operative PES were included (PES-group); 27 patients inducible for aneurysm-related VA received cryoablation (71%). A historical cohort of 39 patients without spontaneous VA, pre-operative PES and anti-arrhythmic surgery served as control group. Patients were discharged with an implantable cardioverter defibrillator (ICD).

Results

During 74±35 months follow-up no arrhythmic deaths occurred. Five-year survival for the total study population was 78%. Twenty-eight patients (36%) experienced ≥1 VA. There were no differences in number and type of ICD therapies between groups: shocks p=0.699; Anti-tachypacing p=0.403. Five-year VA-free survival was 61% for the PES-group and 65% for the control group (hazard ratio 1.67, p=0.290).

Conclusions

The majority of patients referred for SVR without previously documented VA was inducible for aneurysm-related VA. During follow-up, more than one third of patients experienced sustained VA and 25% received appropriate ICD therapy. No difference in VA occurrence or ICD therapy was observed between groups.

INTRODUCTION

Late sudden cardiac death due to ventricular arrhythmias (VA) constitutes 30-50% of mortality in patients with ischemic heart failure.[1] VA may be due to scar-related reentry typically involving the scar-borderzone or to heart failure related mechano-electric changes resulting in altered ion channel and transporter function.[2-4] Surgical ventricular reconstruction (SVR) is an effective treatment to reduce left ventricle (LV) volumes and improve LV function in ischemic heart failure patients with LV anterior-apical aneurysm.[5,6] However, despite improved function and reduced wall stress patients remain at risk for VA.[2,7,8] These VA can be due to reentry in the scar-borderzone which is left in place and excluded by patch material during surgery.[9] Targeting aneurysm scar-borderzone without additional mapping by an encircling cryoablation (EC) has been proven safe and effective for recurrent slow VA in these patients.[10-12] Programmed electrical stimulation (PES) can identify patients at risk for VA after myocardial infarction as it indicates the presence of an arrhythmogenic substrate.[13,14] Patients who undergo SVR for an LV anterior-apical aneurysm without prior VA who are inducible for aneurysm-related reentrant VA, may benefit from substrate modification by concomitant EC of the scar-borderzone referred to as PES-guided EC, to prevent spontaneous VA.

The objective of this study was to evaluate the incidence, type and timing of VAs after PES-guided EC concomitant to SVR for primary prevention of VA during long-term follow-up.

METHODS

Patient population

The investigation is a single center observational study. In 2007 PES-guided EC of the scar-borderzone was added to the standard clinical protocol for patients without documented VA accepted for SVR. The studied population consisted of 38 consecutive patients with ischemic heart failure, an anterior-apical aneurysm, no history of VA and who underwent PES prior to elective SVR and PES-guided EC between 2007 and 2012 (PES-group). Thirty-nine patients who underwent SVR without PES-guided EC with the same indication from 2003 onwards and with an ICD at discharge served as a historical control group. This included a comprehensive preoperative evaluation with echocardiography and coronary angiography. The results were evaluated by a team of cardiologists and cardiothoracic surgeons.

The Dutch Central Committee on Human-related Research allows use of anonymous data without prior approval of an institutional review board provided that the data are acquired for patient care. All data used for this study were acquired for clinical purposes and handled anonymously.

Preoperative electrophysiological evaluation

Before PES, anti-arrhythmic drugs were discontinued for ≥5 half-lives. None used amiodarone at time of PES. Two catheters were inserted through the right femoral vein, one placed at the His position and the second at the right ventricular apex and subsequently in the right ventricular outflow tract to perform PES. The PES protocol consisted of 3 drive cycle lengths (CL) (600, 500, 400ms) with 1-3 ventricular extra stimuli (down to 200ms or refractory period) and incremental burstpacing. An aneurysm-related VA substrate was assumed if PES induced a monomorphic VA, lasting >30s or requiring termination because of hemodynamic compromise, was re-inducible *and* the VA exit site was located at the aneurysm scar-borderzone. The presumed exit site was determined based on the VA 12-lead electrocardiogram morphology.[15] All 12-lead VA electrocardiograms were analyzed by 2 independent observers. In case of discrepancy agreement was reached by consensus. Patients with aneurysm-related VA were candidates for EC concomitant to SVR. Patients without aneurysm-related VA underwent SVR only.

Surgical technique

Patients underwent SVR according to the previously described technique.[6] Operations were performed using cardiopulmonary bypass, aortic cross-clamping and intermittent warm blood cardioplegia. The LV was opened through the infarcted area. At the transitional zone between viable and scarred myocardium, EC was performed using a 4mm diameter malleable cryoprobe (Cardioblate CryoFlex, Medtronic, Minneapolis, USA) using argon gas. Overlapping linear applications, down to -150˚C for 90s, were made to the aneurysm scar-borderzone.[9] After EC, a Fontan-stich was placed at the transitional zone. The residual LV cavity was shaped and sized using a mannequin balloon at 55ml/m^2 body surface-area (TRISVR, Chase Medical, Richardson, USA) and the remaining defect was closed through an endoventricular Dacron patch plasty. Excluded fibrous scar-tissue was sutured over the patch to improve hemostasis. Additional concomitant procedures were performed when indicated. After weaning the patient from extracorporeal circulation, trans-esophageal echocardiography was repeated to assess LV shape and function, patch integrity and valvular competency.

ICD settings

In patients without ICD before surgery one was implanted before discharge based on the preoperative LV ejection fraction (EF) ≤30-35% according to current European Society of Cardiology guidelines. Devices were programmed according to our standard institutional protocol for primary prevention; VA monitor zone (VACL 321-400ms, no therapy), VA zone (VACL 261-320ms, anti-tachycardia pacing (ATP) and if the VA continued ICD shocks), VF zone (VACL ≤260ms, ICD shocks). Settings were adapted when clinically indicated.

Follow-up

Patients were prospectively followed in an outpatient heart failure program and maintained on optimal medical treatment for heart failure. ICDs were interrogated every 6 months. Printouts were reviewed for the occurrence of sustained VA, VACL and therapy mode. VA were classified as sustained when lasting >30s in the ICD monitor zone or when initiated appropriate ICD therapy. Therapy was considered appropriate when occurring in response to any VA. Echocardiography was performed before discharge and afterwards annually. The follow-up started at time of discharge and ended at last outpatient clinic visit up to 2015 or death.

Statistical analysis

Continuous variables are expressed as mean (standard deviation) or median (interquartile range [IQR]) and categorical variables as percentages (%), where appropriate. To compare groups at baseline for continuous variables Student's T-test (normally distributed data) and Mann-Whitney U-test (non-normally distributed data) were used. For categorical data Chi^2-test or Fisher's exact-test (n<5 in any one cell) was used. For analysis purposes, for each patient the mean CL of all induced and/or spontaneous VAs was calculated. Intrapatient comparison for LVEF, NYHA-class and VACL was performed using the paired samples T-test or Wilcoxon paired-test as appropriate. Incidence rate ratio were estimated for counted data. Overall survival and VA-free survival over time were analysed for the total study population by the method of Kaplan-Meier. For calculating follow-up time a time to event approach was used where patients were censored at time of an event. To assess differences and effect of potential confounders on overall survival and VA-free survival between the groups univariable and multivariable Cox regression models were constructed (Table 4 and 5). Selection of potential confounders was based on clinical knowledge and comparing baseline characteristics. To check robustness of the results we performed a propensity score adjusted analysis including the same confounders as included in the Cox model. All tests were 2-sided and a p-value of <0.05 was considered significant. Statistical analyses were performed using SPSS software (version 22, SPSS Inc, Chicago, Ill, USA), and STATA version 14.1 XXX.

RESULTS

Patient characteristics

Thirty-eight patients were included in the PES-group and 39 controls. Baseline patient characteristics are provided in Table 1; both groups were similar except for a worse NYHA class and lower ejection fraction in the control group. Patients were on optimal medical treatment for heart failure before undergoing SVR.

Table 1. Baseline characteristics

	All N=77	PES-group N=38	Control group N=39	P-value
Male, n (%)	60 (78)	28 (74)	32 (82)	0.376*
Age, years	60±10	63±9	58±11	0.051#
Diabetes mellitus, n (%)	16(21)	10 (26)	6 (15)	0.237*
Atrial fibrillation, n (%)	8 (10)	6 (16)	2 (5)	0.125†
MI-SVR duration, months (IQR)	36 (9-144)	48 (10-180)	28 (7-132)	0.133‡
NTproBNP, pg/mL (IQR)	1358 (572-2151)	1346 (616-2253)	1369 (459-1885)	0.518‡
Primary reperfusion, n (%)	25 (32)	8 (21)	17 (44)	0.035*
NYHA,n(%)				<0.001#
Class 2	19 (25)	17 (45)	2 (5)	
Class 3	53 (68)	21 (55)	32 (82)	
Class 4	5 (6)	0	5 (13)	
Euroscore, n (IQR)	6 (4-14)	6 (4-14)	7 (4-18)	0.537‡
LVEF,%	27±8	29±8	25±7	0.015#
LVESV-index, ml/m^2	80±45	81±52	79±39	0.880#
LVEDV-index, ml/m^2	111±53	110±63	112±44	0.894#
ACE-I/ARB, n (%)	74 (96)	37 (98)	37 (95)	0.571*
Beta-blocker, n (%)	74 (96)	37 (98)	37 (95)	0.571*
MRA, n (%)	46 (60)	26 (68)	20 (51)	0.125*

EDV = End-diastolic volume; EF = Ejection fraction; ESV = End-systolic volume; LV = Left ventricle; MI = myocardial infarction; NYHA = New York Heart Association SVR = Surgical ventricular reconstruction
*Chi^2-test`; †Fisher's Exact-test; #Student's T-test; ‡Mann-Whitney U-test

Preoperative electrophysiological evaluation

27/38 patients (71%) were inducible for 31 VAs which were classified as aneurysm-related, based on the 12-lead electrocardiogram. These had a VACL of 259±54ms, 24 VAs (77%) a superior axis, and 19 VAs (58%) had a left bundle branch block-type morphology; 17 VAs (55%) were hemodynamically not tolerated. An additional 3 VA in 3 patients were non-aneurysm related; In 2 patients 1 aneurysm-related and 1 non-aneurysm-related VA were induced. In 1 patient only a non-aneurysm-related VA was induced and was therefore not considered a candidate for concomitant EC.

Surgical characteristics

All patients underwent SVR. EC was applied at the aneurysm scar-borderzone in all patients inducible for aneurysm-related VA. No statistical differences in surgical data were observed between groups (Table 2).

Table 2. Surgical characteristics

	All N=77	PES-group N=38	Control group N=39	P-value
Coronary angiography bypass graft, n (%)	41 (53)	20 (53)	21 (54)	0.915*
Mitral valve repair, n (%)	45 (58)	21 (55)	24 (62)	0.576*
Tricuspid valve repair, n (%)	26 (34)	11 (29)	15 (38)	0.377*
Aortic valve replacement, n (%)	4 (5)	2 (5)	2 (5)	0.979†
Patch-size, cm^2	14±8	12±5	16±10	0.070#
Corporal-pulmonary bypass -time, min	204±58	209±52	194±68	0.349#
Aortic cross-clamp-time, min	141±58	148±41	129±43	0.124#

*Chi^2-test; †Fisher's Exact-test; #Student's T-test

Follow-up

Patients were followed for 74±35 months. 74/77 patients had an ICD during follow-up (96%); 3 patients in the PES-group did not receive an ICD at the preference of the referring cardiologist (LVEF≥35% at discharge, negative PES). There was an improvement in NYHA-class from the majority in 3 at baseline to 2 at 1 year follow-up (p<0.001). Mean LVEF improved from 27±8% pre-operatively to 36±9% after 1 year (p<0.001). No differences were observed between groups after 1 year (Table 3).

VA occurrence and survival

In 28/74 (38%) patients 99 VA episodes were recorded on ICD (VACL 310±58ms, 3[IQR 1-3] VAs/patient), which prompted appropriate ICD therapy in 26/28 patients (93%); 20 patients (25%) received ATP for 58 VAs and 11 patients (14%) received ≥1 shocks for 18 VAs. In 10 patients 15 VA were registered in the VF-zone. No differences were found between groups regarding type of ICD therapy (Table 3). Two patients in the PES-group had 2 VA registered only in the monitor zone of the ICD and did not receive any ICD therapy. None of the patients without ICD had documented or suspected sustained VA. 8/11 patients with a negative outcome at PES had no VA occurrences which generated a negative predictive value of 73%.

Median time to first VA was 11 months (IQR 2-27). 9/28 patients (32%) experienced a first VA while on anti-arrhythmic drugs. Anti-arrhythmic drugs were initiated because of postoperative spontaneous VA (n=4) or atrial fibrillation/flutter (n=5).

VA occurrence was similar between groups; 14/38 (37%) patients in the PES-group experienced 45 VAs (CL 314±50ms; 3 [IQR 1-3] VAs/patient), and 14/39 (36%) in the control group experienced 54 VAs (CL 305±67ms, 3 [IQR 1-3] VAs/patient). VA-free survival was 63% at 5 years for the entire cohort and similar between groups (Figure 1A); 61% for the PES-group and 65% for the control group (hazard ratio 1.13 [p=0.750]; after adjusting for confounders hazard ratio 1.67 [p=0.290], Table 4). A similar hazard ratio was obtained after propensity score adjustment: 1.52 (p=0.39). At multivariable Cox regression analyses for VA occurrence LVEF at

Table 3. Follow-up

	All N=77	PES-group N=38	Control group N=39	P-value
Follow-up, months	74±35	61±25	87±39	<0.001#
Death(all cause), n (%)	25 (32)	12 (32)	13 (33)	0.869*
Cardiac death, n (%)	14 (18)	9 (24)	7 (18)	0.688*
ICD, n (%)	74 (96)	35 (92)	39 (100)	0.115*
Cardiac resynchronization therapy, n (%)	44 (57)	23 (61)	21 (54)	0.299*
Anti-arrhythmic drug, n (%)	36 (47)	17 (42)	19 (49)	0.726*
Sotalol≥160mg/day	26 (34)	13 (34)	13 (33)	0.953*
Amiodarone	21 (27)	10 (26)	11 (28)	0.852*
New atrial fibrillation, n (%)	33 (43)	15 (39)	18 (46)	0.544*
NYHA 1 year follow-up, n (%)				0.052#
Class-1	28 (39)	19 (54)	9 (26)	
Class-2	33 (47)	14 (39)	19 (53)	
Class-3	10 (14)	3 (8)	7 (20)	
LVEF,%	36±9	36±8	35±9	0.845#
LVESV-Index, ml/m^2	50±19	50±19	51±19	0.829#
LVEDV-Index, ml/m^2	77±22	76±23	79±23	0.600#
VA				
Total, n	99	45	54	0.982*
Incidence rate, episodes/total follow-up	0.017	0.016	0.019	1.19 (0.78-1.80)**
Occurrence, patients (%)	28 (36)	14 (37)	14 (36)	0.931#
Time to first VA, months (IQR)	11 (2-27)	8 (2-26)	15 (4-29)	0.511‡
Episodes/patients (IQR)	3 (1-3)	3 (1-3)	3 (1-3)	0.982‡
Cycle length, ms	310±58	314±50	305±67	0.699#
Ventricular fibrillation, n	15	8	7	0.841*
ICD therapy, patients (%)	26 (34)	12 (32)	14 (36)	0.222*
Anti-tachycardia pacing, patients (%)	20 (26)	9 (24)	11 (28)	0.403†
Episodes, n	59	20	39	
Shock, patients (%)	11 (14)	6 (16)	5 (13)	0.699*
Episodes, n	18	9	9	
Monitor zone, patients (%)	8 (10)	6 (16)	2 (5)	0.092†
Episodes, n	22	16	6	
Anti-arrhythmic drug usage during first VA episode	9 (12)	5 (13)	4 (10)	1.0†
Sotalol≥160mg/day	6	4	2	
Amiodarone, n	3	1	2	

Abbreviations as in Table 1 and 2. VA = ventricular arrhythmia; ICD = Internal cardioverter defibrillator

P-value calculated between groups.

*Chi^2-test; †Fisher's Exact-test; #Student's T-test; ‡Mann-Whitney U-test; **Incidence rate ratio (95% confidence interval)

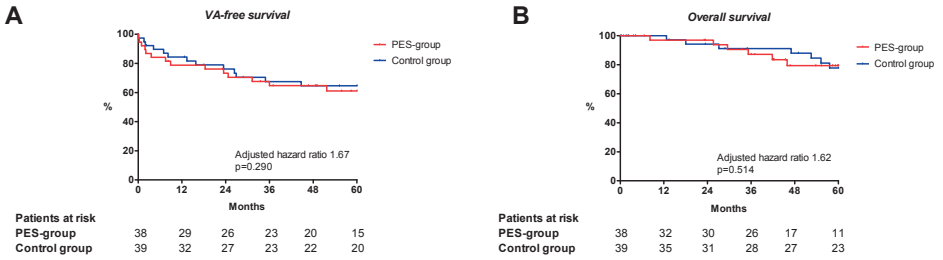

Figuur 1.

A: Kaplan Meier curves of 5 year ventricular arrhythmia (VA)-free survival, groups compared using multivariable Cox regression model. B: Kaplan Meier curves of 5 year overall survival, groups compared using multivariable Cox regression model. Curves are according to the different pre-operative strategies of yes/no programmed electrical stimulation (PES).

baseline demonstrated to influence VA occurrence: lower LVEF increased the risk for VA during follow-up. VA characteristics did not differ between groups (Table 3). One patient in the control group underwent successful catheter ablation of 2 presumptive clinical VAs 46 months after discharge and was free from VA afterwards.

Twenty-five patients (32%) died during follow-up; 16 patients (64%) of heart failure, 9 of non-cardiac causes. No arrhythmic deaths were reported. One patient in the PES-group received a LV assist device as destination therapy 58 months after SVR and 1 patient in the control group underwent heart transplantation after 28 months; both were censored for further follow-up afterwards. Kaplan-Meier analysis revealed a 5-year overall survival of 78%. No difference in 5-year overall survival was observed between groups (PES-group 79% versus control group 78%, Figure 1B): unadjusted hazard ratio 1.05, p=0.932; adjusted hazard ratio 1.62, p=0.514. A similar hazard ratio was obtained after propensity score adjustment: 1.41 (p=0.64). When performing multivariable analyses, only older age remained associated with worse overall survival (Table 5).

Table 4. Cox Regression analyses: VA-free survival

	Univariable		Multivariable	
	HR (CI 95%)	P-value	HR (CI 95%)	P-value
Age	1.02 (0.98-1.07)	0.28	1.03 (0.99-1.08)	0.13
LVEF baseline	0.97 (0.92-1.02)	0.19	0.94 (0.89-1.00)	0.03
NYHA-class*	1.15 (0.53-2.50)	0.72	1.28 (0.51-3.18)	0.60
PES-group	1.13 (0.53-2.41)	0.75	1.67 (0.65-4.30)	0.29
Primary reperfusion	0.81 (0.35-1.84)	0.61	0.83 (0.35-1.99)	0.68
Sex	1.81 (0.62-5.23)	0.28	2.62 (0.87-7.89)	0.09

CI = Confidence interval; HR = Hazard ratio; Abbreviations as Table 1 and 2

* NYHA-class as categorical covariate did not alter outcome

Table 5. Cox Regression analyses: Overall survival

	Univariable		Multivariable	
	HR (CI 95%)	P-value	HR (CI 95%)	P-value
Age	1.10 (1.02-1.18)	0.02	1.12 (1.03-1.22)	<0.01
LVEF baseline	0.98 (0.91-1.05)	0.59	0.94 (0.87-1.024)	0.16
NYHA-class*	1.98 (0.64-6.10)	0.24	2.54 (0.72-8.91)	0.15
PES-group	1.05 (0.35-3.12)	0.93	1.62 (0.38-6.85)	0.51
Primary reperfusion	0.41 (0.09-1.84)	0.24	0.45 (0.09-2.25)	0.33
Sex	2.05 (0.45-9.25)	0.35	2.45 (0.48-12.49)	0.28

CI = Confidence interval; HR = Hazard ratio; Abbreviations as in Table 1

* NYHA-class as categorical covariate did not alter the outcome

Encircling cryoablation and VA characteristics

Overall 11/27 patients (41%) with concomitant EC experienced 37 VA episodes (median 2 [IQR 1-3] episodes/patient). VACL did not differ between patients with or without EC: 308±46ms versus 311±66, p=0.919, respectively. Five VA (14%) were terminated by ICD shock and 19 VA (51%) by ATP. The remaining 13 VA (35%) were registered in the ICD monitor zone. There were no differences in type of ICD therapy between patients with or without EC.

DISCUSSION

The present study is the first to systematically evaluate the incidence, type and timing of VA in patients who underwent PES-guided EC concomitant to SVR for primary prevention of VA thereby targeting two potential VA mechanisms; scar-related reentry and wall stress. The main findings are: (1) the majority of patients referred for SVR without previously documented VA was inducible for aneurysm-related VA; (2) during follow-up more than one third of the patients experienced appropriate ICD therapy, despite concomitant EC targeting the scar-borderzone and significant hemodynamic improvement; (3) no difference in VA occurrence, VACL and ICD therapy was observed during long-term follow-up between patients with PES guided concomitant EC and those without preoperative evaluation and concomitant treatment.

The current investigation comprised of a homogeneous patient group referred for heart failure treatment because of ischemic cardiomyopathy, with an anterior aneurysm after infarction and none treated with amiodarone. Excellent outcome of heart failure parameters after SVR for this indication was previously reported by our group.[16] The STICH trial has reported no clinical benefit of SVR if added to surgery in patients scheduled for CABG.[17] As the primary inclusion criterion for this trial was acceptation for CABG for significant coronary artery disease we feel that the findings of this trial are not fully applicable to the populations reported in the current study.

Pre-operative VA inducibility

Seventy-one percent in the study group were inducible for an aneurysm-related VA prior to surgery, using a standardized and complete PES protocol. Others have reported lower inducibility rates, ranging from 22-58%. However, included patients were more heterogeneous (with/without apical aneurysm; anterior/non-anterior infarction; NYHA-class 1-3; many on sotalol/amiodarone; LVEF >40%) and in several studies the induction protocol was less extensive which is likely to influence inducibility rates in scar-related VA.[13,18-21] Induction of a monomorphic reentrant VA indicates the presence of an arrhythmogenic substrate and has been associated with VA occurrence and sudden death in patients after myocardial infarction, especially in patients with a LV aneurysm.[13,14,22] Based on VA morphology all but 3 VAs had an exit site at the aneurysm scar-borderzone in particular involving the inferior apical septal segments. Therefore, targeting the scar-borderzone by cryoablation may abolish at least parts of the substrate for these VA.

VA occurrence after SVR

Previous studies have demonstrated that the substrate for reentrant VA can persist after SVR and may lead to VA occurrence during follow-up.[10,23] This might be partly due to incomplete elimination of VA substrate by SVR as a significant portion of myocardial scar is left behind the inserted patch for stability and hemostasis. Excluded portion of the scar containing the VA reentry circuit can no longer be approached by endocardial catheter ablation, which may further justify preventive substrate elimination.[9] In the historical control group without additional PES guided EC, 36% experienced spontaneous VA during long-term follow-up supporting the importance of preventive methods to identify and target possible VA substrates. Of importance, in the PES-group, 71% of which underwent EC of the scar-borderzone, a similar high VA occurrence rate was registered (37%). The groups were not randomized, but Cox regression testing for possible confounders does not suggest that PES-guided concomitant EC does prevent late VA.

As VA were registered in 41% of patients who underwent EC of the scar-borderzone the technique seems insufficient to eliminate the VA substrate in our population. Catheter mapping studies of post infarct VA have shown that although reentry circuit exit sites are usually located at the scar-borderzone, which may also involve the mid-wall and subepicardial layers, the critical isthmus is often found in the electroanatomical dense scar.[3,4,24,25] A prior animal study could demonstrate that endocardial cryoablation lesions reach a depth of approximately 4.8mm.[26] Endocardial cryolesions, in particular at the septal scar-borderzone may not create transmural or deep lesions and may not be sufficient to eliminate or exclude the VA substrate, allowing for circuits to remain or the reentrant circuit to exit.

VA occurrence rate after EC in this population without prior VA was higher than previously described recurrence rates in patients who underwent EC for the treatment of recurrent VA.[2,8,10-12] This may be in part explained by the large proportion of patients with an ICD (96%) in the current investigation allowing for reliable monitoring of VA recurrence. The high ICD

implantation rate is different from most prior studies with implantation rates of only up to 9.6% after SVR,[2,10-12] except for the investigation of O'Neill[8] in which 48% of patients were discharged with an ICD. Differences in surgical techniques and the frequent use of amiodarone in the prior studies may have also contributed to lower VA recurrence rates.

Of importance, differences in VA substrate may exist between patients with, as in previous studies, and without, as in the current study, spontaneous VA before surgery. While previous studies mainly included patients with hemodynamically tolerated and often slow VA,[9,11,27] the observed VAs in the present study were often fast, and an important number required ICD shocks to be terminated. As the underlying substrate determines VA characteristics, like CL, the occurrence of fast VAs may reflect differences in the VA substrate between the studied population and patients in previous studies.[28] Fast VAs as observed in our cohort, may be due to small anatomical or even functional reentry circuits. The substrate for these fast VAs may not be sufficiently targeted by EC of the scar-borderzone.

The fact that late VA in both groups were similar regarding CL and response to ATP, supports the conclusion that EC had no sufficient impact on the VA substrate. Progressive remodeling and LV re-enlargement may occur after surgery contributing to arrhythmogenity, which is also supported by the high occurrence rate of atrial fibrillation in patients with VA.[9,21]

Survival

We reported a good overall survival of 78% at 5 years follow-up for the total study population. This is comparable with other centers with a large experience in SVR (70-82% 5 years survival).[2,10] No arrhythmic deaths occurred.

The observed fast VAs terminated by ICD shock in 11 patients (14%), may be considered as aborted arrhythmic deaths. Two prior studies reported similar rates of arrhythmic deaths (17% and 20%).[7,12] In contrast, in 1 study cardiac death constituted 19% of late mortality at follow-up, however sudden cardiac death rate was only 2.5%.[2] Although not all ICD therapy equals aborted sudden death, most of the study period was during the time with relatively short detection times and prior to MADIT-RIT trial results were published, symptomatic and potential fatal VA do occur.[29]

Clinical implications

The majority of patients referred for SVR and without prior VA were inducible for aneurysm-related monomorphic VA prior to SVR. Although all pre-operatively inducible patients underwent concomitant EC targeting the scar-borderzone this was not sufficient to prevent VA in a considerable number of patients. We observed a clinically relevant high VA occurrence rate after surgery in both the PES- and control group. Considering the good long-term survival and high incidence of appropriate ICD therapies, other concomitant antiarrhythmic surgical approaches targeting the potential arrhythmogenic substrate like endocardectomy should be explored, as endocardial encircling cryoablation alone appears not to be sufficient.[30] According to current

guidelines patients after SVR, independently of concomitant anti-arrhythmic treatment, should receive an ICD to prevent sudden cardiac death if they meet the criteria for prophylactic ICD implantation.

Limitations

Because of the retrospective nature of the study the number of patients included is limited. As a consequence of the inclusion of a historical control group, follow-up duration varied among patients. Furthermore, this study was non-randomized. To adjust for baseline-imbalances a Cox regression analysis was performed, the results were checked with a Cox model adjusted for propensity score. Despite this evaluation it should be kept in mind that neither a standard Cox model nor a propensity score can balance for unmeasured confounding. So, residual confounding should still be considered one of the explanations for our results. The adjusted hazard ratio for the PES group increases after adjusting for confounders. This may in part reflect the poorer baseline condition of the control group. As the confidence interval of the adjusted hazard ratio is very wide no definite conclusions with regard the relation between PES guided EC and outcome can be drawn.

No comparison between patients with inducible aneurysm-related VA but without concomitant EC was performed. However, because of the reported favorable results of non-mapping guided cryoablation to treat VA, not performing cryoablation in these high-risk patients was considered unethical. Although the treatment strategy was not allocated in a randomized fashion, groups were comparable and treated by the same team. Because the cohort was small the negative predictive value should be interpreted with caution.

Conclusion

The majority of patients referred for SVR without previously documented VA was inducible for aneurysm-related fast monomorphic VA. Despite concomitant EC targeting the scar-borderzone, postoperative hemodynamic improvement and low all-cause mortality, 5 year VA-free survival was only 64%. No difference in VA occurrence or ICD therapy was observed between patients with or without PES-guided concomitant EC. An ICD should therefore be considered in patients after SVR as they remain at high risk for VA. Consequently, other strategies for targeting the substrate for VA in this patient population are required.

REFERENCES

1. Mosterd A, Cost B, Hoes AW, et al. The prognosis of heart failure in the general population: The Rotterdam Study. *Eur Heart J*. 2001;22:1318-1327.
2. Di Donato M, Sabatier M, Dor V, Buckberg G. Ventricular arrhythmias after LV remodelling: surgical ventricular restoration or ICD? *Heart Fail Rev*. 2004;9:299-306.
3. Hsia HH, Lin D, Sauer WH, Callans DJ, Marchlinski FE. Anatomic characterization of endocardial substrate for hemodynamically stable reentrant ventricular tachycardia: identification of endocardial conducting channels. *Heart Rhythm*. 2006;3:503-512.
4. Arenal A, del Castillo S, Gonzalez-Torrecilla E, et al. Tachycardia-related channel in the scar tissue in patients with sustained monomorphic ventricular tachycardias: influence of the voltage scar definition. *Circulation*. 2004;110:2568-2574.
5. Athanasuleas CL, Buckberg GD, Stanley AW, et al. Surgical ventricular restoration in the treatment of congestive heart failure due to post-infarction ventricular dilation. *J Am Coll Cardiol*. 2004;44:1439-1445.
6. Dor V, Saab M, Coste P, Kornaszewska M, Montiglio F. Left ventricular aneurysm: a new surgical approach. *Thorac Cardiovasc Surg*. 1989;37:11-19.
7. Klein P, Bax JJ, Shaw LJ, et al. Early and late outcome of left ventricular reconstruction surgery in ischemic heart disease. *Eur J Cardiothorac Surg*. 2008;34:1149-1157.
8. O'Neill JO, Starling RC, Khaykin Y, et al. Residual high incidence of ventricular arrhythmias after left ventricular reconstructive surgery. *J Thorac Cardiovasc Surg*. 2005;130:1250-1256.
9. Wijnmaalen AP, Roberts-Thomson KC, Steven D, et al. Catheter ablation of ventricular tachycardia after left ventricular reconstructive surgery for ischemic cardiomyopathy. *Heart Rhythm*. 2012;9:10-17.
10. Guiraudon GM, Thakur RK, Klein GJ, et al. Encircling endocardial cryoablation for ventricular tachycardia after myocardial infarction: experience with 33 patients. *Am Heart J*. 1994;128:982-989.
11. Frapier JM, Hubaut JJ, Pasquie JL, Chaptal PA. Large encircling cryoablation without mapping for ventricular tachycardia after anterior myocardial infarction: long-term outcome. *J Thorac Cardiovasc Surg*. 1998;116:578-583.
12. Demaria RG, Mukaddirov M, Rouviere P, et al. Long-term outcomes after cryoablation for ventricular tachycardia during surgical treatment of anterior ventricular aneurysms. *Pacing Clin Electrophysiol*. 2005;28 Suppl 1:S168-S171.
13. Daubert JP, Zareba W, Hall WJ, et al. Predictive value of ventricular arrhythmia inducibility for subsequent ventricular tachycardia or ventricular fibrillation in Multicenter Automatic Defibrillator Implantation Trial (MADIT) II patients. *J Am Coll Cardiol*. 2006;47:98-107.
14. Buxton AE, Lee KL, Di Carlo L, et al. Electrophysiologic testing to identify patients with coronary artery disease who are at risk for sudden death. Multicenter Unsustained Tachycardia Trial Investigators. *N Engl J Med*. 2000;342:1937-1945.
15. Miller JM, Marchlinski FE, Buxton AE, Josephson ME. Relationship between the 12-lead electrocardiogram during ventricular tachycardia and endocardial site of origin in patients with coronary artery disease. *Circulation*. 1988;77:759-766.
16. Witkowski TG, ten Brinke EA, Delgado V, et al. Surgical ventricular restoration for patients with ischemic heart failure: determinants of two-year survival. *Ann Thorac Surg*. 2011;91:491-498.
17. Jones RH, Velazquez EJ, Michler RE, et al. Coronary bypass surgery with or without surgical ventricular reconstruction. *N Engl J Med*. 2009;360:1705-1717.

18. Piers SR, Wijnmaalen AP, Borleffs CJ, et al. Early reperfusion therapy affects inducibility, cycle length, and occurrence of ventricular tachycardia late after myocardial infarction. *Circ Arrhythm Electrophysiol*. 2011;4:195-201.
19. Wolpert C, Kuschyk J, Aramin N, et al. Incidence and electrophysiological characteristics of spontaneous ventricular tachyarrhythmias in high risk coronary patients and prophylactic implantation of a defibrillator. *Heart*. 2004;90:667-671.
20. Schmitt C, Barthel P, Ndrepepa G, et al. Value of programmed ventricular stimulation for prophylactic internal cardioverter-defibrillator implantation in postinfarction patients preselected by noninvasive risk stratifiers. *J Am Coll Cardiol*. 2001;37:1901-1907.
21. Sartipy U, Albage A, Insulander P, Lindblom D. Surgery for ventricular tachycardia in patients undergoing surgical ventricular restoration: the Karolinska approach. *J Interv Card Electrophysiol*. 2007;19:171-178.
22. Iesaka Y, Nogami A, Aonuma K, et al. Prognostic significance of sustained monomorphic ventricular tachycardia induced by programmed ventricular stimulation using up to triple extrastimuli in survivors of acute myocardial infarction. *Am J Cardiol*. 1990;65:1057-1063.
23. Babokin V, Shipulin V, Batalov R, Popov S. Surgical ventricular reconstruction with endocardectomy along radiofrequency ablation-induced markings. *J Thorac Cardiovasc Surg*. 2013;146:1133-1138.
24. Kaltenbrunner W, Cardinal R, Dubuc M, et al. Epicardial and endocardial mapping of ventricular tachycardia in patients with myocardial infarction. Is the origin of the tachycardia always subendocardially localized? *Circulation*. 1991;84:1058-1071.
25. Stevenson WG, Khan H, Sager P, et al. Identification of reentry circuit sites during catheter mapping and radiofrequency ablation of ventricular tachycardia late after myocardial infarction. *Circulation*. 1993;88:1647-1670.
26. d'Avila A, Aryana A, Thiagalingam A, et al. Focal and linear endocardial and epicardial catheter-based cryoablation of normal and infarcted ventricular tissue. *Pacing Clin Electrophysiol*. 2008;31:1322-1331.
27. Wellens F, Geelen P, Demirsoy E, et al. Surgical treatment of tachyarrhythmias due to postinfarction left ventricular aneurysm with endoaneurysmorrhaphy and cryoablation. *Eur J Cardiothorac Surg*. 2002;22:771-776.
28. Wijnmaalen AP, Schalij MJ, von der Thusen JH, Klautz RJ, Zeppenfeld K. Early reperfusion during acute myocardial infarction affects ventricular tachycardia characteristics and the chronic electroanatomic and histological substrate. *Circulation*. 2010;121:1887-1895.
29. Moss AJ, Schuger C, Beck CA, et al. Reduction in inappropriate therapy and mortality through ICD programming. *N Engl J Med*. 2012;367:2275-2283.
30. Miller JM, Kienzle MG, Harken AH, Josephson ME. Subendocardial resection for ventricular tachycardia: predictors of surgical success. *Circulation*. 1984;70:624-631.

Chapter 8

Endocardial/Epicardial- versus Endocardial Encircling Cryoablation for Ventricular Tachycardia; A Randomized Trial

Carine F.B. van Huls van Taxis, Katja Zeppenfeld, Robert J.M. Klautz, Adrianus P. Wijnmaalen

Accepted for publication in the Journal of Thoracic and Cardiovascular Surgery

INTRODUCTION

Patients remain at risk for ventricular tachycardia (VT) after surgical ventricular reconstruction (SVR).[1-3] During surgery concomitant preventive antiarrhythmic treatment may be of important incremental value. Standard non-mapping guided endocardial encircling cryoablation (ENDO) is unlikely to result in a complete transmural lesion in ventricular myocardium of normal wall thickness.[4] We hypothesised that doubling the lesion depth by combined endocardial-epicardial encircling cryoablation (ENDO-EPI) would lead to a transmural lesion electrically disconnecting the VT substrate from the remaining myocardium thereby preventing future VT. We aimed to determine the electrophysiological effects of ENDO-EPI cryoablation, compared to ENDO cryoablation.

METHODS

The study was designed as a single-center prospective open label parallel group comparison of conventional endocardial- versus new combined endocardial-epicardial encircling cryoablation (1:1 randomization) of the myocardial aneurysm scar-borderzone to treat VT, approved by the institutional ethics committee (P07.257) and registered at the Netherlands Trial Register (NTR3340). The manuscript was prepared according to the CONSORT checklist. Inclusion criteria were acceptation for SVR and inducible aneurysm-related VT at electrophysiology study. Patients were included in our hospital from 2008-2011 by the treating physician and allocated according to the predefined randomization list.

During surgery epicardial pacemaker lead-pairs were placed at the LV and RV, and the aneurysm (Figure 1). No subendocardial resection was performed. Cryoablation was performed with overlapping linear applications (-145˚C, 90s) at the endocardial aneurysm scar-borderzone.[5] In the ENDO-EPI group additional overlapping epicardial applications were applied opposite to the endocardial cryoablation line. Conduction properties were determined by pacing at all 3 pacemaker lead-pairs before and after cryoablation.

The primary endpoint was the presence of ≥50ms conduction delay or bidirectional block after cryoablation. The secondary endpoint was VT occurrence during follow-up.

A detailed further description is provided in the online supplement.

RESULTS

Nine patients were enrolled to the ENDO Group and 10 to the ENDO-EPI Group. One in the ENDO Group withdrew from the study and was excluded from further analysis (see Table 1 and 2 of the online supplement for patient- and peri-operative characteristics). Conduction over

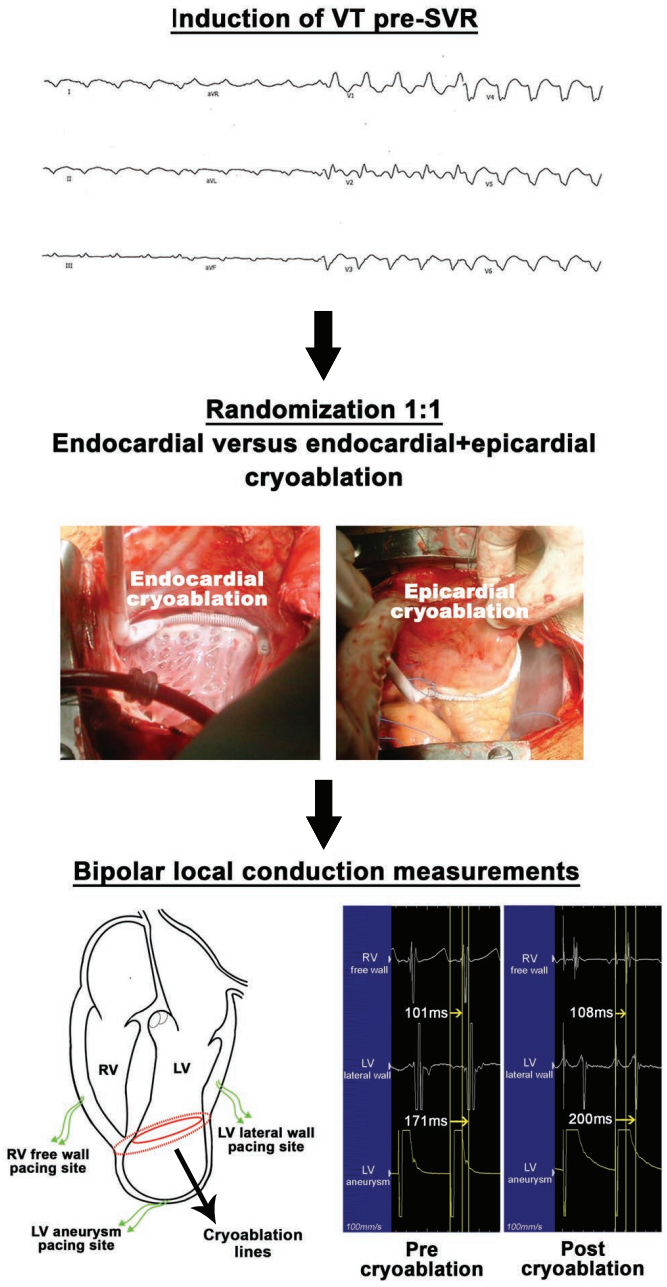

Figure 1. Graphical presentation of the trials' methods and primary outcome. Top: induced VT (ventricular tachycardia) originating from the inferior-apical aneurysm borderzone. Middle: flow chart of the 2 treatment arms. Left bottom: schematic overview of pacemaker lead pairs placements in right and left ventricle and cryoablation lines. Right bottom: example of conduction measurements with no significant conduction delay. LA/RA=left and right atrium; LV/RV=left and right ventricle; SVR=surgical ventricular reconstruction.

the cryoablation line during LV and RV pacing was present in all without conduction delay. In 15 patients pacing at the aneurysm resulted in capture and conduction without delay. In 3 patients pacing over the aneurysm lead-pairs did not result in local capture (1 ENDO, 2 ENDO-EPI) which was judged to be caused by manipulation of the leads during surgery. Two patient died of heart failure postoperatively (1 each group); 16 patients (7 ENDO; 9 ENDO-EPI) were discharged and prospectively followed.

The primary endpoint of a significant conduction delay or block was not established in any patient, therefore after consultation with the institutional ethics committee it was decided to terminate the inclusion.

VT occurred in 2/7 patients in the ENDO group; both had multiple VTs in a brief period, 1 shortly after surgery (27 VTs) managed by catheter ablation and 1 years after (14 VTs) managed by Sotalol. VT occurred in 5/9 patients in the ENDO-EPI group 25 (9-66) months after cryoablation (1-3 VT episodes/patients). Because of small numbers we could not evaluate differences between groups regarding the secondary endpoint.

CONCLUSION

During SVR both ENDO and ENDO-EPI encircling cryoablation did not create sufficient lesions to significantly delay conduction from aneurysm scar to the functional LV. VT occurrence rate was high in both groups. Although the results are limited by the small number of patients, it appears encircling cryoablation did not prevent VT, and therefore other surgical techniques like endocardectomy should be considered.

REFERENCES

1. Klein P, Bax JJ, Shaw LJ, Feringa HH, Versteegh MI, Dion RA, et al. Early and late outcome of left ventricular reconstruction surgery in ischemic heart disease. *Eur J Cardiothorac Surg.* 2008;34:1149-1157.
2. Di Donato M, Sabatier M, Dor V, Buckberg G. Ventricular arrhythmias after LV remodelling: surgical ventricular restoration or ICD? *Heart Fail Rev*. 2004;9:299-306.
3. van Huls van Taxis CF, Wijnmaalen AP, Klein P, Dekkers OM, Braun J, Verwey HF, et al. Programmed electrical stimulation-guided encircling cryoablation concomitant to surgical ventricular reconstruction for primary prevention of ventricular arrhythmias. *Eur J Cardiothorac Surg*. 2018;54:98-105.
4. Guiraudon GM, Thakur RK, Klein GJ, Yee R, Guiraudon CM, Sharma A. Encircling endocardial cryoablation for ventricular tachycardia after myocardial infarction: experience with 33 patients. *Am Heart J.* 1994;128:982-989.
5. Wijnmaalen AP, Roberts-Thomson KC, Steven D, Klautz RJ, Willems S, Schalij MJ, et al. Catheter ablation of ventricular tachycardia after left ventricular reconstructive surgery for ischemic cardiomyopathy. *Heart Rhythm*. 2012;9:10-17.

Chapter 8

Endocardial/Epicardial- versus Endocardial Encircling Cryoablation for Ventricular Tachycardia; A Randomized Trial

Supplement

METHODS

Patient population

The study was designed as a single center prospective open label parallel group comparison of endocardial versus combined endocardial-epicardial cryoablation of myocardial scar borderzone to treat VT, approved by the institutional ethics committee, between 2008 and 2011. Inclusion criteria were acceptation for SVR according to Dor in the Leiden University Medical Center, ischemic heart failure (New York Heart Association class 2-4) and age older than 18 years. Exclusion criteria were inability to comply with the protocol due to hemodynamic instability or to sign informed consent.
The manuscript was prepared according to the CONSORT checklist.

Endpoints

The primary endpoint and assumed optimal acute electrophysiological outcome of non-mapping guided encircling cryoablation was the electrical isolation of the scar area to exclude the arrhythmogenic part from the ventricles.

The normal left ventricular wall thickness at midventricular level is between 5,6±1.1mm (minimum) and 9,5±1.9mm (maximum) in men.[1] As cryoablation has shown to result in transmural lesions of 4mm in the atrium and 6mm lesion depth in ventricular myocardium the creation of encircling transmural lesions on de scar border applying standard endocardial cryoablation is unlikely.[2,3] In addition our clinical observation showed that patients who underwent encircling cryoablation experienced VTs during follow-up to a similar rate as patients who did not undergo encircling cryoablation, indicating failure of the standard therapy to isolate the substrate in a large proportion of patients. It was therefore assumed that endocardial encircling cryoablation would result in isolation in a minority of patients. A high percentage of transmural lesions after combined endo-epicardial cryoablation (doubling the lesion depth) was thought to be reasonable.

The secondary endpoint was occurrence of any sustained ventricular arrhythmia registered by the ICD or electrogram during follow-up.

Clinical evaluation

Prior to surgery, patients underwent extensive clinical evaluation consisting of careful history taking, echocardiography, coronary angiography and ICD interrogation. The results, including the functional status, presence of a LV anterior-apical aneurysm, concomitant valve disease and remaining coronary artery disease, were carefully evaluated by a team of cardiologists, electrophysiologists and cardiothoracic surgeons according to the institutional protocol.

Assessment myocardial wall thickness

To evaluate whether the wall thickness assumed based on literature applied to the current patient population, diastolic wall thickness was measured at the healthy myocardium side of the scar border in the cine-MRI images. Imaging planes and walls assessed were: 4 chamber view: septal and lateral; 2 chamber view: anterior and inferior, short axis: 6 segments.

Preoperative electrophysiological evaluation (PES)

Two catheters were inserted through the right femoral vein, one placed at the His position and the second at the right ventricular apex and subsequently in the right ventricular outflow tract to perform PES. The PES protocol consisted of 3 drive cycle lengths (600, 500, 400ms) with 1-3 ventricular extra stimuli (down to 200ms or refractory period) and incremental burst pacing. An aneurysm-related VT substrate was assumed if PES induced a monomorphic VA, lasting >30s or requiring termination because of hemodynamic compromise and the VT exit site was located at the aneurysm scar-borderzone. The presumed exit site was determined based on the VT 12-lead electrocardiogram morphology.[4] All 12-lead VT electrocardiograms were analyzed by 2 independent observers. In case of discrepancy agreement was reached by consensus. Patients with aneurysm-related VT were candidates for participation in the trial and asked to participate. After signing the informed consent form, patients were randomly assigned in a 1:1 fashion to either the conventional surgical VT therapy of endocardial encircling cryoablation (ENDO Group) to serve as a control group, or the newly proposed therapy of combined endocardial-epicardial encircling cryoablation (ENDO-EPI Group).

Surgical technique

Patients underwent SVR according to the previously described technique.[5] Surgery was performed using cardiopulmonary bypass, aortic cross-clamping and intermittent warm blood cardioplegia. Epicardial temporary pacemaker lead-pairs were placed at the LV and RV, and the aneurysm. Then, the LV was opened through the infarcted area. At the transitional zone between viable and scarred myocardium, endocardial encircling cryoablation was performed with a 4mm diameter malleable cryoprobe (Cardioblate CryoFlex, Medtronic, Minneapolis, USA) using argon gas. As mentioned above, the myocardium thickness targeted by encircling cryoablation is likely between 6 and 11mm. The available studies have mainly been performed in, thinner ±4mm, atrial tissue where 60sec of cryoapplication (-150ºC) resulted in transmural lesions. Therefore we extended the freezing time with 50%, so 90 seconds per application, to achieve an assumed lesion depth of at least 6mm in endocardial and 12 mm in combined endo- and epicardial cryoablation. Overlapping linear applications, down to -145˚C for 90s, were made to the aneurysm scar-borderzone. In the ENDO-EPI group additional overlapping epicardial cryoablation lesions were applied opposite to the endocardial cryoablation line.

After cryoablation, a Fontan-stich was placed at the transitional zone. The residual LV cavity was shaped and sized using a mannequin balloon at 55ml/m2body surface-area (TRISVR, Chase

Medical, Richardson, USA) and the remaining defect was closed through an endoventricular Dacron patch plasty. Excluded fibrous scar-tissue was sutured over the patch to improve hemostasis. Additional concomitant procedures, such as valve surgery and/or coronary artery bypass grafting, were performed when indicated. After weaning the patient from extracorporeal circulation, trans-esophageal echocardiography was repeated to assess LV shape and function, patch integrity and valvular competency. Conduction properties between LV, RV and aneurysm were measured by sequentially pacing at all 3 pacemaker lead-pairs consecutively before and after cryoablation.

No endocardial resection was performed during surgical ventricular restoration in our cohort prior to this study. Prior investigation by Guiraudon and colleagues demonstrated promising results by performing only encircling cryoablation concomitant to SVR.[6] Therefore we adapted this strategy. Additionally, not resecting the myocardial scar has been for enhancement of surgical stability of the SVR and improved hemostasis during the procedure.

ICD settings

In patients without ICD before surgery one was implanted before discharge based on the preoperative LV ejection fraction (EF) ≤30-35% according to current European Society of Cardiology guidelines. Devices were programmed according to our standard institutional protocol for primary prevention; VT monitor zone (VACL 321-400ms, no therapy), VT zone (VACL 261-320ms, anti-tachycardia pacing) and if the VT continued ICD shocks), VF zone (VACL ≤260ms, ICD shocks). Settings were adapted when clinically indicated.

Follow-up

Patients were prospectively followed in an outpatient heart failure program and maintained on optimal medical treatment for heart failure. ICDs were interrogated every 6 months. Printouts were reviewed for the occurrence of sustained VA, VACL and therapy mode. VT were classified as sustained when lasting >30s in the ICD monitor zone or when initiated appropriate ICD therapy. Therapy was considered appropriate when occurring in response to any VA. Echocardiography was performed before discharge and afterwards annually. The follow-up started at time of discharge and ended at last outpatient clinic visit up to June 2016 or death.

Statistical analysis

We used a Two Independent Proportions Power Analysis to determine group size. It was assumed that 80% of the patients in the study group and 30% in the control group would reach the primary outcome. Group sample sizes of 18 in the study group and 18 in the control group achieved a 91% power to detect a 50% difference between groups in regarding the primary endpoint. The test statistic used was the two-sided Z test with pooled variance. The significance level of the test was targeted at 0.05.

Continuous variables are expressed as mean (standard deviation) or median (interquartile range [IQR]) and categorical variables as percentages (%), where appropriate. To compare groups for continuous variables Student's T-test (normally distributed data) and Mann-Whitney U-test (non-normally distributed data) were used. For categorical data the Fishers Exact-test was used. All tests were 2-sided and a p-value of <0.05 was considered significant. General statistical analyses were performed using SPSS software (version 22, SPSS Inc, Chicago, IL, USA). For the power calculation PASS software was used (version 15, NCSS Statistical Software, Kaysville, UT, USA). The randomization list was constructed by R software (version 3.0.1. R Foundation, Vienna, Austria).

RESULTS

Table 1 describes patients characteristics.
Table 2 describes peri-operative characteristics.

Assessment myocardial wall thickness

Wall thickness was determined in a subset of six of 18 patients (2 in the ENDO group, 4 in the ENDO-EPI group) in whom pre-operative MRI data were available. In these patients mean wall thickness of the borderzone was 7.9±1.6mm. Maximal wall thickness was found in the septal segments as was expected (mean 8.7±1.7mm, maximal wall thickness measured 11.3mm).

Programmed electrical stimulation after SVR

Thirteen of the 16 patients who were discharged underwent PES after SVR, using the same induction protocol as pre-operatively. Two patients (1 both groups) died during the post-operative period before PES could be performed (due to heart failure). In 1 patient no PES was performed because of the preference of the patient (ENDO-EPI) and the other 2 patients (1 both groups) experienced VT during the post-operative period so PES was thought to be unnecessary. Both these patients also experienced VTs during follow-up. Only 1 of 13 patients (ENDO group) who underwent programmed electrical stimulation after SVR was inducible for VT, which was aneurysm related. During follow-up this patient did not experience any VT. One other patient (ENDO group) was non-inducible 1 week after surgery but experienced incessant VT 4 weeks later. This patient underwent successful radiofrequency catheter ablation where the clinical VT was terminated at the inferior-apical border of the patch.

Table 1. Baseline characteristics

	Total population N=18	ENDO Group N=8	ENDO-EPI Group N=10	P-value*
Male, n (%)	15(83)	6(75)	9(90)	0.559†
Age, years	64±10	62±9	66±11	0.390‡
LV ejection fraction,%	27±6	27±5	27±6	0.979‡
LV end diastolic volume -index, ml/m^2	112±44	129±58	102±34	0.230‡
LV end systolic volume -index, ml/m^2	82±36	97±49	74±25	0.260‡
Diabetes mellitus, n (%)	5 (27)	0	5 (50)	0.036†
Atrial fibrillation, n (%)	4 (22)	1 (13)	3 (33)	0.588†
Medication, n (%)				
Beta-blocker	18 (100)	8 (100)	10 (100)	1.0†
ACE-inhibitor/ Angiotensin II receptor blockers	18 (100)	8 (100)	10 (100)	1.0†
Mineralocorticoid receptor antagonists	11 (61)	4 (50)	7 (70)	0.630†
Antiarrhythmic drugs	4 (22)	0	4 (40)	0.092†
New York Heart Association class, n (%)				1.000†
Class 2	8 (44)	4 (50)	4 (40)	
Class 3	10 (66)	4 (50)	6 (60)	
Creatinine clearance, ml/min*1.73 m^2	72±27	70±20	73±33	0.812‡
Euroscore, n (IQR)	10 (5-24)	6 (4-20)	19 (8-25)	0.203¥
Coronary artery disease, n	1.9±0.7	1.9±0.8	1.9±0.6	0.941‡
Left anterior descending artery, n (%)	18 (100)	8 (100)	10 (100)	
Right coronary artery, n (%)	9 (50)	6 (75)	3 (30)	
Ramus circumflexus, n (%)	7 (39)	4 (50)	3 (30)	
Time from myocardial infarction to surgical ventricular reconstruction, months (IQR)	53 (10-213)	51 (12-170)	53 (5-294)	0.762¥
Characteristics induced VT, n	22	10	12	
VTs/patient, n	1.2±0.5	1.3±0.5	1.2±0.6	0.854‡
Cycle length	267±56	267±63	267±53	0.961‡
Left axis	14 (64)	7 (70)	7 (58)	0.380†
Left bundle branch block	10 (46)	5 (50)	5 (42)	0.666†

**P*-value calculated between groups
LV = left ventricle; VT = ventricular tachycardia
†Fisher's exact-test; ‡Student's T-test; ¥Mann Whitney U-test

DISCUSSION

Limitations

The study was designed as a prospective open label parallel group comparison. The non-blinded nature of the study may be associated with an inherent bias. Reliable blinding of those involved in performing the conduction measurements was however considered to be unfeasible as these

Table 2. Peri-operative characteristics

	Total population N=18	ENDO Group N=8	ENDO-EPI Group N=10	P-value*
Coronary artery bypass grafting, n (%)	12 (67)	5 (63)	7 (70)	0.737‡
Mitral valve plasty, n (%)	9 (50)	3 (38)	6 (60)	0.343†
Tricuspid valve plasty, n (%)	4 (22)	1 (13)	3 (30)	0.375†
Aortic valve replacement, n (%)	1 (11)	1 (13)	0	0.250†
Cardiopulmonary bypass, min	212±67	200±75	222±62	0.509‡
Aortic cross-clamping, min	135±47	126±62	142±39	0.516‡
Postoperative stay, days	11 (8-15)	11 (8-14)	11 (9-18)	0.573¥
Post-operative mortality, n	2 (11)	1 (13)	1 (10)	1.0†
Post-operative echocardiography				
LV ejection fraction (%)	32±12	35±6	30±15	0.429‡
LV end diastolic volume-index, ml/m^2	77±17	73±16	79±19	0.514‡
LV end diastolic volume-index, ml/m^2	48±17	46±12	50±20	0.626‡

**P*-value calculated between groups
LV = left ventricle
†Fisher's exact-test; ‡Student's T-test; ¥Mann Whitney U-test

included the surgeon and those involved during the surgery. The treatment and measurements were done according to a standard protocol. Utmost care was taken to correctly assess the conduction prior to and after surgery.

The study was terminated after inclusion of 19 patients as the primary endpoint was not met in any of the participants. As no histopathological evaluation of the myocardial cryolesions was performed it is not possible to determine the exact reason for failure of combined endo- epicardial cryoablation. Although VTs occurred in both groups the resulting size of the study population is too small to make a relevant comparison between groups regarding the secondary endpoint (VT occurrence).

REFERENCES

1. Kawel N, Turkbey EB, Carr JJ, Eng J, Gomes AS, Hundley WG, et al. Normal left ventricular myocardial thickness for middle-aged and older subjects with steady-state free precession cardiac magnetic resonance: the multi-ethnic study of atherosclerosis. *Circ Cardiovasc Imaging*. 2012;5:500-508.
2. Doll N, Kornherr P, Aupperle H, Fabricius AM, Kiaii B, Ullmann C, et al. Epicardial treatment of atrial fibrillation using cryoablation in an acute off-pump sheep model. *Thorac Cardiovasc Surg.* 2003;51:267-273.
3. d'Avila A, Aryana A, Thiagalingam A, Holmvang G, Schmidt E, Gutierrez P, et al. Focal and linear endocardial and epicardial catheter-based cryoablation of normal and infarcted ventricular tissue. *Pacing Clin Electrophysiol*. 2008;31:1322-1331.
4. Miller JM, Marchlinski FE, Buxton AE, Josephson ME. Relationship between the 12-lead electrocardiogram during ventricular tachycardia and endocardial site of origin in patients with coronary artery disease. *Circulation.* 1988;77:759-766.
5. Dor V, Saab M, Coste P, Kornaszewska M, Montiglio F. Left ventricular aneurysm: a new surgical approach. *Thorac Cardiovasc Surg*. 1989;37:11-19.
6. Guiraudon GM, Thakur RK, Klein GJ, Yee R, Guiraudon CM, Sharma A. Encircling endocardial cryoablation for ventricular tachycardia after myocardial infarction: experience with 33 patients. *Am Heart J.* 1994;128:982-989.

Chapter 9

Summary, Conclusions and Future Perspectives

SUMMARY

Ablation of ventricular arrhythmias (VA) in patients with and without structural heart disease has become an important therapeutic option and is increasingly being performed. The aim of the current thesis was to study new strategies and techniques in VA ablation that facilitate and thereby potentially improve procedural and long-term outcome after ablation. Chapter 1 provides an historical overview of the developments in surgical- and catheter ablation treatment strategies of VA in patients with and without structural heart disease and the currently applied ablation techniques.

Part I of this thesis focuses on radiofrequency catheter ablation (RFCA) of premature ventricular contractions (PVCs). High idiopathic PVC burden has been associated with PVC-induced cardiomyopathy. However, frequent PVCs may also worsen a pre-existing cardiomyopathy. RFCA of frequent PVC in patients with left ventricular (LV) dysfunction is usually restricted to patients with suspected PVC-induced cardiomyopathy. N-terminal pro-brain natriuretic peptide (NT-proBNP) and BNP are markers for increased ventricular wall stress and has been demonstrated to be a reliable marker to monitor heart failure. **Chapter 2** describes the results of a prospective multicentre study regarding 80 consecutive patients with frequent PVCs and LV dysfunction and referred for catheter ablation. Twenty-seven patients (34%) had a diagnosis of structural heart disease (of which 17 patients with ischemic heart disease). The neurohormonal, structural and functional recovery pattern was evaluated after PVC ablation. After 12 months follow-up left ventricular ejection fraction (LVEF) recovered from 34% to 46%, BNP decreased from 140pg/mL to 40pg/mL and New York Heart Association functional class improved from 2 to 1 after successful ablation, all regardless of a potential PVC-induced or PVC-worsened cardiomyopathy. Twenty patients who underwent successful ablation had a class I indication for ICD implantation prior to ablation but had no such indication 6 months after ablation. Improvement in LVEF was related to the baseline PVC burden and the persistence of acute ablation success. Given the magnitude of the obtained benefit and its consistency in unselected patients, all patients with depressed LVEF should be evaluated for the presence of frequent PVCs, especially those meeting criteria for primary prevention ICD implantation, as the benefit might modify the clinical decision making.

In addition, patients with frequent PVCs may be symptomatic before LV dysfunction develops. It is still unclear which patients develop a PVC-induced cardiomyopathy, as not all patients with frequent PVCs develop LV dysfunction. In **Chapter 3**, 80 consecutive patients with frequent symptomatic idiopathic PVCs and a preserved LV function undergoing PVC ablation were analysed. In addition to NT-proBNP, circumferential end-systolic wall stress (cESS) on echocardiography is also a marker for increased ventricular wall stress. Type of symptoms analysed included palpitations, fatigue, (near-) syncope. The use of NT-proBNP and cESS were tested in this patient population, also in relation to type of symptom. NT-proBNP was elevated in 41% of the total patient group. Only fatigue, but not palpitation or (near-) syncope, was

associated with higher baseline NT-proBNP and cESS. In patients after sustained successful ablation NT-proBNP and cESS decreased significantly. Furthermore, fatigue was independently associated with a significantly larger reduction in NT-proBNP. In patients after non-successful ablation NT-proBNP and cESS remained unchanged.

According to current recommendations, catheter ablation can be useful in patients with frequent symptomatic PVCs if antiarrhythmic drugs are not effective, tolerated or desired. Ablation is not indicated for asymptomatic PVCs that are not suspected of causing or contributing to ventricular dysfunction. We could demonstrate for the first time that fatigue, which is often considered a nonspecific symptom and not typically related to PVCs, was associated with elevated NT-proBNP levels and cESS on echocardiography. NT-proBNP and cESS are markers for ventricular wall stress and both normalized after successful ablation accompanied by relief of symptoms of fatigue. Although we cannot prove causality, the current findings suggest that fatigue may be associated with PVC-induced ventricular wall stress, which can be successfully treated by catheter ablation. In the light of the these findings, clinicians may therefore consider catheter ablation of PVCs in patients presenting only with fatigue, even in the absence of LV dysfunction, classical PVC related symptoms (such as palpitations or [near-]syncope), or a certain PVC burden. Whether elevated NT-proBNP level and fatigue as presenting symptom identify patients at risk to develop PVC-induced cardiomyopathy requires further investigation.

As described above, frequent PVCs in the absence of structural heart disease are a common entity. The majority of idiopathic PVCs originate from the right ventricular outflow tract (RVOT). Ablation is an effective treatment and although considered safe, serious complications may occur and the application of a limited number of radiofrequency lesions particular is preferred. In **Chapter 4** the value of reversed polarity of adjacent bipolar electrograms to predict a successful ablation site in idiopathic RVOT arrhythmias was evaluated. Twenty-five consecutive patients undergoing RFCA for RVOT PVCs were studied. Electrograms of ablation sites and of points within a 15mm radius to the successful site were evaluated for local activation time, unipolar electrogram morphology and the presence of reversed polarity of adjacent bipolar electrograms. Electrogram characteristics of successful ablation sites were compared to non-successful ablation sites. The spatial distribution of each electrogram characteristic was studied. Successful ablation sites more often demonstrated reversed polarity and had an earlier local activation time than non-successful ablation sites. A wide spatial distribution was observed for unipolar electrograms with a QS-configuration around the successful ablation site. Mapping based on local activation time and reversed polarity had a higher predictive value for a successful ablation site compared to mapping strategy based on local activation time and a unipolar QS-configuration. The presence of reversed polarity is easily to obtain and has a high predictive value to identify a successful ablation site in idiopathic focal RVOT arrhythmias. Combining local activation time and reversed polarity can predict a successful ablation site with higher accuracy than the conventional mapping strategy based on local activation time and unipolar QS-configuration. Its clinical application is likely to reduce the number of RFCA applications and radiation exposure to both patient and operator.

In **Part II** of this thesis, image integration during ablation of ventricular arrhythmias is analysed to facilitate the ablation procedure. Epicardial substrate determination and RFCA for VA is limited by the presence of coronary arteries and epicardial fat. In **Chapter 5** we aimed to evaluate epicardial ablation failure using real-time image integration and reversed registration of MDCT data and electroanatomical mapping (EAM). Twenty-eight patients underwent combined endocardial-epicardial EAM. Prior to the procedure, MDCT derived coronary anatomy and epicardial fat meshes were loaded into the EAM system. Real-time registration of MDCT data was performed after endocardial EAM and before epicardial EAM. The left main artery was used as a single landmark to merge both images. The distance between epicardial ablation target sites and coronary arteries was assessed by registered MDCT and angiography. Ablation was withheld within 5mm from a coronary artery confirmed by coronary angiography. After the procedure, mapping and ablation points were superimposed on the MDCT using a reversed registration matrix for head-to-head comparison of mapping data and local fat thickness. Real-time image integration of pre-acquired MDCT data with EAM was safe, accurate and feasible and available before epicardial EAM (surface registration error 2.8±1.3mm). Forty-six VA were targeted; 25 were abolished by RFCA and in 21 RFCA was not successful. In 8 VA no target site could be identified. In 2 VA ablation was withheld due to His-bundle vicinity and in 7 due to proximity of coronary arteries. In 4 VA RFCA was ineffective. At ineffective ablation sites mean epicardial fat layer was 16mm (range 7-22mm), compared to successful ablation sites were the mean epicardial fat layer was 1.5mm (range 0-6mm). Subsequently, epicardial fat layers of >7mm and the presence of coronary arteries were important reasons for epicardial ablation failure. Furthermore, bipolar voltages decreased with increasing fat thickness therefore making the exact delineation of fat based on bipolar voltage mapping poor. It may be even worse if subepicardial scar is present. Visualization of the MDCT derived coronary anatomy and epicardial fat thickness prior to epicardial mapping is therefore of importance for the identification of potential harmful and ineffective ablation sites and the correct interpretation of local bipolar electrograms and. In addition, accurate image integration after endocardial ablation failure for focal VA may even prevent unnecessary pericardial access and thereby potential complications in selected patients

Using the same technique of real-time image integration and a reversed registration matrix EAM data were additionally to MDCT superimposed on contrast-enhanced magnetic resonance imaging (CE-MRI) data to analyse scar information. This allowed us to combine both scar and fat information with EAM data and evaluate how they influenced unipolar and bipolar voltages. In **Chapter 6** this combined image integration technique is described in 10 patients with non-ischemic cardiomyopathy who underwent combined endocardial- and epicardial VA ablation. At the epicardium EAM may be challenging because differentiation between scar from viable myocardium is hindered by the presence of fat which influences bipolar voltages. It was illustrated that bipolar voltage ≤1.8mV and unipolar voltage of ≤7.95mV were the optimal cut-off points to distinguish scar from viable myocardium in epicardial regions devoid of ≥2.8mm fat. In

addition, only unipolar voltage could detect intramural scar. Both bipolar voltages and unipolar voltages were reduced by epicardial fat. Specific electrogram morphologies were not affected by fat, but were present at only one quarter of all scar sites. A newly developed algorithm combining unipolar voltage and electrogram characteristics could differentiate between scar and viable myocardium. These findings provide important insights into epicardial EAM in patients with non-ischemic cardiomyopathy, which is essential for successful ablation.

Part III concentrates on surgical encircling cryoablation for VA in patients undergoing surgical ventricular reconstruction (SVR). SVR is an effective treatment to improve LV function in patients with ischemic heart failure and an LV anterior-apical aneurysm**.** VA is an important cause for morbidity and mortality in these patients. Additional encircling endocardial cryoablation (EC) targeting the VA-substrate may therefore be required. Programmed electrical stimulation (PES) can identify patients at risk for VA. **Chapter 7** structurally evaluated the incidence of VA in patients after SVR with an ICD for primary prevention. Patients referred for SVR underwent PES pre-operatively. When inducible for aneurysm-related VA patients received concomitant EC to SVR. All patients received an ICD according to current guidelines. The efficacy of PES-guided EC concomitant to SVR for primary prevention of VA was assessed in patients inducible for VA pre-operatively.

Thirty-eight patients without spontaneous VA referred for SVR underwent pre-operative PES. A historical cohort of 39 patients without spontaneous VA, pre-operative PES and anti-arrhythmic surgery served as a Control group. The majority (71%) was inducible for aneurysm-related VA pre-operatively. During long term follow-up (>5 years) no arrhythmic deaths occurred. Five-year overall survival was high, but VA-free survival was low despite concomitant EC in patients inducible for aneurysm-related VA. Twenty-seven patients (35%) experienced 1 or more VA during follow-up. No difference in VA occurrence between patients who did and did not undergo PES-guided EC was observed and was high in both groups. Pre-operative PES could consequently not identify patient at risk for VA during long-term follow-up after SVR. Although all pre-operatively inducible patients underwent concomitant EC this was not sufficient to prevent VA in a considerable number of patients and no difference in VA occurrence rate was observed between patients with or without EC. Improvement in hemodynamics and concomitant EC appeared not to be sufficient to prevent VA in this patient population. Anti-arrhythmia surgery targeting the arrhythmogenic substrate, should therefore be considered in patients with documented VA or with a suspected substrate for reentry tachycardia. Other strategies should therefore be explored to identify patients at risk for VA and to prevent them in this high risk patient population.

In light of these results a randomized controlled trial was conducted which compared endocardial encircling cryoablation (ENDO) with a combined endocardial-epicardial (ENDO-EPI) cryoablation. In **Chapter 8** these results are described. Eighteen patients in whom aneurysm related VA was induced during PES prior to SVR, were included. Patients were randomized in

a 1:1 fashion to ENDO or ENDO-EPI group. During surgery 3 epicardial pacing wire pairs were placed on either side of the presumed ablation line to assess conduction properties before and after encircling cryoablation. All patients received an ICD. VA incidence was evaluated during long term follow-up.

Eight patients were randomized to ENDO and 10 to ENDO-EPI cryoablation. After SVR, a significant conduction delay (≥50ms) or bidirectional conduction block was achieved in none after cryoablation. During long-term follow-up 6 of 16 discharged patients (38%) had spontaneous VT registered on ICD. Long-term follow-up revealed no difference in VA occurrence between both groups (2 ENDO, 4 ENDO-EPI). In addition, no differences in VA cycle length, VAs per patients or VA-free survival could be identified between both groups. These results suggest that a change in surgical approach for anti-arrhythmic treatment is desirable. Perhaps subendocardial resection would improve VA free survival. This has not been structurally explored yet.

CONCLUSIONS AND FUTURE PERSPECTIVES

In all patients with frequent PVCs, irrespectively of the presence of structural heart disease, RFCA should be considered as all patients demonstrated significant improvement in LV dimensions, reduction of NT-proBNP and relieve of symptoms after successful ablation. Not all patients develop LV dysfunction due to frequent PVCs. However, up till now a proper tool to stratify was lacking. NT-proBNP might be used to detect patients who might be prone to develop LV dysfunction as it is a marker for increased ventricular walls stress. Furthermore, fatigue might be a due to increased ventricular wall stress in patients with frequent PVCs. Patients undergoing PVC ablation for frequent idiopathic PVCs are mostly healthy and young. It is therefore important to limit the number of RF applications. The use of reversed polarity can facilitate this as it identifies successful ablation sites very accurately. In all patients undergoing epicardial VA ablation, real-time image integration with MDCT and CE-MRI improved pre-procedural planning, substrate identification and delineation, and can guide to areas containing critical isthmus sites but also identifies inappropriate ablation sites due to coronary arteries and thick epicardial fat layers thereby facilitating successful ablation sites. Finally, it was demonstrated that endocardial and combined endocardial-epicardial encircling cryoablation were both not effective in preventing VA in patients after SVR. This is important because the VA circuits may resides beneath the patch material not accessible for catheter ablation. Other surgical treatments such as (non-mapping guided) endocardectomy should be opted to prevent VA in this high risk patient population. The studies described in this thesis illustrated new ablation strategies and techniques for VA which potentially could improve procedural success and long-term outcome after ablation.

Chapter 10

Nederlandse Samenvatting

NEDERLANDSE SAMENVATTING

Ablatie van ventriculaire ritmestoornissen is een belangrijke therapeutische optie geworden voor patiënten met- en zonder structurele hartziekten. Het doel van dit proefschrift was om nieuwe behandel strategieën en ablatie technieken ter verbetering van procedurele- en lange termijn ablatie uitkomsten te bestuderen. **Hoofdstuk 1** beschrijft de historische ontwikkelingen van katheter ablatie- en chirurgische strategieën bij patiënten met ventriculaire ritmestoornissen.

Deel 1 van het proefschrift betreft de behandeling van radiofrequente katheter ablatie van premature ventriculaire contracties (PVCs). **Hoofdstuk 2** beschrijft de resultaten van een prospectieve multicenter studie waarbij 80 patiënten werden geïncludeerd met frequente PVCs en een verminderde linker ventrikel (LV) functie. Al deze patiënten waren verwezen voor katheter ablatie. Zevenentwintig patiënten (34%) waren gediagnostiseerd met een structurele hartziekten (waarvan 17 met ischemische cardiomyopathie). Twaalf maanden na de behandeling was de LV ejectiefractie hersteld van 34% naar 46%, het brain natriuretisch peptide (BNP) verlaagd van 140pg/mL naar 40pg/mL en New York Heart Association functionele klasse verbeterd van 2 naar 1 na succesvolle ablatie, onafhankelijk van een mogelijke PVC-geïnduceerde of PVC-verslechterde cardiomyopathie. Twintig patiënten hadden voorafgaand aan de ablatie een indicatie voor een interne cardioverter defibrillator (ICD). Zes maanden na de ablatie was de LV functie dermate hersteld dat de indicatie kwam te vervallen. Verbetering in LV ejectiefractie was gerelateerd aan de PVC burden en het aanhoudende ablatie succes van de frequente PVC. Onafhankelijk van de aanwezigheid van structurele hartziekten zorgde succesvolle katheter ablatie van frequente PVCs in patiënten met een verminderde LV functie voor een klinische en functionele verbetering. De verbetering van hartfalen parameters was gerelateerd aan baseline PVC burden en het blijvende ablatie succes.

In **Hoofdstuk 3** werden 83 patiënten met frequente idiopathische PVCs en een behouden LV functie, die een PVC ablatie ondergingen, geanalyseerd. Patiënten kunnen symptomatisch zijn voordat LV dysfunctie optreedt ten gevolg van de frequente PVCs. N-terminal proBNP (NT-proBNP) en circumferentiële eind-systolische wandspanning (cESS) op echocardiografie, die beide markers zijn voor verhoogde ventriculaire wandspanning, werden getest in relatie tot de PVC burden en de verschillende symptomen (hartkloppingen, vermoeidheid, duizelingen/flauwvallen). Baseline NT-proBNP was verhoogd in 41% van de patiënten. Alleen vermoeidheid was geassocieerd met een hogere uitgangswaarde van NT-proBNP en cESS. Bij blijvend succes van de katheter ablatie daalde het NT-proBNP en cESS significant. Verder was vermoeidheid onafhankelijk geassocieerd met significant grotere reductie in NT-proBNP vergeleken met andere symptomen. In patiënten bij wie de ablatie faalde bleven NT-proBNP en cESS onveranderd. Deze bevindingen zijn een aanwijzing dat vermoeidheid mogelijk veroorzaakt kan worden door verhoogde ventriculaire wandspanning welke door frequente PVCs wordt veroorzaakt, zelfs in

patiënten met een normale LV functie. Patiënten met vermoeidheid en/of verhoogd NT-proBNP zouden daarom kunnen profiteren van een katheter ablatie procedure, zelfs in de afwezigheid van typische PVC-gerelateerde symptomen of een verminderde LV functie.

Hoofdstuk 4 evalueerde de waarde van 'reversed polarity' (tegenovergestelde polariteit van lokale elektrogrammen) om een succesvolle ablatie locatie te identificeren in idiopathische rechter kamer uitstroombaan aritmieën. Vijfentwintig patiënten die een katheter ablatie procedure ondergingen werden bestudeerd. Elektrogrammen van alle ablatie locaties en geregistreerde locaties binnen een straal van 15mm van de succesvolle ablatie locatie werden geëvalueerd. Er werd gekeken naar (1) lokale activatie tijd, (2) unipolaire QS-configuratie en (3) de aanwezigheid van 'reversed polarity'. De elektrogam karakteristieken van succesvolle ablatie locaties werden vergeleken met niet-succesvolle ablatie locaties. Verder werd de spatiale distributie van iedere electrogram bestudeerd. Succesvolle ablatie locaties toonden significant vaker reversed polarity en hadden een vroegere lokale activatie tijd vergeleken met niet-succesvolle ablatie locaties. Een brede spatiale distributie werd geobserveerd voor een unipolair QS-morfologie rondom de succesvolle ablatie punten. De nieuwe mapping strategie waarbij lokale activatie tijd en reversed polarity wordt gebruikt hadden een hogere voorspellende waarden voor succesvolle ablatie punten dan een mapping strategie met lokale activatie tijd en een unipalair QS-patroon. Deze nieuwe strategie kan er voor zorgen dat er minder ablatie applicaties nodig zijn om de ritmestoornis uit de rechter ventrikel uitstroombaan te termineren

In **Deel II** van dit proefschrift werd 'real-time image integratie' tijdens katheter ablatie procedures van ventriculaire aritmieën beoordeeld. Epicardiale substraat determinatie en katheter ablatie van ventriculaire aritmieën wordt bemoeilijkt door de aanwezigheid van kransslagvaten en epicardiaal vet. **Hoofdstuk 5** evalueert het gebruik van 'real time image integratie' en 'reversed registratie' van CT scans met elektro-anatomische mapping gegevens van epicardiale ablatie procedures. Achtentwintig patiënten die gecombineerde endocardiale-epicardiale mapping procedure hadden ondergaan werden geïncludeerd. De CT scan was voorafgaand aan de mapping procedure vervaardigd om de coronair anatomie en epicardiale vet distributie in kaart te brengen. Pre-procedureel werd de CT data in het 3D-mapping systeem geladen. Ablatie werd niet verricht wanneer de oorsprong van de ritmestoornis <5mm van een kransslagvat gelegen was. Dit werd bevestigd middels coronair angiografie. Alle mapping data werden vervolgens post-procedureel op de CT scan geprojecteerd. In alle patiënten was de real time image integratie succesvol en accuraat verricht. Zesenveertig ritmestoornissen werden geanalyseerd waarvan er 25 (54%) succesvol middels katheter ablatie waren getermineerd. Eenentwintig ritmestoornissen werden niet succesvol geäbleerd; in 8 kon de oorsprong van de ritmestoornispunt niet worden geïdentificeerd; in 9 ritmestoornissen werd geen ablatie verricht omdat het te dicht op een kransslagvat lag of in de buurt van de His-bundel. Bij 4 ritmestoornissen was de ablatie niet effectief. Op deze plekken was de gemiddelde epicardiale vetlaag 16.9mm (range 7-22mm). Opvallend was dat de gemiddelde epicaridale vet dikte bij succesvolle ablatie punten 1.5mm was (range 0-6mm). Concluderend bleek dat 'real time image integratie' van

CT scans realiseerbaar en accuraat is. Epicardiale vet dikte van >7mm en de aanwezigheid van kransslagvaten waren de belangrijkste reden voor het niet slagen van ablatie procedures.

Met dezelfde techniek van 'real time image integratie' werden mapping data naast CT scans, ook op MRI scans geprojecteerd. Hierdoor kon vet en litteken informatie gecombineerd worden met de mapping data en geëvalueerd worden hoe dit de unipolaire en bipolaire voltages beinvloedden. In **Hoofdstuk 6** wordt deze image integratie techniek beschreven in 10 patiënten met een non-ischemische cardiomyopathie. Deze patiënten ondergingen een gecombineerde endocardiale-epicardiale ablatie procedure in verband met ventriculaire ritmestoornissen. Epicardiale voltage mapping wordt gehinderd door vetweefsel, welke bipolaire electrogram amplitudes beïnvloeden, met als resultaat dat het soms moeilijk was om te differentiëren tussen litteken en gezond myocard. Verder kon worden aangetoond dat bipolaire voltages ≤1.8mV en unipolaire voltages van ≤7.95mV de optimale afkapwaarden zijn om litteken te onderscheiden van gezond myocard in epicardiale regio's zonder vet. Echter, bipolaire en unipolaire voltages waren beide verlaagd in regio's waar epicardiaal vet aanwezig was. Specifieke electrogram morfologiën werden niet beïnvloed door de aanwezigheid van vet, maar waren enkel aanwezig in 25% van alle litteken regio's. Een algoritme werd geconstrueerd om te differentiëren tussen littekenweefsel, gezond myocard en vet. Deze bevindingen geven belangrijke inzichten in epicardiale substraat mapping bij patiënten met een non-ischemische cardiomyopathie, wat essentieel is voor een succesvolle ablatie.

Deel III richt zich op chirurgische omcirkelende cryoablatie van ventriculaire tachycardieën (VTs) in patiënten die een chirurgische linker kamer reconstructie ondergaan. Zo'n reconstructie is een effectieve behandeling om de linker kamer functie in patiënten met ischemische hartziekten en een apicaal aneurysma te verbeteren. Eerder werd omcirkelende cryoablatie beschreven als therapie voor VTs in patiënten met frequente recidiverende episodes. Echter, tot nu toe was het onduidelijk of endocardiale omcirkelende cryoablatie ook VTs kan voorkomen in patiënten die een chirurgische linker kamer reconstructie ondergaan. Ventriculaire tachycardieën zijn een belangrijke oorzaak voor toegenomen morbiditeit en mortaliteit in deze patiënten groep. Additionele anti-aritmische chirurgie waarbij het substraat van de aritmie wordt behandeld zou daarom van toevoegende waarde kunnen zijn. **Hoofdstuk 7** evalueert op gestructureerde wijze in 38 patiënten de incidentie, type en timing van VTs nadat er naast de chirurgische linker kamer reconstructie, ook omcirkelende cryoablatie werd verricht. Deze additionele cryoablatie werd alleen toegepast wanneer er tijdens een pre-operatief elektrofysiologisch onderzoek VTs opwekbaar waren. Een historische cohort van 39 patiënten zonder spontane VTs en/of pre-operatief elektrofysiologisch onderzoek werden gebruikt als controle groep. In 27 (71%) van de 38 patiënten waren VTs opwekbaar die hun oorsprong in het aneurysma gebied hadden. Deze 27 patiënten kregen allen additionele omcirkelende cryoablatie. Zesennegentig procent van de patiënten hadden bij ontslag een ICD. 5-jaar VT-vrije overleving was laag in beide groepen; 61% in de onderzoeksgroep en 65% in de controle groep (hazard ratio 1.67, p=0.290). In totaal ontwikkelde 28 patiënten (36%) ≥1 VTs tijdens follow-up. Er waren geen verschillen meetbaar

in het aantal en type ICD therapieën tussen de 2 groepen. Kaplan-Meier analyse liet een 5-jaars overall overleving van 78% zien. Er waren tevens geen verschillen in overall overleving tussen beide groepen (onderzoeksgroep 79% versus controle groep 78%). Er waren geen patiënten overleden ten gevolg van VTs. De nieuwe voorgestelde strategie van pre-operatief elektrofysiologisch onderzoek en additionele omcirkelende cryoablatie was derhalve niet toereikend in het voorkomen van VTs in deze patiënten populatie.

Gezien bovenstaande resultaten werd een single-center gerandomiseerde studie georganiseerd welke het elektrofysiologische effect van endocardiale omcirkelende cryoablatie (ENDO) vergeleek met gecombineerde endocardiale-epicardiale omcirkelende cryoablatie (ENDO-EPI). In **Hoofdstuk 8** worden deze resultaten beschreven. Negentien patiënten bij wie een aneurysma gerelateerde VT opwekbaar was tijdens pre-operatief elektrofysiologisch onderzoek werden geïncludeerd in de studie. Patiënten werden gerandomiseerd in ENDO (n=9) en ENDO-EPI (n=10). Tijdens de operatie werden 3 tijdelijke epicardiale pacemakerdraden ingehecht in het myocard op 3 verschillende plaatsen (rechter kamer, linker kamer, aneurysma) om de geleidings-eigenschappen voor- en na cryoablatie te evalueren. Een significante geleidingsvertraging (>50ms) of bi-directioneel geleidingsblok werd bij niemand bewerkstelligd. Patiënten werden vervolgens met een ICD naar huis ontslagen. Tijdens follow-up hadden 7 van de 16 ontslagen patiënten (44%) spontane VTs welke op de ICD geregistreerd waren. Concluderend leidden ENDO en/of ENDO-EPI omcirkelende cryoablatie niet tot een transmurale laesie waarbij het aneurysma litteken elektrisch wordt afgesloten van het gezonde myocard. Er werd geen voordeel gevonden in de nieuwe ablatie strategie en daarom werd de inclusie van patiënten vervroegd beëindigd.

CONCLUSIE EN TOEKOMST PERSPECTIEVEN

Ventriculaire aritmieën, met name PVCs, komen vaak voor in hartfalen patiënten met een gedilateerde linker kamer en een verminderde linker kamer functie. We konden aantonen dat in patiënten met frequente monomorfe PVCs, onafhankelijk van de aanwezigheid van structurele hartziekten, een succesvolle katheter ablatie leidt tot significante verbetering van de linker kamer afmetingen, vermindering van het (NT-pro)BNP en verbetering van symptomen. Gezien het voordeel dat patiënten hebben van een succesvolle ablatie, zouden patiënten met een verminderede linker kamer functie geëvalueerd moeten worden voor de aanwezigheid van frequente PVCs. Met name de patiënten die in aanmerking komen voor een ICD voor primaire preventie zouden hierop onderzocht moeten worden aangezien dit de beslissing tot het plaatsen van een ICD zou kunnen beïnvloeden. Tot op de dag van vandaag is het onduidelijk welke patiënten met frequente PVCs een PVC-geïnduceerde cardiomyopathie ontwikkelen. Preventie van zo'n cardiomyopathie is echter wel wenselijk. Een instrument dat patiënten op de juiste manier stratificeert is er nog niet. Wij konden voor het eerst aantonen dat vermoeidheid geas-

socieerd is met verhoogde NT-proBNP waarden en cESS. NT-proBNP en cESS normaliseerde allebei na een succesvolle ablatie. Tevens werden de vermoeidheidsklachten minder. Alhoewel we de causaliteit niet konden aantonen, lijken de resultaten te suggereren dat vermoeidheid geassocieerd is met PVC-geïnduceerde verhoogde ventriculaire wandspanning, die met succes konden worden behandeld met katheter ablatie. In het kader van deze bevindingen zouden clinici katheterablatie moeten overwegen bij patiënten die zich presenteren met vermoeidheid, zelfs wanneer de linker kamer functie goed is en andere typische PVC-gerelateerde symptomen ontbreken (zoals hartkloppingen, duizeligheid) of een bepaalde PVC burden. Of een verhoogde NT-proBNP waarde en vermoeidheid patiënten kan identificeren die een verhoogd risico lopen op een PVC-geïnduceerde cardiomyopathie is nog onduidelijk. Daarvoor zou extra onderzoek nodig zijn.

De meerderheid van idiopathische ventriculaire ritmestoornissen hebben hun oorsprong in de rechter kamer uitstroombaan. Patiënten die verwezen worden voor ablatie in verband met deze ritmestoornis zijn vaak jong en gezond. De accuraatheid van elektro-anatomische mapping om een succesvolle ablatie locatie in de rechter kamer uitstroombaan te identificeren kan worden verbeterd door 'reversed polariy' te gebruiken. Dit is een beter criterium dan lokale activatie tijd en/of unipolair QS patroon. Wanneer 'reversed polarity' gebruikt wordt, zijn er minder ablatie laesies nodig om de ritmestoornis te beëindigen, en dit is erg belangrijk ik deze patiënten groep.

In alle patiënten die een epicardiale ablatie procedure ondergaan kunnen real-time image integratie met CT en MRI de pre-procedurele planning en substraat identificatie verbeteren, en tevens niet-succesvolle ablatie locaties identificeren nabij coronair arteriën en dik epicardiaal vet. Bovendien kan het de ablatie procedure zelf faciliteren doordat het de kritische isthmus locaties kan aantonen en daardoor ook succesvolle ablatie locaties kan identificeren. Het nieuwe algoritme helpt om epicardiaal littekenweefsel, gezond myocard en epicardiaal vet te stratificeren. Deze bevindingen geven belangrijke inzichten in epicardiaal mapping bij patiënten met een non-ischemische cardiomyopathie welke essentieel zijn om tot een succesvolle ablatie te komen. Echter, door de aanwezigheid van ICDs of pacemakers wordt het vervaardigen van MRIs beperkt, en zelfs als het wel kan, zijn er belangrijke artefacten aanwezig. CT is daarentegen beschikbaar in alle patiënten en is belangrijk voor zowel het aantonen als uitsluiten van epicardiaal vet. De combinatie van CT data, unipolaire voltages en electrogram karakteristieken kunnen tezamen de accuraatheid van epicardiale substraat mapping verbeteren, welke belangrijk is voor om een succesvolle katheter ablatie te kunnen verrichten.

Na chirurgische linker kamer reconstructie blijven patiënten een hoog risico houden op VTs ondanks additionele omcirkelende endocardiale cryoablatie. Dit is een belangrijk gegeven want katheter ablatie is bij deze patiënten meestal niet meer goed mogelijk in verband met de aanwezigheid van een kunststof patch die over het aneurysma litteken is ingehecht. Om dit te voorkomen was epicardiale omcirkelende cryoablatie toegevoegd aan de endocardiale cryoablatie lijn. De gedachte was dat deze extra ablatie een transmurale laesie zou creëren

waarbij het aneurysma litteken elektrisch zou worden afgesloten van het resterende en gezonde myocard. Wij konden deze hypothese niet bevestigen in een gerandomiseerde studie. Bij geen van de patiënten werd een significante geleidingsvertraging bewerkstelligd na cryoablatie. Verder was de incidentie van VT tijdens follow-up hoog. Daarom concluderen wij dat omcirkelende cryoablatie alleen niet voldoende is om VTs te voorkomen in deze patiënten populatie. Andere anti-aritmische chirurgische opties om VTs te voorkomen zijn echter wel wenselijk. Mogelijk zou (non-mapping gestuurde) endocardectomie een uitkomst bieden, waarbij een groot deel van het VT substraat wordt gereseceerd. Een studie welke de VT incidentie evalueert op een gestructureerde manier is tot op heden nog niet uitgevoerd.

Conclusie

De studies die in dit proefschrift beschreven staan evalueren nieuwe ablatie strategieën en technieken voor de behandeling van ventriculaire aritmieën en procedurele- en lange termijn uitkomsten na ablatie. Verder werden er nieuwe ablatie strategie-algoritmes geïntroduceerd. Het gebruik van (NT-pro)BNP en real-time image integratie van CT en MRI hebben toegevoegde waarde in de behandeling van verschillende subgroepen met ventriculaire ritmestoornissen. Ten slotte wijzen deze resultaten erop dat bij patiënten met ischemisch hartfalen die een linker kamer reconstructie ondergaan andere aanvullende behandeling dan omcirkelende cryoablatie dient te worden overwogen aangezien zij een hoog risico hebben op het ontwikkelen van ventriculaire ritmestoornissen.

Appendix

List of Publications
Dankwoord
Curriculum Vitae

LIST OF PUBLICATIONS

1. **CF van Huls van Taxis**; K Zeppenfeld, RJ Klautz, AP Wijnmaalen. Endocardial/epicardial-versus endocardial encircling cryoablation for ventricular tachycardia; a randomized trial. *Accepted for publication in the Journal of Thoracic and Cardiovascular Surgery*
2. **CF van Huls van Taxis**; AP Wijnmaalen; P Klein; OM Dekkers; J Braun; HF Verwey; MJ Schalij; RJ Klautz; K Zeppenfeld. Programmed electrical stimulation guided encircling cryoablation concomitant to surgical ventricular reconstruction for primary prevention of ventricular arrhythmias*. Eur J Cardiothorac Surg.* 2018;54:98-105
3. **CF van Huls van Taxis,** SR Piers, M de Riva Silva, OM Dekkers, DA Pijnappels, MJ Schalij, AP Wijnmaalen, K Zeppenfeld. Fatigue as presenting symptom and a high burden of premature ventricular contractions are independently associated with increased ventricular wall stress in patients with normal left ventricular function. *Circ Arrhythm Electrophysiol.* 2015;8:1452-1459.
4. K Dyrda, SR Piers, **CF van Huls van Taxis**, MJ Schalij, K Zeppenfeld. Response to Letter by Chhabra and Spodick regarding article, "Influence of steroid therapy on the incidence of pericarditis and atrial fibrillation following percutaneous epicardial mapping and ablation for ventricular tachycardia" by Dyrda et al. Zeppenfeld K. *Circ Arrhythm Electrophysiol.* 2014;7:992.
5. K Dyrda, SR Piers, **CF van Huls van Taxis**, MJ Schalij, K Zeppenfeld. Influence of steroid therapy on the incidence of pericarditis and atrial fibrillation after percutaneous epicardial mapping and ablation for ventricular tachycardia. *Circ Arrhythm Electrophysiol.* 2014;7:671-676.
6. SR Piers, Q Tao, **CF van Huls van Taxis**, MJ Schalij, RJ van der Geest, K Zeppenfeld. Contrast-enhanced MRI-derived scar patterns and associated ventricular tachycardias in nonischemic cardiomyopathy: implications for the ablation strategy. *Circ Arrhythm Electrophysiol.* 2013;6:875-883.
7. D Penela, **CF van Huls van Taxis**, L Aguinaga, J Fernández-Armenta, L Mont, MA Castel, M Heras, JM Tolosana, M Sitges, A Ordóñez, J Brugada, K Zeppenfeld, A Berruezo. Neurohormonal, structural, and functional recovery pattern after premature ventricular complex ablation is independent of structural heart disease status in patients with depressed left ventricular ejection fraction: a prospective multicenter study. *J Am Coll Cardiol.* 2013;62:1195-1202.
8. SR Piers, DP Leong, **CF van Huls van Taxis**, M Tayyebi, SA Trines, DA Pijnappels, V Delgado, MJ Schalij, K Zeppenfeld. Outcome of ventricular tachycardia ablation in patients with nonischemic cardiomyopathy: the impact of noninducibility. *Circ Arrhythm Electrophysiol.* 2013;6:513-521.
9. SR Piers, **CF van Huls van Taxis**, Q Tao, RJ van der Geest, SF Askar, HM Siebelink, MJ Schalij, K Zeppenfeld. Epicardial substrate mapping for ventricular tachycardia ablation in patients

with nonischemic cardiomyopathy: A new algorithm to differentiate between scar, myocardium and fat developed by simultaneous integration of CT and contrast-enhanced MRI. *Eur Heart J*. 2013;34:586-596.

10. **CF van Huls van Taxis,** AP Wijnmaalen, SR Piers, RJ van der Geest, MJ Schalij, K Zeppenfeld. Real-time integration of MDCT-derived coronary anatomy and epicardial fat: impact on epicardial electroanatomic mapping and ablation for ventricular arrhythmias. *JACC Cardiovasc Imaging.* 2013;6:42-52
11. Q Tao, J Milles, **CF van Huls van Taxis**, HJ Lamb, JH Reiber, K Zeppenfeld, RJ van der Geest. Toward magnetic resonance-guided electroanatomical voltage mapping for catheter ablation of scar-related ventricular tachycardia: a comparison of registration methods. *J Cardiovasc Electrophysiol.* 2012;23:74-80.
12. **CF van Huls van Taxis**, AP Wijnmaalen, DW den Uijl, M Gawrysiak, H Putter, MJ Schalij, K Zeppenfeld. Reversed polarity of bipolar electrograms for predicting a successful ablation site in focal idiopathic right ventricular outflow tract arrhythmias. *Heart Rhythm.* 2011;8:665-671.
13. SR Piers, AP Wijnmaalen, CJ Borleffs, **CF van Huls van Taxis**, J Thijssen, JB van Rees, SC Cannegieter, JJ Bax, MJ Schalij, K Zeppenfeld. Early reperfusion therapy affects inducibility, cycle length, and occurrence of ventricular tachycardia late after myocardial infarction. *Circ Arrhythm Electrophysiol.* 2011;4:195-201.
14. AP Wijnmaalen, RJ van der Geest, **CF van Huls van Taxis**, HM Siebelink, LJ Kroft, JJ Bax, JH Reiber, MJ Schalij, K Zeppenfeld. Head-to-head comparison of contrast-enhanced magnetic resonance imaging and electroanatomical voltage mapping to assess post-infarct scar characteristics in patients with ventricular tachycardias: real-time image integration and reversed registration. *Eur Heart J.* 2011;32:104-114.
15. AP Wijnmaalen, V Delgado, MJ Schalij, **CF van Huls van Taxis**, ER Holman, JJ Bax, K Zeppenfeld. Beneficial effects of catheter ablation on left ventricular and right ventricular function in patients with frequent premature ventricular contractions and preserved ejection fraction. *Heart.* 2010;96:1275-1280.

DANKWOORD

Dit proefschrift is gebaseerd op onderzoek dat is uitgevoerd op de afdeling Hartziekten van het Leids Universitair Medisch Centrum. Een groot aantal mensen zijn direct en indirect betrokken geweest bij het tot stand komen van dit proefschrift. Ik wil graag de medewerkers van de afdeling Hartziekten en mijn “tuin” en “serre” collega’s bedanken voor de goede samenwerking en inspiratie.

Graag zou ik een aantal mensen in het bijzonder willen bedanken. Ten eerste wil ik mijn dank uitspreken aan mijn promotores prof. Zeppenfeld en prof. Schalij voor alle begeleiding en het in mij gestelde vertrouwen. Mijn co-promotor, beste Hadrian, dank je wel voor al je goede adviezen en eeuwige geduld.

“Het VT-team”; Sebastiaan, Marta en Gijs, dank voor de goede en gezellige samenwerking in- en rond het cath-lab.

Lieve Mariëlle en Jaap, dank jullie wel voor de hechte vriendschap en alle gezelligheid die we met elkaar en de kids hebben beleefd en gaan beleven.

Lieve Eleanore, we hebben veel tijd samen doorgebracht op de afdeling en daarnaast, jij kan niet ontbreken als mijn paranimf. Dank je wel voor alle pep-talks en je positivisme. Lieve Antoinette, lief zusje, dank je wel voor alle niet-wetenschappelijke input tijdens het schrijven van dit proefschrift. Fijn dat ik altijd op je kan rekenen en dat je mijn paranimf bent.

Lieve Henk en Toos, dank jullie wel voor jullie oneindige flexibiliteit.

Lieve Papa, Mama en Jan Willem, dank voor jullie onvoorwaardelijke steun (op alle vlakken) en interesse tijdens het schrijven van dit proefschrift.

Mijn lieve Joris, dank je wel dat je er altijd bent. Jij bent mijn steun en toeverlaat. Thuis met onze Cato en Aimee zijn we een team en is ons leven één groot feest.

CURRICULUM VITAE

De auteur van dit proefschrift werd geboren op 12 augustus 1984 te Leiden. In 2002 deed zij eindexamen VWO aan het Rijnlands Lyceum te Wassenaar. Hierna startte zij met de opleiding Geneeskunde aan de Universiteit Leiden, waar zij in maart 2009 het artsexamen haalde. Tijdens haar studie was zij werkzaam op de afdeling thorax intensive-care als Joshua (IC-ondersteuner) waar de interesse in de cardiologie ontstond.

Direct na haar afstuderen startte zij in het Leids Universitair Medisch Centrum haar promotie onderzoek onder leiding van Prof. Dr. K. Zeppenfeld en Prof. Dr. M.J. Schalij naar nieuwe ontwikkelingen in ablatie technieken van ventriculaire aritmieën. De resultaten hiervan werden op meerdere (inter)nationale congressen gepresenteerd en staan beschreven in dit proefschrift.

Per 1 december 2012 is zij begonnen aan haar opleiding tot cardioloog vanuit het Leids Universitair Medisch Centrum (opleider: Prof. Dr. M.J. Schalij). Op dit moment heeft zij de vooropleiding Interne Geneeskunde in het HMC Bronovo Ziekenhuis te Den Haag (opleider: Dr. Y.W.J. Sijpkens) en het perifere opleidingsjaar cardiologie in het Groene Hart Ziekenhuis te Gouda (opleider: Dr. M.W.J. Van Hessen) voltooid. Heden vervolgt zij haar opleiding cardiologie in het Leids Universitair Medisch Centrum.